

---

An Evaluation of the Canopy Layer Urban Heat Island Through Regional Air  
Temperatures in Cheltenham, Gloucestershire, 1990 to 2000.

---

Thomas Ashfield



'A thesis submitted to the University of Gloucestershire in accordance with the  
requirements for the degree of Master of Science by Research in the School of  
Natural and Social Sciences'

February 2022

Word Count: 26,480

## **Abstract**

The urban heat island (UHI) is the difference in equivalent temperatures of a city when compared with its rural surroundings. Interactions between natural and anthropogenic activity have been proposed as key driving mechanisms towards UHIs, and this is often exacerbated by anticyclonic conditions and extreme weather phenomena. Typical studies of the UHI focus on populous and mega-cities rather than smaller towns and cities. The aim of this study was to investigate what factors help to explain why Cheltenham was ranked the hottest town in the United Kingdom (UK) between the years 1990 to 2000 and to what extent the effects of weather and the natural and artificial landscape influenced the magnitude and geographical extent of the UHI in Cheltenham. Data from MIDAS weather stations in Gloucestershire were used for statistical analyses to test and infer the associations between the canopy layer urban heat island (CUHI) in Cheltenham and cloud cover, precipitation, population, and changes in land cover between 1990-2000. Sunspot cycles were used as an experimental surrogate for solar intensity. Air temperature profiles show Cheltenham demonstrates higher temperatures when compared with its rural surroundings with temperatures exceeding 3.43°C (maximum) and 0.95°C (minimum). Correlation analyses show that cloud cover has a significant, weak, negative correlation with maximum and minimum CUHI. The CUHI shows a weak negative correlation with precipitation. In addition, CUHI minimum shows a strong, significant relationship with population growth. This study concludes that small towns and cities demonstrate an urban heat island effect. Furthermore, that Cheltenham's CUHI is conditioned by fluctuations in cloud cover, precipitation, and changes in population over time.

## Declaration

I declare that the work in this thesis was carried out in accordance with the regulations of the University of Gloucestershire and is original except where indicated by specific reference in the text. No part of the thesis has been submitted as part of any other academic award. The thesis has not been presented to any other education institution in the United Kingdom or overseas.

Any views expressed in the thesis are those of the author and in no way represent those of the University.

Signed Thomas Ashfield

Date 02/02/2022

doi:10.46289/LB58VW72

## **Acknowledgements**

First and foremost, I would like to show my appreciation and gratitude towards the University of Gloucestershire and the supportive staff who helped me throughout every step during my academic studies. I would like to thank my primary supervisor, Professor Frank Chambers for his continued interest, guidance, and feedback throughout this research project. Furthermore, I would like to thank Dr. Robert Berry for his support and guidance during the preliminary stages of this thesis. Finally, I would like to extend my special thanks to Dr. Lucy Clarke, without her assistance and dedication through the final stages of this research project, this paper would never have been accomplished.

I would also like to show my utmost appreciation for my family, friends and loved ones, for their wise counsel and unparalleled support from the beginning. Without them, I would not be where I am now.

## Table of Contents

### Contents

Abstract.....	ii
Declaration.....	iii
Acknowledgements.....	iv
Table of Contents.....	v
Chapter 1: Introduction.....	1
1.1 Background.....	1
1.1.1. The Urban Heat Island (UHI).....	5
1.2 Study Area and Research Focus.....	6
1.3. Aim.....	10
1.3.1. Research questions.....	10
1.3.2. Objectives.....	10
Chapter 2: UHIs: Concepts and Previous Research Emphasis.....	12
2.0. Introduction.....	12
2.1. UK Heatwave Events.....	12
2.1.1 The 1990 Heatwave.....	13
2.1.2 UK Heatwave Events since 1990.....	15
2.2 Global Energy Exchange and Energy Balance.....	17
2.3 Driving Mechanisms to the UHI.....	19
2.3.1 Natural Driving Mechanisms.....	19
2.3.2 Anthropogenic Driving Mechanisms.....	22
2.4. Urban Heat Islands (UHIs).....	26

2.4.1 Types of UHI.....	29
2.5. UHI Intensity .....	34
2.5.1. Calculated UHI Intensity .....	35
2.6. Analysis and Visualization of the UHI .....	35
Chapter 3: Methods .....	38
3.1 Introduction.....	38
3.2 Weather data.....	38
3.2.1 Temporal analysis of the air temperature.....	42
3.2.2 Interpolation of air temperature data .....	42
3.2.3 Urban Heat Island (UHI) Intensity .....	44
3.3 Land cover.....	45
3.3.1 Land Classification .....	47
3.4 Population data.....	49
3.5 Sunspot cycle data .....	49
3.6 Topographic data.....	49
3.7 Data analysis.....	50
Chapter 4: Results .....	52
4.1 Temperature.....	52
4.1.1 Decadal Temperature Profile .....	52
4.1.2 Daily and Monthly Mean Air Temperature .....	56
4.2 Land Classification .....	65
4.3 Heat Maps.....	70
4.4 Weather Variables and Extra-Terrestrial Influences.....	72

4.4.1 Sunspot Cycle .....	72
4.4.2 Precipitation.....	73
4.4.3 Cloud Cover .....	75
4.5 Urban Heat Island (UHI) Intensity .....	76
4.6 Sunspot Cycles and Urban Heat Island (UHI) Intensity.....	79
4.7 Analysis of relationships .....	81
4.7.1 Correlation and Regression Analysis of maximum CUHI .....	81
4.7.2 Correlation and Regression Analysis CUHI Minimum .....	83
5. Discussion .....	85
5.1 Air Temperature Trends.....	85
5.2 Impact of Weather and Population on the CUHI .....	88
5.2.1 Impact of Cloud Cover .....	88
5.2.2 Relationship of Precipitation and CUHI .....	92
5.2.3 Population Growth and CUHI.....	95
5.3 Relationship Between Sunspot Cycles and CUHI .....	97
5.3.1 Isolating Sunspot Cycle and CUHI.....	99
5.3.2 Examination of Sunspot Cycles on Weather and Temperature .....	101
5.4 An Evaluation of the CUHI in Cheltenham .....	103
5.4 Topography, Land Classification and CUHI .....	109
Chapter 6: Conclusion.....	113
6.1 Limitations to the Study .....	119
6.2 Suggestions for Future Research .....	122
References .....	125

## **Chapter 1: Introduction**

### **1.1 Background**

Weather and climate are governed by inter-terrestrial and extra-terrestrial processes.

Inter-terrestrial processes can be defined as processes which exist and occur inside the Earth and its atmosphere; these include atmospheric, oceanic, climate, and weather (Holden, 2018). In contrast, extra-terrestrial processes are those which are governed by the Sun and its interactions with Earth (Stewart and Mills, 2021).

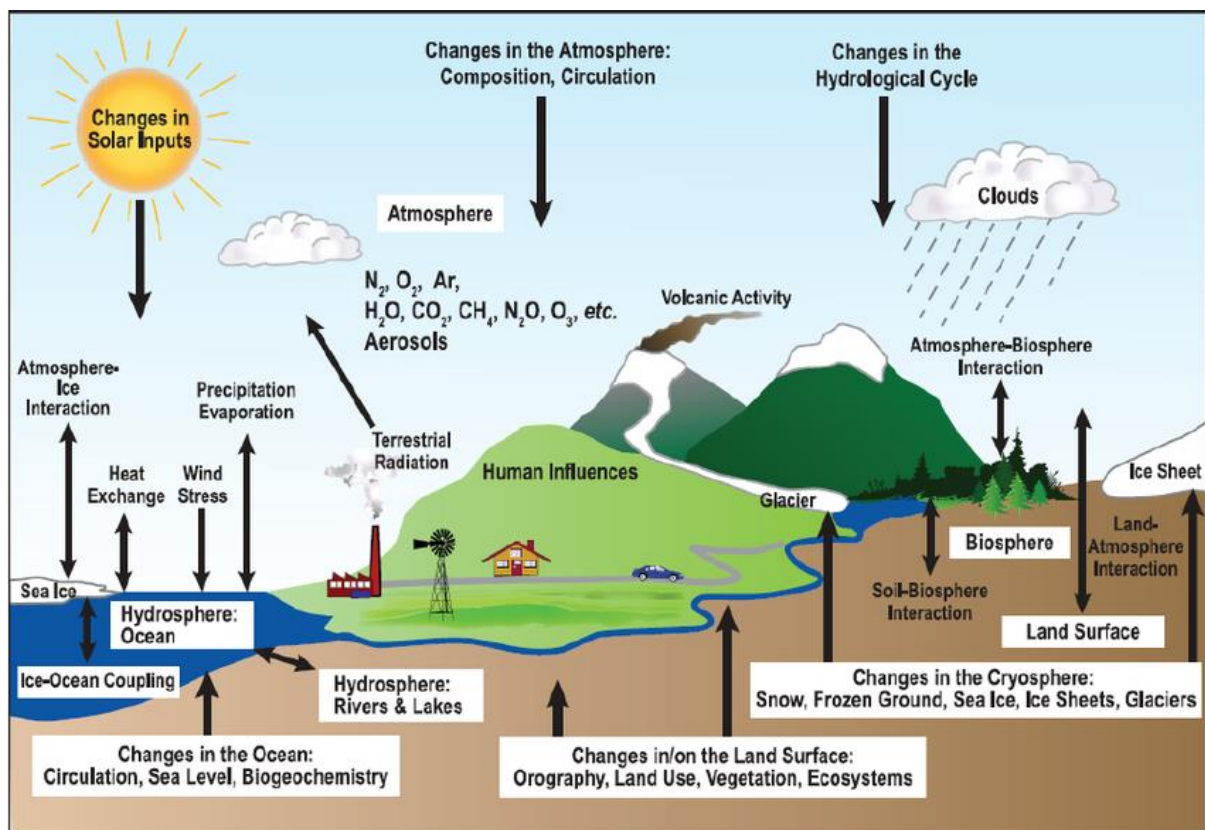
Weather can be defined as the totality of atmospheric processes over short-term periods (Atkinson, 1998); it concerns the conditions prevailing from hours, days, weeks, and a year (Gobo 2014) over a small area (Atkinson. 1998). It is the instantaneous state of the atmosphere and consists of short-term variations in temperature, precipitation, humidity, air pressure, cloudiness, radiation, wind, and visibility (Schmittner, 2018). Climate is defined as the long-term processes of the atmosphere, which are influenced by underlying surface features and extra-terrestrial influences (Atkinson, 1998). As such, the climate system concerns all major components of the natural environment on the planet (Houghton et al., 1996).

Both climate and weather are closely related, as Linacre and Geerts (1997) explain climate is an aggregate or composite of weather. Various atmospheric processes and surface features explain the weather and that in turn explains the climate (Robinson and Henderson-Sellers, 1999). The main difference between these two systems is the measure of time between the two.

Earth's climate system is primarily composed of five bodies. The atmosphere, hydrosphere, cryosphere, biosphere, and lithosphere. These components interact through exchanges in energy (shown in Figure 1.1). Variations in latitude, elevation,



orientation to the Sun, and distance from the sea affect both the weather and climate of an area.



**Figure: 1.1** Overview of components of the climate system, processes, and interactions (Gobo, 2004).

Figure 1.1 shows that both natural and artificial forcings affect the climate system, with the main source of energy that drives Earth's climate being solar radiation. Around 31% of incoming solar radiation is reflected away by the atmosphere, clouds, and Earth's surface (Trenberth et al., 2000). A further 20% is absorbed by the atmosphere and clouds resulting in 49% of net incoming solar radiation being absorbed by the Earth's surface. The planet and its atmosphere must radiate, on average the same amount of energy back to space (Trenberth et al., 2000). If the balance is altered, by changes in solar radiation the Earth will respond by either warming or cooling until a new balance is achieved (Hill et al., 2010). In simple

terms, the interaction between incoming and outgoing energy fluctuations within the Earth's climate systems is defined as the energy balance. Climates can change because of natural changes within the climate system, fluctuations in solar energy, volcanic activity, alterations to atmospheric composition, or land-use (Figure 1.1). An additional emerging factor is the effect of human activities on climate (Trenberth et al., 2000). The energy that is not reflected back to space is absorbed by the Earth's atmosphere and surface. Increased anthropogenic activity has resulted in alterations to the atmosphere with increased contributions of greenhouse gas, especially carbon dioxide, emissions, Changes to the landscape have also changed the energy balance of the urban and natural landscape, these alterations change the radiative properties of the surface and affect the energy balance on both local and global scales (Oke, 2017; Schmittner, 2018; Le Treut et al., 2021). To expand, complex interactions among urban albedo, increased thermal mass per unit, city roughness, anthropogenic, heat and decreased evaporative areas change the radiative properties of the surface (Taha et al., 1988), predominantly within urban landscapes where there are increases in impervious surfaces and lacking vegetation. To reiterate, changes to natural and urban landscapes create positive feedbacks in the energy balance resulting in warming on both local and global scales (Taha et al., 1988; Schmittner, 2018).

In studies of climate change, long-term cycles of the Earth's systems and processes relate to the effects of past climates (Holden, 2017), through the processes and effects of Milankovitch cycles, extra-terrestrial influences on climate and weather over long periods of time (Atkinson, 1998; Schmittner, 2018; Oke, 2017). To elaborate, the Quaternary period demonstrates rhythmic changes in climate. these cyclic variabilities are driven by astronomical influences which operate at frequencies

that range from tens to hundreds of thousands of years, these cycles are known as Milankovitch cycles (Lowe et al., 2013). These cycles are dictated by Earth's orbit around the Sun which corresponds to changes in both global temperatures and glacial-interglacial cycles. Furthermore, within these cycles are abrupt changes that are lesser understood but reflect mechanisms operating within the Earth-Atmosphere system. Within contemporary climate research, evidence shows the present climate is being affected by anthropogenic activities (Lowe et al., 2013). Brunetti (2003), reviews the literature on 11-year solar cycles and states that influences on temperature were induced by the Sun. Reichel et al., (2001) show that cause-and-effect ordering is present in smoothed solar cycle length and cycle mean for the Northern Hemisphere land air temperature for the twentieth century with a 99% significance level. In sum, Reichel et al., (2001) link variations in solar activity to variations in climate. Although, there are some disputes with inquiries into solar cycles and temperature as Thejll and Lassen (2000), conclude that the relationship between solar cycle and temperature breaks down after 1975 in solar records, concluding that anthropogenic warming is likely for the breakdown in this relationship.

In comparison with the focus on glacial-interglacial cycles, there is less knowledge and evaluation into the direct effects and relationships short-term cycles may have on climate, both globally, regionally, and locally, the weather. Within contemporary climate change, there is also a focus on the anthropogenic relationships with changes in weather and climate (Robinson and Henderson-Sellers, 1999; Oke, 2017). The field of climate and weather is far more convoluted and complex than just a primary focus on human interactions or anthropogenic causalities as the literature might imply.

Owing to the nature of energy transference, specific and latent heat capacities of urban and rural environments, the natural landscape has direct effects on energy transference, weather, and climate.

### **1.1.1. The Urban Heat Island (UHI)**

The urban heat island (UHI) can be defined as the difference between urban temperatures when compared with their rural surroundings (Stewart and Mills, 2021; Oke, 2017), related to anthropogenic heating in towns and cities (Bassett et al., 2017). These differences in temperatures are primarily determined by the urban configuration and local meteorology. UHI intensity is calculated by subtracting the temperature at a reference rural station from an urban weather station (Stewart, 2011).

The study of the UHI has developed significantly over time since Howard (1833) first observed urban environments were distinctly warmer when compared to their rural surroundings. Observations and modelling of the UHI over time have shown that they are prevalent in cities and towns of all climate types (Cardoso et al., 2017). Expanding on these initial observations, further research has been made into the influence of UHI intensity on humans, flora, and fauna as well as investigations into methods to mitigate UHIs, derived from initial physical studies of the phenomena (Yow, 2007). These studies show common findings which show that UHI will work in conjunction with large-scale climate change to significantly shift ranges of numerous species, increase growing seasons and induce earlier flowering data, affecting both flora and fauna (White et al., 2002; Lavoie and Lachance, 2006; Yow 2007).

Although many advancements have been made in this field, there continues to be a focus on investigating the prevalence of UHIs in cities and mega-cities (Peng et al.,

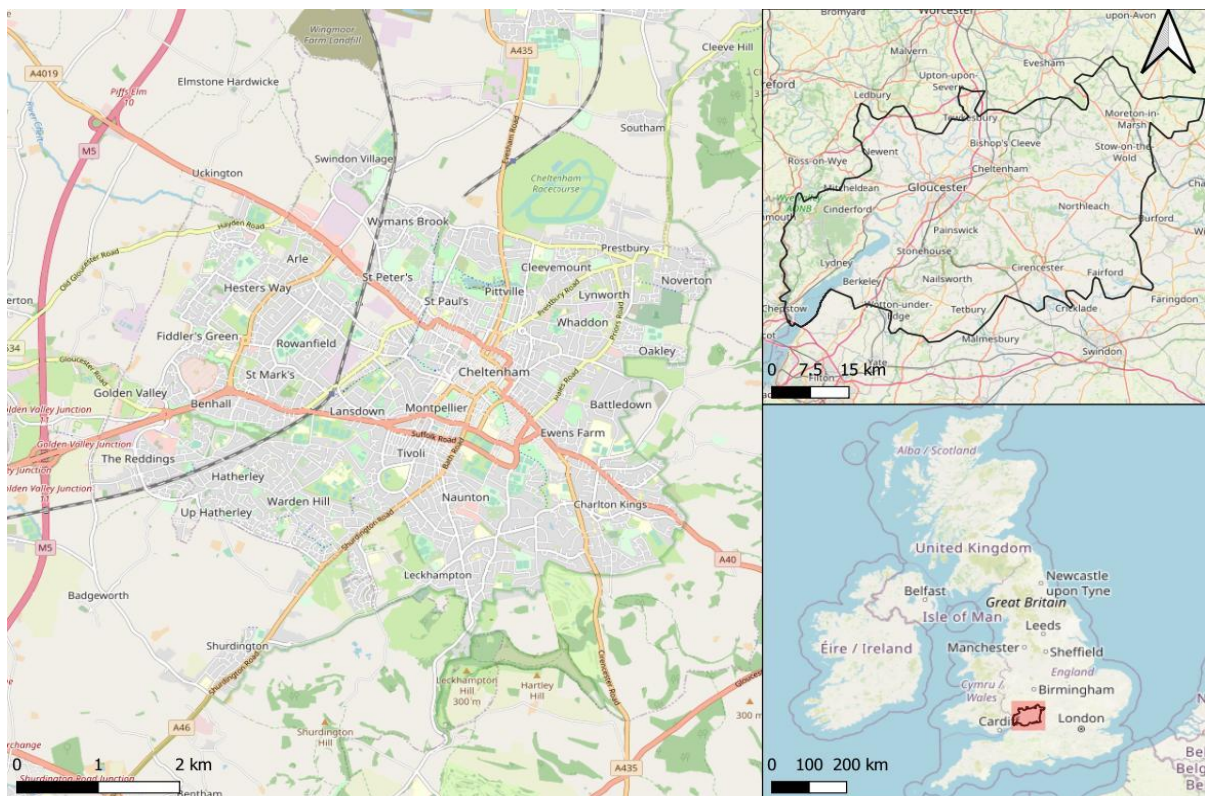
2011). To address this there needs to be more emphasis on the impact of the UHI in smaller urban areas, which this project is aiming to do.

City size and high population densities have been correlated to the magnitude of a city's UHI (Oke, 1973). Population and population density are key anthropogenic causes of UHI formation and magnitude (Oke, 1995). The intensity of the UHI varies with population size and by extension, population density (Manoli et al., 2019). Links between urban warming and city size as measured by population were first proposed by Oke (1973). Later studies support that the size of a city has the strongest influence on the UHI intensity, furthermore, compactness and the degree to which cities stretch influence to a lesser degree UHI intensity (Zhou et al., 2017). Yunfei et al., (2020) model parameters of gross building volume and city size against UHI intensity and show strong correlations between the elevated near-surface air temperatures and anthropogenic factors. The result of this quantifies the relationship between urban factors and UHI intensity (Yunfei et al., 2020). Further concepts of anthropogenic drivers and the UHI are explained in Chapter 2.

## **1.2 Study Area and Research Focus**

Cheltenham is situated within Gloucestershire, South-West England (51°53'N 002°04'W) bordering the Cotswolds Area of Outstanding Natural Beauty (Figure 1.2). The town is situated 58 m above mean sea level, with Cleeve Hill on the eastern edge of the town at the highest elevation of 330m. Cheltenham is a conurbation with the surrounding areas such as Leckhampton, Bishops Cleeve, and Charlton Kings merging with the central area of Cheltenham. Cheltenham was established as a Spa town in 1790, its increased popularity led to the construction of Regency terraces, crescents and villas (Cheltenham Council, 2021). The urban infrastructure reflects this and is composed of both Regency period and modern buildings, with the River

Chelt flowing through and under the town. Over the last hundred years, Cheltenham has developed rapidly with an area of 46.62km<sup>2</sup> (ONS, 2016), expanding as a centre for business and administration. It is accessible by the A40, railway, M5, and private airport connections, furthermore, it is host to major key players such as GCHQ, the University of Gloucestershire and the Cheltenham Festivals which bring in business, tourism and education (Cheltenham Council, 2021).



**Figure 1.2:** Map of Cheltenham, Gloucestershire with reference to its relative location in the county of Gloucestershire and the wider United Kingdom (Google Earth, 2018). Crown copyright and database rights 2022 Ordnance Survey (100025252); Contains OS data © Crown copyright and database right 2022.

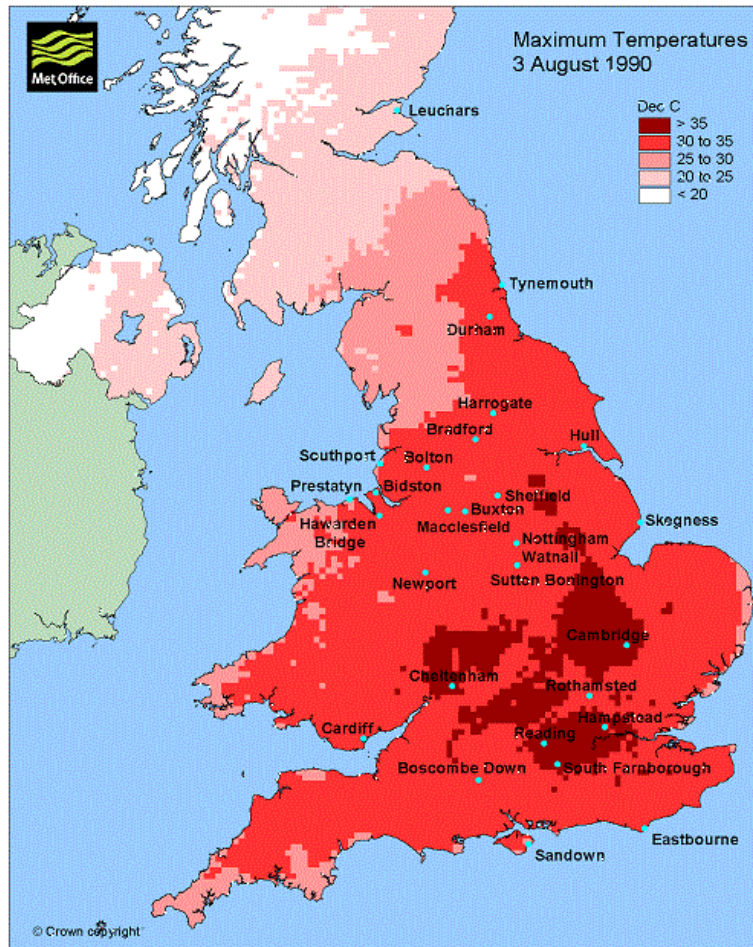
In 1990, Cheltenham had a population of 107,102, with an average population density of 2297.34 inhabitants/km<sup>2</sup> which had grown to 109,282 in 2003 with an average population density of 2344.10 inhabitants/km<sup>2</sup> (ONS, 2018). According to current mid-population estimates from the ONS, in 2020 Cheltenham had a

population of 116,043 (Inform Gloucestershire, 2020). This is an increase of 8941 inhabitants since 1990, with a current population density of 2489.12km<sup>2</sup>.

The local climate for the study area can be classified as a temperate oceanic climate (or Cfb), according to the Koppen climate classification (Lohmann, 1992). On average, Cheltenham has an annual temperature of 14.7°C with an average maximum temperature of 19.1°C and an average minimum temperature of 10.3°C (Met Office, 2017). The average seasonal temperatures from 1981 to 2010 are: Spring 14.0°C, Summer 21.8°C, Autumn 14.9°C and Winter 7.3°C (Met Office, 2019).

In 1990 the UK experienced an unprecedented, short-lived heatwave that affected the British Isles (Burt, 1991); in particular, this impacted the Midlands and the south-east area of the country (Figure 1,3) which are subject to the Central European Blocking High, which diverts depressions northward resulting in warmer climates and higher temperatures (Kennedy et al., 2016). Blocking highs are climatic episodes that occur during thermic and rainfall anomalies (Andrei and Liviu, 2016). The zonal movement of air is blocked which leads to weak vorticity of air. Examples of these occurred during both 1990 and 2003 heatwave events (Andrei and Liviu, 2016), which further exacerbate the effects of heatwave events through anticyclonic systems leading to positive anomalies for temperature. During this, on August 3<sup>rd</sup>, 1990, Cheltenham recorded the highest British maximum temperature of 37.7°C (Met Office, 2012); Cheltenham held this record for 13 years before being overtaken by Faversham, Kent, which recorded a new maximum of 38.5°C in 2003 (Met Office, 2012). Since then, the record has been surpassed again, most recently in 2019 with Cambridge recording 38.7°C (Met Office, 2019). Heatwaves can induce or exacerbate existing UHIs within built-up environments.





**Figure 1.3:** Maximum temperatures in the UK during the heatwave on August 3<sup>rd</sup>, 1990 (source: Met Office, 2012).

Urban heat islands are a typical feature of urban climates, regardless of size or population (Blazejczyk et al., 2006). However, there is limited research available investigating the heat island effect in small cities or towns, as well as cities in specific locations (Blazejczyk et al., 2006).

The purpose of this study is to investigate the urban heat island effect through regional air temperatures by using Cheltenham as a case study. Although comparative studies have been utilized to compare and evaluate the urban heat island effect with larger cities and megacities, these studies typically evaluate two similar locations by metric of population or size. Owing to the limited nature of



research into urban heat islands in smaller towns and cities, this study will solely focus on exploring the urban heat island effect for Cheltenham, Gloucestershire.

### **1.3. Aim**

The overall aim of this study is to advance the understanding of the UHI effect within Cheltenham. Specifically, this study will quantify and model the presence and degree of the UHI in Cheltenham and explore their spatial and temporal extent of this between 1990 and 2000. This study will explore the relationship between geographical and meteorological variables using secondary data.

#### **1.3.1. Research questions.**

There are two main research questions:

1. To investigate and explain why Cheltenham was ranked the hottest town in the UK between the years 1990 to 2000. An in-depth analysis of the literature will provide context to the main driving forces behind the formation and magnitude of the UHI.
2. To investigate the extent and the effects that both weather and the natural and artificial landscape have on the UHI in Cheltenham. Interactions between the natural and artificial landscape may have exacerbated the impact of the heatwave induced by the background weather conditions and this will be investigated.

#### **1.3.2. Objectives**

The objectives of the study are:

1. Use spatial analysis of secondary data to explore the variables influencing the UHI around Cheltenham.

2. Acquire temperature data from weather stations in the Cheltenham locality and use these to create and evaluate temperature profiles for each and calculate the UHI.
3. Analyse the relationship between the UHI intensity, temperature, and other meteorological variables.
4. Use the data collected to explain the formation and extent of the UHI in Cheltenham between 1990 to 2000.

## **Chapter 2: UHIs: Concepts and Previous Research Emphasis**

### **2.0. Introduction**

This chapter begins with an overview weather synopsis of UK heatwaves relevant to this study. To understand the presence of the UHI effect it is necessary to outline the main driving forces behind the formation and presence of the UHI. This chapter will review the relevant literature published within this field of study to help define the different types of UHI, including the several sub-types of UHI that have been identified. A focus on the natural and anthropogenic driving forces behind the formation and magnitude of the UHI will also be provided. This chapter will conclude with an overview of the methods that have been used to analyse and visualise UHIs.

### **2.1. UK Heatwave Events**

Heatwaves are defined as prolonged periods of unusually high temperatures, lasting several days to weeks (McCarthy et al., 2019; WMO, 2018). A heatwave requires three consecutive days in which the daily maximum temperature exceeds a heatwave threshold ranging between 25°C and 28°C (McCarthy et al., 2019). The heatwave threshold pertains to the 90th percentile of the July daily maximum temperature for the 1981 – 2010 climatological reference period using gridded observations (Hollis et al., 2019).

The frequency and intensity of heatwaves have increased worldwide (Baldwin et al., 2019; Perkins-Kirkpatrick and Lewis, 2015). An investigation into the frequency and intensity of global heatwaves from 1950 to 2017 by Perkins-Kirkpatrick (2020) shows that the average number of global heatwave days has increased from five (1950) to eighteen days (2017). Furthermore, decadal trends in heatwave intensity have increased from 18°C (1950) to 24°C (2017), further supporting Baldwin et al., (2019), showing that both the frequency and intensity of heatwaves have increased globally.

In tandem with the warming of background climate systems, the average temperature for the period 2009–2018 has been 0.9°C above the 1961–1990 reference climate (Kendon, 2019). However, an analysis of historical heatwaves in the UK using gridded temperature pushes this figure to 1°C higher than average for UK summer maximum temperatures based on the 2000 – 2018 figures when compared against the 1960 – 1979 figures (Beckett and Sanderson, 2021). Their study further states that, heatwave events for the UK which record temperatures of 25°C to 30°C have increased in frequency and duration over time, increasing by an average of 1 – 2 days to 4 – 6 days respectively from 1960 to 2020 (Beckett and Sanderson, 2021).

### **2.1.1 The 1990 Heatwave**

Changes in pressure can lead to the formation of cyclones and anticyclones which in turn can affect weather and climate on a local to regional scale. Anticyclones are high-pressure systems associated with fair weather conditions, in contrast, cyclones are low-pressure systems associated with unstable weather conditions (White et al., 1998).

In mid to late 1990 an anticyclonic system over the British Isles resulted in a high-pressure system with clear, warm weather conditions over the country leading to an increase in the mean temperatures of 1.0°C above the 1951 to 1980 mean (Burt, 1992). Temperatures for the UK reached or exceeded 26°C every day from July 11th onwards with a small break in trends at the end of July (Burt, 1992) and maximum temperatures exceeding 34°C. Brugge (1991) compared monthly sunshine totals taken from 40 weather stations during 1989 and 1990 against the 1951 – 1980 sunshine totals and found that many stations in southern and eastern parts of England recorded an increase up to 20% above average. Furthermore, there was a

lack of rain in 1989-90 with low levels in reservoirs and hose-pipe bans, in tandem with the 1990 heatwave (Brugge, 1991). The prolonged effects of increased mean temperatures have profound effects on both atmospheric and topographical processes; the results can induce, or exacerbate on a local scale, the effects of the UHI.

Burt (1992) notes that four essential conditions led to the hot weather: (1) a high soil moisture deficit owing to the lack of rainfall; (2) a lack of soil moisture retention resulted in a lack of evapotranspiration (a key cooling process as heat energy is transported when moisture evaporates and changes state into a gas whereby heat is transported); (3) the lack of moisture in the soil allowed for more energy to be available as sensible heat, this is the energy required to change the temperature of a substance with no phase change; and (4) as no moisture is available to change state and remove heat from the surface, surfaces can heat up quickly and efficiently, allowing for more solar radiation to be concentrated on the surface. According to Tursilowati et al. (2018) reduced moisture content and enhanced trapping of heat and solar energy within a localized urban environment would be exacerbated owing to the heat capacity of buildings and the ratio of the number of mixed surfaces. This positive feedback loop allows for both regional and localized heating within both rural and urban environments, exacerbating the heatwave.

By the end of July 1990, a small anticyclone formed over the English Channel that was fed from warm air from the European continent which accelerated the effects of the heatwave. On 3<sup>rd</sup> August 1990, the main axis of high pressure extended east-west over the central parts of the British Isles (Martin, 2005); a direction that would favour the development of a slight anticyclonic foehn off the Cotswold's towards Cheltenham (Martin, 2005). A foehn is a strong downslope wind that introduces

warmer air to lower elevations on the lee side of mountains (Elvidge and Renfrew, 2016). It is the result of drying and warming of observed downwind after moisture has been lifted from upwind air after turbulent mixing. The downwind air is relatively dry owing to removed moisture and latent heat from the condensation of water (Linacre and Geerts, 1997; Elvidge and Renfrew, 2016). To place this in context, Cheltenham is situated within a 'basin', surrounded by escarpments to the east of Cheltenham. Escarpments are steep slopes that occur from erosion and faulting which separate two relatively level areas of differing elevations (Monkhouse, 1995). The topography, therefore, predisposes Cheltenham to the foehn effect, the meteorological effects of which are dry adiabatically heating on the downwind side. This results in warm, dry wind on the downward side towards Cheltenham. Therefore, warmer temperatures at lower elevations induce further warming in and around Cheltenham.

### **2.1.2 UK Heatwave Events Since 1990**

Within the 13-year period in which Cheltenham held the British maximum, there were two subsequent major heatwave events recorded within the UK in 1995 and 2003.

The 1995 heatwave occurred during late July and late August following a smaller heatwave event in late June, and it was recorded as one of the warmest summers and Augusts in many locations throughout the UK (Met Office, 2017). A key driving mechanism of this heatwave was the dry conditions in the UK. In the summer of 1995 (Webb and Meaden, 2000) 19 weather stations in the UK recorded less than 50% of their average rainfall, with some locations recording less than 20%. During the heatwave, many locations recorded peak temperatures at the start of August. The highest temperature recorded was 35.2°C on 1<sup>st</sup> August in Boxworth, Cambridgeshire (Webb and Meaden, 2012), and towards the end of the heatwave

event, many locations recorded average temperatures of around 30°C. Of the 19 stations outlined by Webb and Meaden (2000) Cheltenham recorded three consecutive days with a temperature of 32°C from 20<sup>th</sup> – 22<sup>nd</sup> August, with the highest temperature reaching 33.6°C on August 22<sup>nd</sup>.

In 2003 the UK experienced another heatwave event; this heatwave was one of the hottest summers in UK history and was experienced at a continental scale, affecting most of Europe and the British Isles (Met Office, 2019). High-pressure systems persisted over most of Western Europe and these anti-cyclonic conditions introduced a dry, tropical continental air mass to the UK (Burt, 2004). A cold front movement from Iceland progressed southeast over England, slowly losing intensity before weakening over the English Channel, intensifying the effects of the high-pressure system that dominated the UK (Burt, 2004). Although the effects of the heatwave were widespread over the UK, daily maximum temperatures recorded highs of 38°C predominantly within the London metropolitan area southeast of England.

Temperatures in the southeast of England exceeded 32°C on three consecutive days between August 4<sup>th</sup> – 6<sup>th</sup>, and a further five consecutive days between August 8<sup>th</sup> - 12<sup>th</sup>. On 10<sup>th</sup> August 2003, Faversham, Kent recorded the highest temperatures in the UK, 38.5°C, which exceeded that held by Cheltenham since 1990.

Gloucestershire experienced high temperatures as a result of the heatwave, but maximum temperatures only reached ~32°C (Burt, 2004).

Since 2003 there have been a further five heatwave events recorded in the British Isles (Kendon et al., 2020; Beckett and Sanderson, 2021) in 2013, 2018, and 2019 with two events occurring in 2021. The effects of the heatwaves recorded maximum temperatures of 33.5°C, 28.1°C, 34°C and 31.6°C respectively, all occurring within the London area (Met Office, 2021).

## 2.2 Global Energy Exchange and Energy Balance

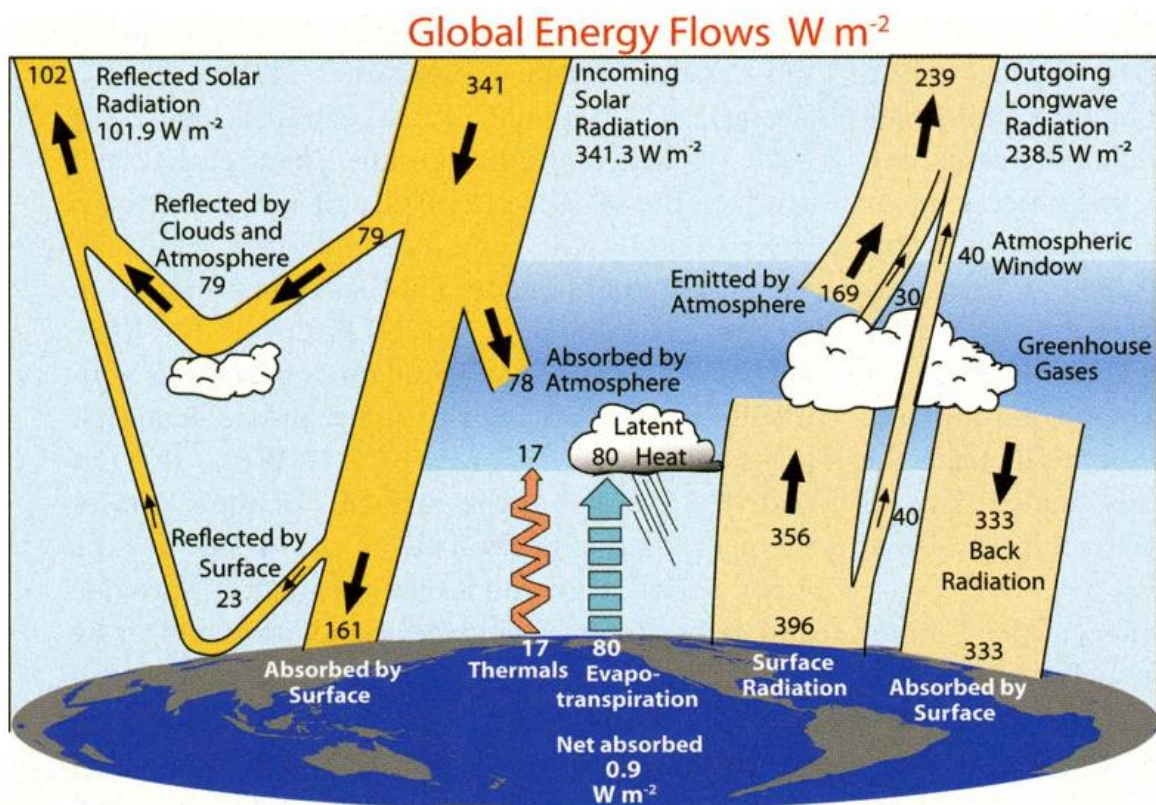
Heat can be transported to and from a system in three ways, radiation, conduction, and convection. Radiation is both a form of energy and a means of transfer, with this energy travelling in the form of waves at the speed of light ( $300 \times 10^6 \text{ m s}^{-1}$ ) (Stewart and Mills, 2021). Conduction occurs by molecular action and is slow; the speed of sensible energy transfer through a medium depends on its conductivity (Robinson and Henderson-Sellers, 1999). Convection describes the exchanges that occur as a body of air and their properties mix. This term is typically used to describe the vertical mixing of sensible heat (Robinson and Henderson-Sellers, 1999). The transmission of energy from the Sun to the Earth is almost entirely radiative. Some mass flux is associated with particles of solar wind, but the amount is too small to have a measurable effect on Earth's surface temperature (Hartmann, 2009).

The Earth's climate is largely driven by its energy budget (Liang et al., 2019), this is the balance between incoming radiation that reaches Earth from the Sun and the energy that flows from Earth back out to space. To understand the energy balance of the Earth the first law of thermodynamics must be defined, this states that the heat added to a system is equal to the change in internal energy minus the work extracted (Hartmann, 2009); energy cannot be created nor destroyed, it can only be transferred from one state to another.

Incoming solar radiation interacts with both the Earth's surface and the atmosphere (Robinson and Henderson-Sellers, 2009), summarized in Figure 2.1. The Earth-atmosphere system is constantly trying to maintain the balance between incoming and outgoing radiation. Upon encountering a medium, radiation can be transmitted, absorbed, or scattered (Stewart and Mills, 2021). The absorption of incoming radiation occurs mostly at the Earth's surface, whereas most of the emissions in the



atmosphere are scattered (Hartmann, 2009). Absorption results in heating, with the ability to absorb being equal to the ability to emit, i.e. the emissivity (Stewart and Mills, 2021). Dependent on the medium the radiative properties (i.e. the object's albedo and its emissivity) vary (Oke et al., 2017). Albedo is the proportion of light reflected from a surface (Perkins, 2019). On a global scale, Earth is a patchwork of dark and light surfaces, which varies from highly reflective ice caps and clouds to less reflective, dark surfaces such as lava beds (Perkins, 2019). On average, 30% of sunlight is reflected back to space from Earth. On a more local scale, the properties of urban and natural landscapes consist of a matrix of varying surfaces with differing reflective and emissive properties (Oke et al., 2017; Stewart and Mills, 2021).



**Figure 2.1:** The global annual mean energy budget for Earth and its interactions. Broad arrows indicate the flow of energy in proportion to their importance (Trenberth et al., 2009).

## **2.3 Driving Mechanisms to the UHI**

Both natural and artificial driving mechanisms contribute towards increased urban temperatures and affect the intensity of the UHI. These range from alterations in the natural and artificial landscape, reduction of the natural landscape, urban form, fabric and function, urban geometry, anthropogenic interactions, weather, and geography (Oke et al., 2017; Oke, 1985, Stewart and Mills, 2021, Nuruzzaman, 2015, NOAA, 2021). These will be covered in this section.

### **2.3.1 Natural Driving Mechanisms**

Natural factors can have a direct impact on both global and local climates. Solar intensity, which is the amount of solar radiation that reaches the surface (Robinson and Henderson-Sellers, 1999), is dependent on latitude, terrain, season and atmospheric conditions (Oke, 2017; Robinson and Henderson-Sellers, 1999). High solar intensity is a key natural contributor of localized heating (Burt, 1992). Solar azimuth is the given angle of the Sun relative to its position at a given place on Earth (Martinez-Gracia et al., 2019) and changes in this can affect local changes in climate, with a higher zenith angle creating a higher concentration of solar energy on the surface (Burt 1992; Stewart and Mills, 2021); which has been noted as a possible cause of the 1990 heatwave.

Solar cycles also affect the environment and exacerbate UHIs. These are 11-year cycles which mark variations in the number of sunspots on the solar surface and have been attributed to fluctuations in solar output (Linacre and Geerts, 1997). The immediate source of energy to heat the Earth is solar radiation; shortwave radiation (light and ultraviolet) passes through the atmosphere and is absorbed and re-radiated from the ground as longwave radiation (infrared) (Stephens and L'Ecuyer, 2015). The long-wave radiation is one of the key contributors to the heating of

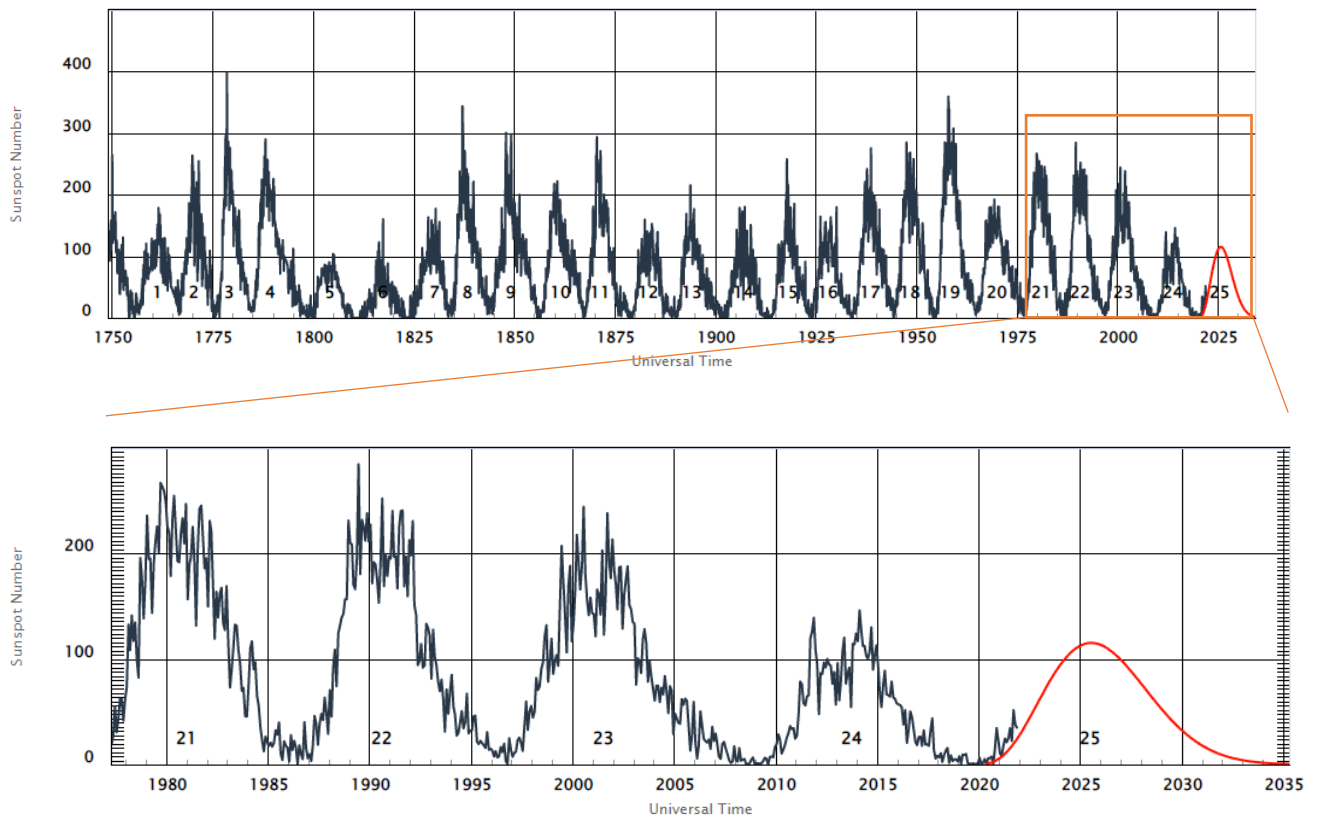
surfaces and urban environments. Changes in received net radiation through fluctuations in solar intensity or solar cycles affect the energy balance. These factors have been considered a putative driving mechanism of UHIs owing to direct and diffuse radiation and the interactions with the radiative properties of the urban environment (Liang et al., 2019; Oke, 2017; Stewart and Mills, 2021).

In urban areas, solar radiation is absorbed through low albedo surfaces and buildings at both global and local scales, this results in increased absorption of radiation which is re-emitted in the form of latent heat. The radiative properties of urban constructs forces air temperatures to increase within the built-up environment. The latent heat varies depending on the heat capacity of the material and its radiative properties (Oke et al., 2017). Within urban environments incoming radiation is trapped, reflected, and re-emitted resulting in localized heating (Stewart and Mills, 2021; Oke et al., 2017) known as the *urban canyon* effect (Oke et al., 2017).

Furthermore, the form and function of cities (i.e. the street geometry) can cause a lack of vertical mixing and transportation of heat, further amplifying urban air temperatures within the canopy layer (Ningrum, 2018).

Solar sunspot cycles refer to the number of observed sunspots on the surface of the Sun (Linacre and Geerts, 1997), the cycle from 1750 to present day is shown in Figure 2.2. Sunspot cycles are typically cyclical in nature as they increase and decrease in strength over time. The temporal behaviour of a sunspot cycle is described by international sunspot numbers with four parameters: starting time, rise time (duration), asymmetry (the result of fast-rising and declining of peak intensity), and amplitude (strength) (Hathaway et al., 1994). They have been associated with increased solar activity, increased outgoing solar radiation, and solar flares (Liang et al., 2019), which can impact the energy balance and thus air temperatures.

Although, the relationship between solar intensity, sunspot cycles, and natural processes have been explored in regard to their relationship with the energy balance and local and global changes in climate over time, natural processes such as solar sunspot cycles have not been recorded in the contribution of UHIs but have a dominating effect on global and local climate.



**Figure 2.2:** Sunspot cycle graph mapping the observed (black line) and predicted (red line) solar cycle, measured through observed sunspot number (NOAA, 2021). Insert highlights contemporary solar cycles (21-25). The black line represents the monthly average observed sunspot number. The forecasted sunspot numbers are outlined in red, depicting the predicted values for solar cycle 25 (NOAA, 2021).

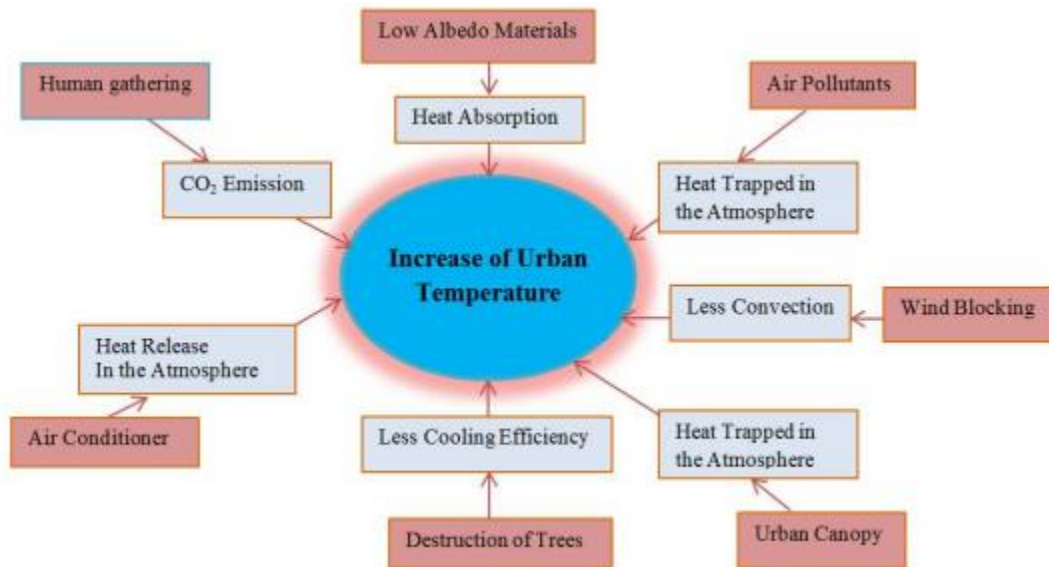
Radiation at the Earth's surface is not distributed equally, the amount of radiation received by the Earth from the Sun is governed by the geometry of Earth's motions (Linacre and Geerts, 1997). The combined motions of Earth's diurnal and annual revolution around the Sun cause daily and seasonal changes in the receipt of solar

radiations at different latitudes (Oke et al., 2017). Placing this in context of the UHI, daytime radiation surplus at the surface is conducted in the form of sensible heat or convected by turbulent transport into the lower atmosphere. At night, these processes are reversed, where the surface becomes a net emitter of radiation and the surface cools forming a temperature inversion (Oke et al., 2017; Stewart and Mills., 2021), resulting in higher nocturnal UHI temperatures when compared with the daytime UHI.

The variation of incoming solar radiation at different latitudes varies the angle of incoming solar radiation, which influences temperatures at higher or lower latitudes. At higher latitudes, the angle of solar radiation is dissipated over a larger area, resulting in lower surface temperatures. Conversely, the radiation received at lower latitudes lead to higher temperatures owing to higher concentrations of received solar radiation, as radiation is dissipated over less area (Linacre and Geerts, 1997; Robinson and Henderson-Sellers, 1999). Therefore the UHI maximum tends to increase from low to high latitudes. (Wienert and Kuttler, 2005). Factors such as the time of the day, season, atmospheric and geographic features, and land surface types influence the intensity of receipt solar radiation at the Earth's surface (Matzinger et al., 2003; Ayoola et al., 2014). Although, natural driving mechanisms such as solar radiation and variations in latitude have a confounding effect on both temperatures and UHI, it appears that in relation to Wienert and Kuttler (2005), anthropogenic activities have a more profound effect on UHI intensities.

### **2.3.2 Anthropogenic Driving Mechanisms**

Anthropogenic activities change atmospheric composition and are considered a key factor in the contribution of UHIs, these can be summarised in Figure 2.3.



**Figure 2.3:** Visual summary of the anthropogenic factors that can exacerbate urban heat islands (UHIs) (Nuruzzaman, 2015).

Modifications to the environment that affect local UHI intensity include reduced albedo, lack of vegetation, increased surface roughness, larger surface areas, heat fluxes from buildings and vehicles (Oke et al., 2017; Naruzzaman, 2015), and radiation trapping in urban canyons (Oke, 1985) owing to building geometries. This heat is reflected by taller buildings which are known as the urban canopy (Masson, 2006). The presence of buildings results in the blocking of wind velocity (Naruzzaman, 2015). This results in the reduction of convective processes which lessens the degree of cooling processes and the vertical mixing of warmer air (Privadarsini, 2008). Additionally, with increased urbanization, mass deforestation takes place to meet demands for urban facilities (Nuruzzaman, 2015); trees intercept solar heat, decrease heating due to increased surface roughness, and absorb carbon dioxide (CO<sub>2</sub>) through photosynthesis, therefore cooling the environment (Akabari et al., 2001; Oke et al., 2017). Alterations to the convective processes within urban environments owing to multi-layer buildings increases the net warming

effect experienced within urban environments, having a confounding effect on both boundary layer and canopy layer UHI (Oke et al., 2017).

The albedo of a city varies on the arrangement of surfaces, orientation, and emissive properties of materials (Bouyer et al., 2009; Oke et al., 2017). Urban environments typically have a lower albedo than their surrounding rural environments (Basset et al., 2017); lower albedos result in greater heat absorption as they store more solar energy, thus increasing the relative urban temperature.

Human gathering is prominent within city centers, the influx of population gathering relates to increased concentrations of CO<sub>2</sub> emissions. The increased concentrations of CO<sub>2</sub> in urban areas further trap heat causing localized atmospheric heating (Nuruzzaman, 2015). The consequence further exacerbates the formation, magnitude and extent of the UHI. Increased aerosols from greenhouse gas emissions and air pollutants can also contribute towards increased urban temperatures. As cities grow, the increase in emissions from industrial processes, domestic heating and transport using fossil fuels causes the UHI effect becomes stronger, creating an artificial heating trend within urban environments (Nica et al., 2019). Lim et al. (2021) states that climate warming will increase already high temperatures in heat island areas.

Furthermore, pollution and increased aerosols result in the increased trapping of direct and diffuse solar radiation within the urban canopy and boundary layer (Bose, 2009). Increased trapping of solar radiation, results in increased temperatures and by extension increased UHI intensity (Nuruzzaman, 2015). Moreover, air conditioners provide cooling within buildings, however, release heat into the

atmosphere (Okwen, 2011). This release in net heating to the atmosphere results in increased atmospheric temperatures.

The temporal and spatial characteristics of the UHI vary with changes in local urban form and function. Local meteorological conditions and geography of an area affect the magnitude of an UHI (Bassett et al., 2017). By extension, population was originally a surrogate measure of the population density associated with UHI intensity (Oke, 1973). Marx (1981) research into cities, buildings and the environment, postulates the theory of urban metabolism to explain this. It is the exchange of materials and energy between nature and society. The concept derives from the desire to quantify urbanization to change and improve relationships between socioeconomics and nature. The combined effects of these changes have recently been estimated to account for  $40\% \pm 16\%$  of the human-caused global radiative forcing from 1850 to the present day (Hibbard et al., 2017). In a review of studies quantifying temperatures in urban areas, Hibbard et al., (2017) predicts that the heat island effect will strengthen in the future as the structure, spatial extent, and population density of urban areas change and grow.

In summary, processes of industrialization, urbanization and the burning of fossil fuels affect the environment owing to intensive and insufficient use of resources in building and modifying urban infrastructure in towns and cities. Furthermore, the contribution of aerosols and anthropogenic interactions with the environment and atmosphere provides means for increased temperatures in urban environments (Naruzzaman, 2015). Changes in land use and land cover due to human activities produce physical changes in land surface albedo, latent and sensible heat, and atmospheric aerosol and greenhouse gas concentrations (Hibbard et al., 2017). The changes to land type and function result in changes to the surface properties.



Surfaces that were once moist and permeable become more impermeable and drier through the process of urbanization. Impermeable surfaces refer to surfaces that do not allow water to penetrate, in contrast, permeable surfaces are porous surfaces that allow water to percolate into the soil and recharge the water Table (Collins, 2007). Due to the heat-absorbing qualities of urban constructs and paving materials, sites with higher ratios of impermeable surfaces increase ambient air temperatures and require more energy for cooling (McGrane, 2016; Collins, 2007). These interactions have a profound relationship with the energy balance of urban environments and thus result in positive forcing effects which exacerbate UHI intensity.

#### **2.4. Urban Heat Islands (UHIs)**

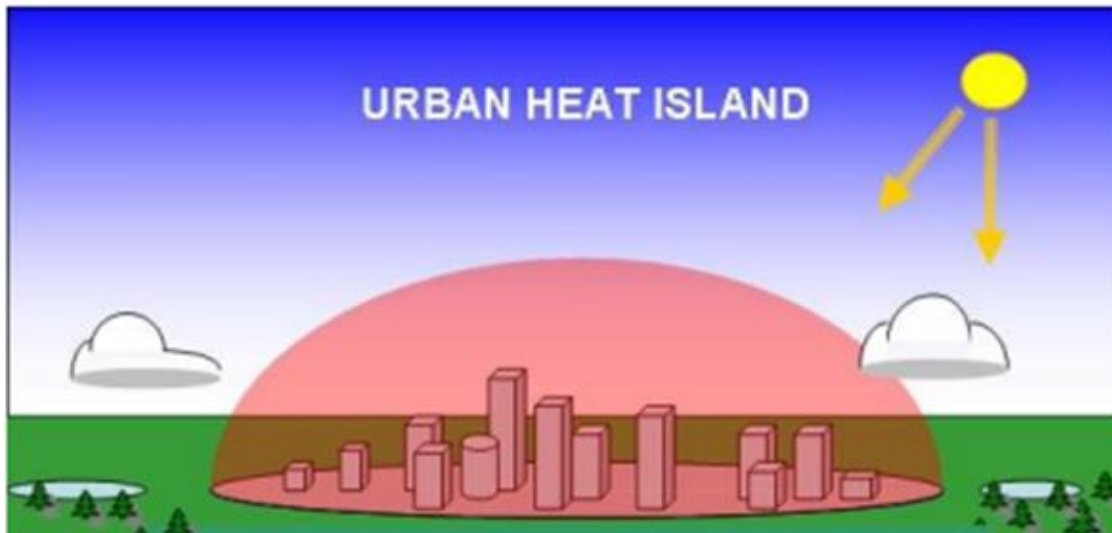
Most cities and towns exhibit UHI effects relative to predevelopment conditions (Aremu et al., 2017). The individual intensities of the UHI experienced for each locality depends on several factors; these include, geography, topography, land use, population density, and physical layout (Aremu et al., 2017).

Urban and suburban areas experience increased temperatures when compared with their rural counterparts, with urban-rural air temperature differences ranging between 1°C – 3°C for populations with one million or more (EPA, 2008; Oke, 1997) and in rare circumstances, under optimum conditions (clear, calm nights), can reach up to 12°C (Oke, 1987). Even smaller towns and cities produce UHIs. Cardoso et al., (2017) investigated the urban morphology and land cover of three small to mid-size cities in Brazil to determine their influence on UHI magnitude and found that UHIs can develop regardless of city size. Through analysis of their temperature profiles, they verified that built density is a key contributor to UHI magnitude, whereas vegetation is related to lower temperatures. Their research shows UHI magnitude

varied between 1.3°C (for increased vegetated areas) to 3.5°C (for increased urbanized areas – commercial buildings). However, Peng et al., (2019) and Oke (2006) both agree that there is a focus on UHIs in both cities and mega-cities in the literature.

UHIs are caused by several factors, including anthropogenic causes like energy emissions from industrial activities, vehicles, the heat capacity of buildings and the ratio of the number of mixed surfaces (EEA, 2013; Tursilowati et al., 2018). Energy emissions refer to the release of aerosols and gasses within the canopy and boundary layers, which interact vertically with the atmosphere. Almost all hotspots have a lack of vegetation or greenspace (Effat and Hassan, 2014).

As urban areas develop, the resulting changes in the landscape and their infrastructure reduce the degree of open land and vegetative cover. Alterations to the natural and artificial environment change the reflective and emissive properties, increases in urbanization and anthropogenic functions, therefore increasing the specific heat capacity of the urban environment (Oke, 2017). This increased heat capacity in tandem with changes in the albedo and emissive properties of the urban environment leads to net warming as incoming solar radiation in the form of longwave radiation is trapped within the urban environment and re-emitted later leading to thermal inversion (Oke, 2017; Stewart and Mills; 2021). This thermal inversion results in increased temperatures owing to the trapping and releasing of heat (Figure 2.4).



**Figure 2.4:** Visual representation of and UHI (Tursilowati et al., 2018). The figure represents a 'dome' of increased heat over urban environments which dissipates outwards towards the cooler rural surroundings.

Figure 2.4 shows the phenomenon as 'an island' or 'dome' in which hot surface air is concentrated in urban areas, with surface or air temperatures decreasing towards the suburban and rural areas. Changes in landscape and urban infrastructure cause changes to the radiative energy balance, which leads to radiative forcing of the microclimate. The concentration of solar radiation, lack of vegetation and evapotranspiration in the urban environment causes cities and towns to remain warmer than their surrounding rural areas. The energy stores itself within the heat capacity of surfaces and constructs, releasing its energy over time. The increased trapping of outgoing radiation owing to low albedo, evapotranspiration and increase in anthropogenic heat flux (Akbari et al., 2001; Oke, 1987) as anthropogenic or solar radiation is absorbed and not radiated back into space. This process of energy release is most notable within diurnal cycles when heat energy is released from surfaces and constructs during nocturnal hours.

Buildings and urban development affect the local micro-climate. Local climatic changes owing to UHIs differ from global climate change, as their effects and

magnitude are limited to a small scale. The magnitude of a heat island's impact decreases the further away from its epicentre. Although there is a difference in global and local climate change, climate change typically refers to global mean surface temperature, whereas local climate change refers to the internal variability of temperature and weather of a city or area (Wake, 2015; Karlický et al., 2020). Climate change can exacerbate the effects and magnitude of UHIs. According to Kirtman et al., (2013), modelling the projected changes in extreme weather and air pollution indicate heatwaves are very likely to become more frequent, and intense and last longer in the future. Feedbacks from local emissions, aerosols and changes in vegetation can increase impacts during heat wave events (Lee et al., 2006).

#### **2.4.1 Types of UHI**

It is important to distinguish the difference between the different types of UHI.

Although the UHI is a collective term used to describe the difference between urban and rural temperatures, each sub-type follows different methods of investigation and differences in the definition of the UHI itself. Oke (1995) notes that there are several distinct sub-types of UHI: Sub-Surface, Surface, Canopy Layer and Boundary Layer.

Sub-surface UHIs exist underneath the surface of the Earth. They are affected by the combined effects of ground heat flux, heat flow from the Earth's interior, thermal properties of soil and anthropogenic stimulation from overlying urban infrastructure (Menberg et al., 2013). Temperature measurements from 40 monitoring wells measured sub-surface UHIs in Manitoba, Canada showed that sub-surface UHIs typically extend between 50 – 150 metres below the surface and are typically observed and measured through indirect measurements taken through the use of monitoring wells situated within the ground (Ferguson and Woodbury, 2007). From

this work, they propose sub-surface UHIs to be the result of underlying heat flow mechanisms correlating to the variability in the above land use.

Surface UHIs are defined as the increased temperatures in urban areas when compared with their rural surroundings (Oke, 2017) measured through indirect measurements, typically identified through remote sensing methods that observe land surface temperatures as opposed to air temperatures (Sobrino et al., 2003). More specifically, thermal remote sensors observe the surface heat island and observe spatial patterns of upwelling thermal radiance received by the detector and use it to estimate thermal surface temperatures (Voogt and Oke, 2003). At sufficient heights, the observed urban surface consists of differing constructs such as rooftops and streets. At lower heights, observations can be seen to depict walls and structures, from an oblique perspective. Surface UHIs are present at all times during the day and night. However, they are most intense both spatially and temporally during the day and in summer periods. The assessment and analysis of this heat island varies on how representative these observations are.

The magnitude of surface UHIs varies seasonally owing to changes in solar intensity and are typically largest in the summer (Oke, 1982). As mentioned, the main driver in the energy balance is the Sun and incoming solar radiation and intensity. Factors such as urban function or street geometry, exposed urban surfaces and changes in weather have a direct influence on temperature changes in urban areas (Oke, 1982).

The temporal and spatial characteristics of the UHI vary with changes in the local urban form and function (Oke, 1995; Stewart and Mills, 2021). Urban function relates to the rudiments which shape the morphological characteristics of urban space; its location, size and shape (Živković, 2018), once of the key elements of this is the

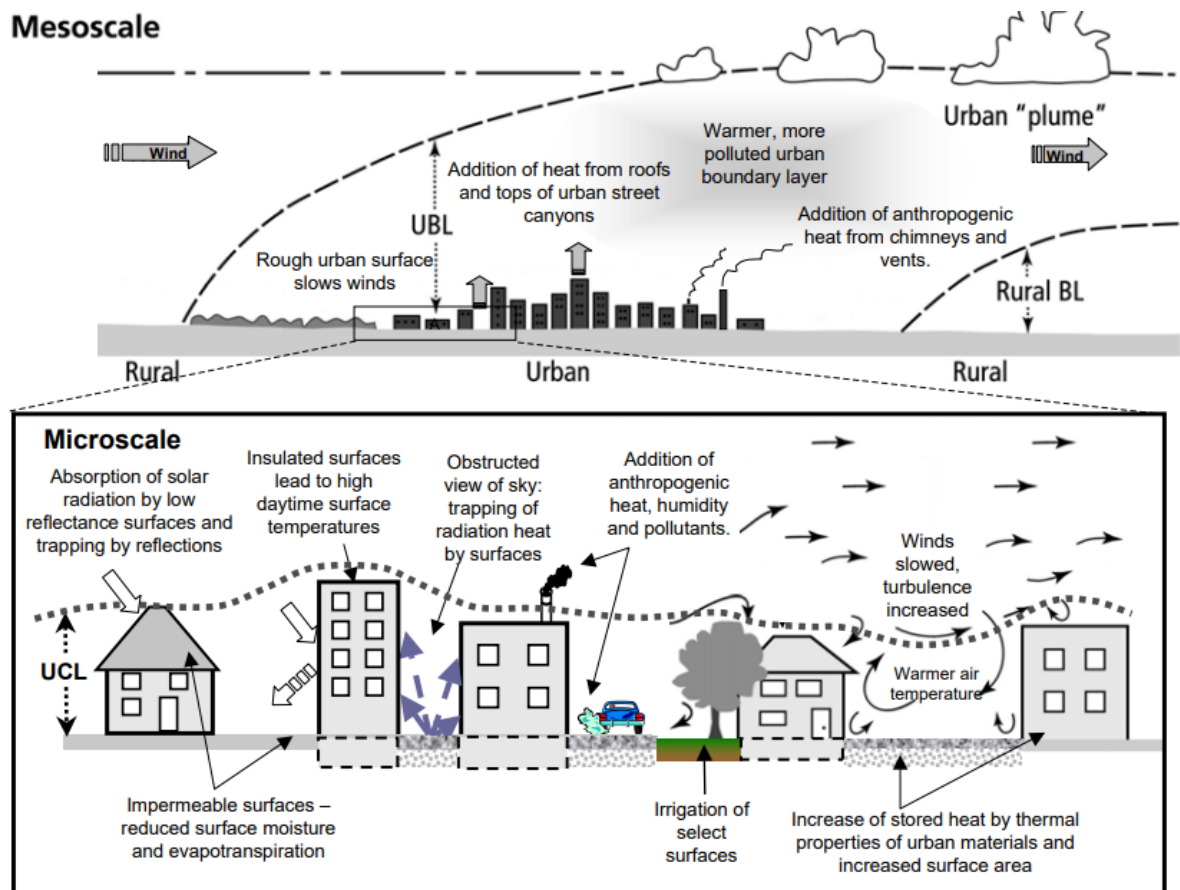
street geometry. Street geometry has several distinct impacts on energy exchanges within the canopy layer; it causes shortwave radiation to be reflected multiple times before exiting the canyon and longwave radiation to be emitted from one facet to another (Stewart and Mills, 2021), thus, increasing the direct absorption of radiation, resulting in increased temperatures. Street geometry also reduces near-surface airflow (Stewart and Mills, 2021) and the vertical mixing of air, which means that there is a lack of evapotranspiration and wind to transport heat away from the urban environment (Oke et al., 2017; Ningrum, 2018). Research by Nunez and Oke (1977) measured net radiation fluxes at walls of north-south orientated alley in Vancouver over a summer. The results of the study support the concept that the urban canyon has profound effects on the surface energy balance and by extension, the energy exchange and fluctuations in temperature.

Typically, rural areas or areas with a high moisture content or shade cover remain closer to average recorded air temperatures while urban areas mark higher recorded temperatures. Thermal remote sensors observe the surface heat island and the display of spatial patterns of upwelling thermal radiance received by the detector. The observations recorded can then be used to calculate and estimate thermal surface temperatures for an area (Voogt and Oke, 2003).

The main focus of this study is the investigation of the atmospheric UHI, which are measured through direct measurements, typically identified through fixed weather station methods (Steenveld et al., 2011). Atmospheric UHIs are defined as areas of warmer air in urban areas as compared with cooler air in rural surroundings (Macintyre, 2017). Professional meteorological networks provide objective, indirect measurements of local weather and climate and can be supplemented by hobbyist

weather stations, which can provide high-resolution data and fill gaps within the network coverage (Steenveld et al., 2011).

Atmospheric UHIs can be divided into two categories: Canopy and Boundary Layer UHIs (Figure 2.5). The Canopy Layer UHI (known from hereon as CUHI) exist in the layer of air that is occupied by humans (Stewart and Mills, 2021). They are defined as the area from the surface to approximately mean building height (canopy) (Fabrizi et al., 2011) The Canopy Layer is the most commonly measured form of heat islands and is often the one in which the key definition of UHI derives from (Oke, 1982). It appears at the surface and throughout the lower atmosphere from the canopy to the boundary layer (Rao 1972; Oke, 1976). Grounding it within the energetic basis, the underlying physics of the UHI imply that it exists anywhere that humans have urbanized land surface in a manner that perturbs the surface energy budget from its natural background (Smoliak et al., 2015; Nunez and Oke, 1977).



**Figure 2.5:** Processes of urban heat islands (UHIs) for the Urban Boundary Layer (mesoscale) and the Urban Canopy Layer (microscale) (Ningrum, 2018).

The Boundary Layer UHIs extends from rooftop height upwards to where the urban landscape no longer influences the atmosphere (Figure 2.5). This region typically extends up to 1.5 km (1 mile) above the surface (Oke, 1982). According to Fabrizi et al., (2011), the boundary layer extends approximately 1 km in thickness or more during the daytime and shrinks to hundreds of metres or less at night owing to heating and cooling processes of the urban atmosphere. Similarly, they are measured through air temperature data from fixed or mobile stations. Data typically compare the urban-rural difference in temperature. Observations of each type have distinct and varying methodologies, incorporating the use of stationary points to



mobile traverses for Canopy Layer UHI, infrared and remote sensed for Surface and Sub- Surface UHI, and for Boundary Layer, the use of radiosonde data (Oke,1995).

The UHI is dependent on several climatic processes, these being wind speed, solar radiation, cloud cover and resultant anthropogenic interactions (Figure 2.5), the influences and interactions for the boundary and canopy layer are synonymous. The processes that affect the Urban Boundary Layer at a mesoscale are dominated by higher thermal inversions during the daytime. In contrast to this, the Urban Canopy Layer is affected by processes at the microscale as lower altitude inversion is prevalent during the night-time (Ningrum, 2018). At microscale, incoming solar radiation is absorbed by low-reflectance surfaces and trapped by reflections of urban constructs. In addition to this, aerosols and pollutants from anthropogenic activity trap further, incoming net radiation and by extension increase localized heating within urban environments.

Feedbacks at a microscale contribute to observations made at mesoscale. At mesoscale, the interactions of increased surface roughness of the urban surface lead to a slowing of wind speed due to increased turbulence (Figure 2.5). Reduced wind speeds result in warmer air temperatures due to the lack of thermal mixing (Oke, 2017). Anthropogenic emissions contribute to the mesoscale further, resulting in an urban plume, and a build-up of pollutants and aerosols which further exacerbate urban warming due to the trapping of net heat and radiation.

## **2.5. UHI Intensity**

UHI intensity within the canopy layer is defined as the difference between the urban and background rural temperatures (Basset et al., 2017). These temperature

differences are dictated primarily by the configuration of urban environments under study and the effects of the local meteorology.

Extended urban areas consisting of several towns merging with the suburbs of a central area or city are defined as conurbations. UHIs are most pronounced under anticyclonic conditions, which influence and emphasise the differential heating and cooling rates between urban and rural areas (Basset et al., 2017; Burt 1992). The increased extension of urban areas through conurbations emphasises the effects and magnitude of the UHI with a significant increase in anthropogenic changes to the landscape.

### **2.5.1. Calculated UHI Intensity**

UHI intensity is calculated by subtracting the recorded air temperature at a reference rural station from the air temperature recorded at an urban station (Stewart, 2011). This variable is either measured in degrees Celsius (°C) or Kelvin. The calculated UHI intensity describes quantitatively the increased air temperature of either the urban surface or the urban atmosphere compared to its rural surroundings owing to increased or increasing anthropogenic activities (Oke, 1987; Voogt, 2004).

### **2.6. Analysis and Visualization of the UHI**

A climate element is one of the various properties of the atmosphere that can specify the state of weather or climate at a given place and time (Linacre, 2004). It is not possible to measure climate, only the individual variables that comprise it, such as air temperature, cloud cover, precipitation, radiation, sunshine duration, and humidity (Oke, 2006; Jin, 2012; Basato et al., 2014). These variables can be extrapolated from weather stations at each locality and trends inferred between them to produce high-resolution maps.

Traditionally, the CUHI is quantified through observations from one or few sites over urban and surrounding regions using air temperature data from screen-level weather stations (Jin, 2012). A variety of approaches can be used to analyse and visualize the UHI such as fixed weather stations, mobile transverse surveys and remote sensing (Xu et al., 2016; Min et al., 2019). Stationary surveys involve air temperature sensors placed at fixed points in or around a city whereas mobile surveys are carried out over urban-rural transects. To evaluate the CUHI weather stations with either a minimum of two (one urban, one rural) stations or a network of multiple stations are required (Stewart and Mills, 2021).

Fixed station surveys focus on short-term data to assess UHI (Busato et al., 2014). However, Stewart and Mills (2021) argue that if stations are fixed for long periods of time, extending months to years, the outputs can be used to analyse the climatology and changing magnitude of the CUHI.

Geographic Information Systems (GIS) applications can be used to perform spatial analysis of meteorological data. Typical analysis of the UHI using GIS produce overlays of temperature patterns in the form of isotherm maps or UHI heatmaps which can explore the spatial extent and magnitude of the UHI. Further analysis of this can be carried out through correlation analysis between UHIs and land changes. In conjunction with this, the Urban Canopy Layer can be modelled in GIS using data acquired from weather stations (Sakakibara and Matsui, 2005). More complex analyses can produce multi-dimensional spatialization (Bottyan and Unger, 2003) through the accompaniment of different environmental information such as climate and terrain as potential predictors for the UHI (Svensson et al., 2002).

Remote sensing methods enable the analysis of the UHI on larger scales, which can provide information to improve the understanding of the UHI and its effects (El-Hattab et al., 2018). According to Tian et al., (2021) typically carried out using a variety of satellite thermal bases images such as MODIS Landsat-TM to study and quantify different land classifications and spatial coverage of the study area and identify and evaluate the UHI through thermal channels.

UHIs can be quantified and modelled using climate models. An advantage of modelling of UHIs can be used to simulate building performance (energy consumption, heat capacity and thermal emissivity), from a range of inputs. These inputs include building materials and geometry, street geometry, shading, ventilation, heating and cooling load and location and climate (Macintyre, 2017). However, many climate models are not efficient enough to be able to run fine enough spatial scale models that can capture detailed characteristics. Regional scale simulations or projections make it possible to run models at finer spatial/regional scales to project the effects and magnitude of urban surfaces on atmospheric or surface temperatures.

## **Chapter 3: Methods**

### **3.1 Introduction**

This research is based solely on the use of secondary data. Secondary data analysis offers methodological benefits that can contribute to research by generating new knowledge (Heaton, 2008; Johnston, 2012). This employs opportunities for researchers to replicate, re-analyse and re-interpret existing research and data collected from pre-existing studies and samples of data (Johnston, 2014). Although it is not without its issues, secondary data within the field of environmental sciences permit the ability to test new ideas, theories, frameworks and models of research design (Johnston, 2014). One of the main limitations when using secondary data is miscommunication in the methods of how data were collected and processed, unless effective metadata is provided or readily available (Perez-Sindin, 2017).

The research design for this study employs a quantitative methodology. Quantitative research is about quantifying the relationships between variables through numerical, empirical data (Linacre, 2004). The data sources and methods will now be outlined.

### **3.2 Weather data**

Weather data for this project was derived from the UK Meteorological Office MIDAS weather stations, which are taken from the Centre for Environmental Data Analysis (CEDA) archive. These secondary data have a high temporal resolution, recorded daily at 24-hour max/min values (Met Office, 2021) with extensive historical records dating back to 1901, recording a range of meteorological variables (Fabrizi et al., 2011). Depending on the availability of data (temporally and spatially) and sensors for fixed weather stations, data recorded include: precipitation; mean, minimum and maximum air temperature; humidity; mean wind speed and direction; cloud cover; incoming solar radiation; and soil temperature. Although these stations can record

and collect high temporal resolution data, the data are limited to one geographical point. Weather patterns can be compared to evaluate links and patterns of existing environmental conditions with the UHI effect (Arnfield, 2003). Several evenly distributed weather stations would be required to interpolate an accurate thermal isomap of a region over a set period of time, and long-term trends can provide diurnal, seasonal, annual and decadal trends. In this study, metadata for MIDAS weather stations are not readily available, scattered amongst several archives and limited by permissions required to view said data.

Cloud cover and precipitation data were provided as a gridded time-series dataset containing cloud cover (%) and precipitation (mm) interpolated for the UK covering the period 1901-2017. The data used within this study extracted values from 1990 to 2000 for the region of Gloucestershire and extracted monthly mean cloud cover and precipitation values pertaining to the study area.

The air temperature will be used to: (1) aggregate temperature data to perform monthly, yearly and decadal temperature profiles for each site and the region, and (2) two weather stations - one urban and one rural - will be used to investigate UHI intensity between 1990 and 2000.

To determine which weather stations to use for air temperature a set of criteria were used:

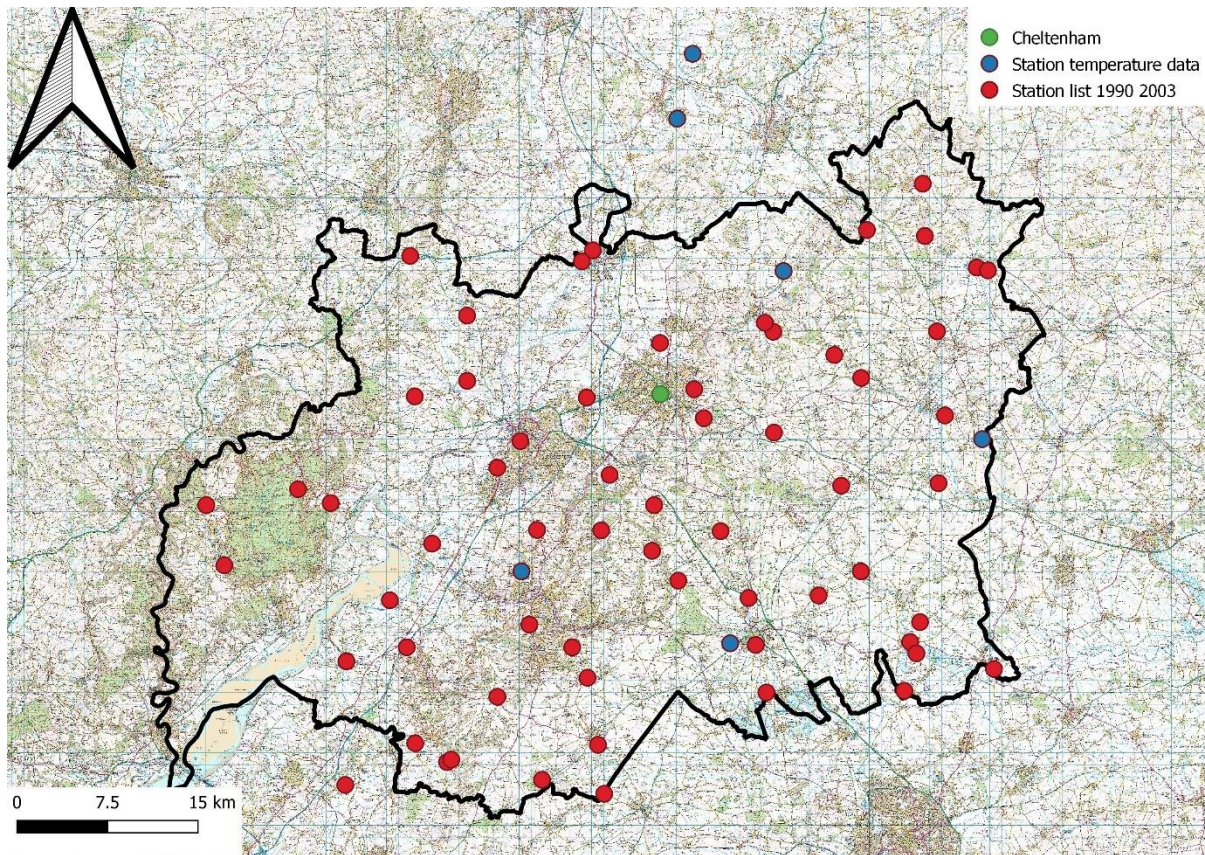
1. Weather stations must exist within or around the boundary of Gloucestershire and/or within 25 miles of Cheltenham;
2. They must measure air temperature;

3. They must have complete records between 1990 and 2000. There must be consideration of missing values to evaluate whether to use select weather stations or to omit them (Sui and Hart, 2012).

Preliminary investigations showed that sixty-six weather stations met the location requirements (Figure 3.1). All stations are situated ~ 2 metres above the ground, following World Meteorological Organization (WMO) guidelines (Oke, 2008).

Measurements are recorded automatically daily between 0900 and 2100 hours with an hourly frequency of data recordings. Following examination of the datasets this was narrowed down as only eleven of these stations contained any recordings of air temperature and only eight of them contained sufficiently long histories of air temperature data with ~90% or more complete data for 1990 – 2000 with a tolerance of 5% for missing data; following the guidance by Bennett (2001) that statistical analysis is more likely to be biased when more than 10% of data are missing.

Therefore, these seven ground-based weather stations were used (Figure 3.1 and Table 3.1).



**Figure 3.1:** Map showing all available weather stations within the study area (red) and those used within the study (blue). Contains OS data © Crown copyright and database right 2022; Crown copyright and database rights 2022 Ordnance Survey (100025252).

**Table 3.1:** A list of all MIDAS weather stations used within the study with reference to their ID, location, running time and completeness of data records.

Screen Id	Station	Start	End	Postcode	% Missing Data
687	Cheltenham	01/01/1874	31/01/2001	GL50 1	0.3%
688	Cirencester	01/01/1948	Current	GL7 6	6.0%
692	Little Rissington	01/01/1942	Current	GL54 2	14.4%
657	Pershore	01/01/1953	Current	WR10 2	9.8%
658	Pershore College	01/01/1952	Current	WR10 3	6.0%
682	Randwick	01/01/1989	01/03/2004	GL6 6	0.1%
691	Westonbirt	01/01/1976	Current	GL8 8	0.1%



### **3.2.1 Temporal analysis of the air temperature**

An analysis of the air temperature trends over varying timescales between 1990 and 2000 was done by creating an air temperature profile for each site. Daily air temperature data was imported into SPSS. Daily minimum and maximum air temperatures were transformed into a 10-year running average for each station to create a decadal temperature profile to show the average annual temperature profile change from 1990 to 2000 for each locality. A 10-year running average of the region was also calculated using the average of all daily air temperature (minimum and maximum) for each location to create a single, regional average for minimum and maximum air temperature. Daily and monthly air temperature trends at each station were also calculated to produce a time-series of daily mean air temperature for each site to produce a time-series plot of mean daily air temperature over time.

### **3.2.2 Interpolation of air temperature data**

Minimum and maximum air temperature data was aggregated and imported into QGIS. Inverse Distance Weighted (IDW) interpolation was then used to interpolate air temperature data from fixed weather stations. IDW interpolates unknown values for any geographic point based on averaging values of sample data from known points. The closer the known points are to each other, the more weight it has on the averaging process; however, there can be a reduction in the quality of the interpolation the more distance and unevenly distributed the points are from each other (Mitas and Mitasova, 2005). Owing to the distance between points, a distance coefficient of two was used; specifying lower distance coefficients gives more influence to points that are farther away, therefore resulting in a smoother interpolation and output (Menke, 2019). Experimentation with larger distance coefficients produced exaggerated interpolated temperature values, presenting

rougher interpolated values between each station. The output was reclassified into 10 equal interval classifications; these break down the range of data into equal divisions based on the number of classes defined (Kennedy, 2013). This number of classifications was decided as it complements the continuous data used and aids in visual inferences to be made about the data presented.

Owing to the requirements for the weather data (see Section 3.2) only seven stations were deemed to be suitable for use to investigate the UHI effect. Spatial interpolation is the process of using a set of point data to create surface data (Longley et al., 2005; Slocum et al., 2005). The point data used contains values for certain locations, within the study area. The surface data produced from the interpolation results in data values for every location inside the study area, regardless of whether it was sampled or not.

Within the context of this study, interpolation allows for illustrating regional air temperature. The output results in an accurate representation of air temperature across the study area, however, the resolution of the output is dependent on the number of points or stations available for interpolation. To expand, the interpolated surface produced using a low number of stations results in a reduced resolution output and decreases the detail and preciseness of the output, but the output still provides an adequate representation. However, with an increased number of stations present, the resolution of the surface output would be higher. Moreover, if a higher number of stations existed within a town or city, such as Cheltenham, a higher resolution output for a localized urban heat island would be able to be produced.

Another key limitation of this method is that sensitive to outliers. Outliers influence the output surface generated, whether this is a numerical or spatial outlier. It is by

this limitation that outliers from surrounding areas may have a confounding effect.

This issue can present itself in two ways (Longley et al., 2005). Firstly, the presence of other urban areas within the boundaries of the study area may produce bias in the surface generated. Secondly, the increased distance between two points increases the distance by which data are interpolated which further introduces bias in the surface generated.

Should more data points be available, the resulting surface produced through the method of interpolation would yield more precise and accurate results. The surface generated would be a superior representation of the urban heat island within the study area and potentially result in outlining how surrounding conurbations influence the heat island at greater spatial distances.

### **3.2.3 Urban Heat Island (UHI) Intensity**

There are different methods proposed to calculate the UHI effect. Some studies propose comparing urban temperatures against all surrounding temperature data (Ackerman, 1985; Ackerman and Knox, 2015 Hardin et al., 2017). However, the standard technique is to use a single urban and rural station to calculate the intensity or difference in temperatures between urban environments and their rural surroundings (Oke, 1973; Stewart and Mills, 2017; Hawkins et al., 2004; Hardin et al., 2017; Unger, 1996). Therefore, this is the method used in this study and will be determined following land cover classification (Section 3.3). Although, the main caveat noted from this method is that there is a notable variability that can arise from picking one dedicated station for each area (Basara et al., 2010).

$\Delta T_{(u-r)(\text{Min and Max})}$  was used to calculate the CUHI intensity for the two sites using minimum and maximum air temperature from 1990 to 2000.

Where:  $\Delta T$  is the change in temperature,  $T_u$  is the urban air temperature,  $T_r$  is the rural reference air temperature, and  $T_{Min}$  and  $T_{Max}$  are representative of the minimum and maximum air temperature values.

The results produced from this were tested against other meteorological and synonymous variables associated with changes in the UHI intensity using correlation and regression analysis. The extent and magnitude of the UHI was also calculated using the decadal air temperature data for all seven stations.

### **3.3 Land cover**

Local climate zones are defined as regions of uniform surface cover, structure material and human activity around a fixed point (Stewart and Oke, 2012), usually captured in field around existing weather stations. Typically, local climate zones (Oke, 2004; Sakakibara and Matsui, 2005) are used to calculate the different land classifications around weather stations (Siu and Hart, 2012). However, the historical nature of this study prevents the collection of accurate infield measurements of sky view factors. Therefore, the land cover data from the timeframe under investigation was used instead.

Land cover data used in this study was derived from the Centre for Ecology and Hydrology (CEH) landcover maps of Great Britain for both 1990 and 2000. These datasets are derived from satellite data collected by the Landsat 5 Thematic Mapper. The data provides pre-classified classifications of land cover types into 25 classes at a 25m resolution (UKCEH, 2020). These were used to provide land classifications and infer changes in land use over time. These are georeferenced and so can be opened directly in GIS.

There are small variations in the classifications and accuracies for classification between 1990 and 2000 imagery and blurring between pixels of land classifications was prominent within 2000 land cover data, similar to the issues experienced within Rembold et al., (2000). To amend this, reclassification of land cover was performed into larger homogenous land cover classifications as proposed by Aremu et al., (2017). The classifications suggested by LaGro (2005) were used to create seven homogenous classifications of forest land, agriculture, rangeland, wetland, water, barren and urban (shown in Table 3.2). This was done in QGIS (version 3.14) using the R.Reclass tool.

**Table 3.2:** Reclassification of CEH land cover types following LaGro (2005) methods.

<b>Land classification Year</b>	<b>Reclassification Values</b>	<b>Original Classification Values</b>
1990	1 - Urban	20, 21
	2 - Agriculture	18, 14, 23
	3 - Rangeland	5, 6, 7, 8, 9, 10, 11, 12, 13, 19, 25
	4 - Forest Land	15, 16
	5 - Water	1, 2
	6 - Wetlands	4, 17, 24
	7 - Barren	3, 22
2000	1 - Urban	171 172
	2 - Agriculture	41 42 43
	3 - Rangeland	51 52 61 71 81 91 101 102 151
	4 - Forest Land	11 21
	5 - Water	131 221
	6 - Wetlands	121 212
	7 - Barren	161 181 191 201 211

All assessments and training samples were processed using the Semi-Automatic Classification plug-in in QGIS (V3.14). An accuracy assessment of the land classification data returned an accuracy of 83.4%

### **3.3.1 Land Classification**

To determine the dominant land classification (i.e. the proportion of each land cover and whether these are urban or rural in composition) for each station a 250m buffer was created around each weather station; this acts as a 'circle of influence, which is a parameter that allows for classification of local climate zones around each fixed weather station (Oke, 2004; Sakakibara and Matsui, 2005). Then zonal statistics (an analytical tool that calculates the average, sum, minimum and maximum values within a zone or area of interest) were used to determine the maximum and majority values of land cover at each site. To cross-reference the results from the zonal statistics each circle of influence was exported into GIMP v2.10.8, an image manipulation tool, and histogram tools were used to analyse the frequency of each pixel (colour) representing land cover to determine the dominant land cover for each locality (map outputs provided in Appendix 1). According to Hardin et al., (2017), there is no set definition of an urban or rural site within UHI studies, in this study this was determined by using dominant land classifications from pre-classified CEH land classification data (shown in Table 3.3). Sites which featured dominant suburban and rural development and Continuous urban classifications were designated as urban sites. Sites which featured vegetative-based dominant land classifications (such as tilled land, mown and grazed turf) were designated as rural sites. For areas which presented dominant land classifications outside of this, visual analysis and next dominant land classification data was used to verify and contextualize urban/rural designations.

**Table 3.3.** Urban and rural sites assigned based on dominant land cover for 1990 and 2000 derived from pre-processed CEH land classification data.

<b>Station</b>	<b>Dominant Land Cover 1990</b>	<b>Dominant Land Cover 2000</b>	<b>Urban/Rural</b>
Cheltenham	Suburban And Rural Development	Continuous Urban	Urban
Cirencester	Tilled Land	Improved Grassland	Rural
Little Rissington	Mown And Grazed Turf	Improved Grassland	Rural
Pershore	Mown And Grazed Turf	Improved Grassland	Rural
Pershore College	Tilled Land	Improved Grassland	Rural
Randwick	Mown And Grazed Turf	Supra-Littoral Rock	Rural
Westonbirt	Mown And Grazed Turf	Improved Grassland	Rural

This land cover classification resulted in one urban and six rural weather stations (Table 3.3). Using this the weather stations selected for the UHI intensity was Cheltenham as the urban and Randwick as the rural one. Cheltenham was the only urban option available and the focus of this investigation and so was an obvious choice, Randwick was selected based on two criteria, the surrounding land cover around Randwick is characterized by Mown and graze turf and supra-littoral rock classifications, the second dominant land classification for Randwick (2000), was mown and grazed turf, which helps assign Randwick as a rural station. The second criterion used to designate Randwick as the reference rural station was owing to the completeness and continuous temperature data pertaining to that station.

### **3.4 Population data**

For this study, population is a surrogate for measures of urban form (Stewart and Mills, 2021; Oke et al., 2017; Oke, 1985). Population data (P) were derived from the 1981, 1991 and 2001 census data archives recorded by the Office for National Statistics. These data are readily available for public use and have been used to investigate population change over time for Cheltenham. Methods from Oke (1973) will be used to calculate  $\log P$ , using a growth function to logarithmically interpolate population between these dates.  $\log P$  can then be used to test for quantifiable relationships between population change and UHI intensity.

### **3.5 Sunspot cycle data**

Sunspot cycle data were taken from WDC-SILSO. Monthly mean total sunspot number datasets were downloaded from SILSO datafile service, this is calculated by simple arithmetic mean of daily total sunspot numbers over all days of each month. Daily total sunspot number (R) derived by the formula:

$$R = N_s + 10 * N_g$$

Where:  $N_s$  is the number of spots and  $N_g$  is the number of groups counted over the entire solar disk (WDC-SILSO, 2021).

### **3.6 Topographic data**

Topographic (height and elevation) data was extracted from Digital Terrain Models (DTMs) downloaded from Digimap. OS Terrain 50 DTM data were used; this has a 50m spatial resolution and is most useful for investigating regional landforms and surfaces (Ordnance Survey, 2020). Although higher resolution elevation data could have been used, such as Lidar (Light Detection and Ranging), the data is only being used to represent the physical shape of the study area and overlay features for



visual analysis and inferences and therefore deemed appropriate. The data are georeferenced and can be opened directly in QGIS. The DTM data was used to create contour data at 10m intervals across the study area to overlay temperature data on, visual analysis on the influence of elevation and temperature were then made.

Contouring methods were used to overlay contour lines detailing lines of equal values and spectral colourization to produce heatmaps, using isotherms to show temperature. Isotherm maps are the most interpretive format of a CUHI illustration (Stewart and Mills, 2021), they are lines on a map that connect points representing the same temperature.

### **3.7 Data analysis**

Correlation analysis measures the association between two or more variables by examining the covariation in recorded values (Stewart and Mills, 2021), this is the extent to which variation in one variable corresponds with the variation of another.

The UHI is defined as  $\Delta T_{(u-r)}$ . Where  $\Delta T$  is the difference in air temperature,  $u$  is the air temperature recorded at an urban station and  $r$  is defined as the air temperature at the rural reference station (Oke et al., 2017).

In UHI studies the aim is to determine the statistical relationship between magnitude as measured by  $\Delta T_{(u-r)}$  and variables relating to urban form and function (Stewart and Mills, 2021) or synoptic weather conditions.

Tests for normality were performed using histograms to analyse the distribution of the data. Variables were assessed by visual inspection of their respective histograms. The results for the tests of normality produced a bell-curve shape that is characteristic of a normal distribution. Parametric tests were performed on the air

temperature data as it was determined the outliers within the data sets can be associated with the extreme maximum and minimum values with the temperature data used within this study. Pearson's Correlation for tests in relationships between dependant and independent variables (Stewart and Mills, 2021) were used, and the correlation coefficients were tested for statistical validity at 5% level of significance (Norusis, 1988). For this,  $\Delta T_{(u-r)}$  is identified as the dependant variable that responds to changes in the independent variable, identified as population, cloud cover (%), precipitation (mm) and sunspot number.

A natural complement to correlation analysis is regression analysis, which fits a mathematical function that explicitly measures the relationship between a dependant variable to one or more independent variables (Stewart and Mills, 2021). The aim of the regression analysis indicated the relationship between each variable and its associations with temperature recorded. It also holds into account the potential to explain the relationship and association between one or more variables in relation to a continuous variable, temperature. A simple linear regression was used to determine the trend and proportion of variance between UHI intensity of the dependant variable against the independent variables (Pallant, 2010). Trend analysis within this study was carried out using a linear regression method.

## **Chapter 4: Results**

This section details the results and analysis of data handled regarding the UHI under investigation in this study. To meet the aims of this study, this section will focus on describing and analysing trends within the datasets using descriptive statistics to summarize the annual and decadal trends of the temperature data for each weather station. Furthermore, it will use descriptive statistics to describe the trend of the temperature of the region both annual and decadal through the means of graphs and figures, as well as investigating the relationships between the main variables that influence the UHI and an analysis of trends and relationships in the canopy layer UHI.

### **4.1 Temperature**

#### **4.1.1 Decadal Temperature Profile**

One of the objectives of this study is to produce a decadal temperature profile for the study area and sites located therein, showing the variation in maximum and minimum air temperatures for each site from 1990 to 2000. Cirencester showed the least variation in maximum recorded temperatures (only 2.5°C) compared to Randwick which has the greatest variance at 6.5°C. Little Rissington had the least variation for minimum air temperature (4.8°C) for minimum air temperature, while the greatest variance was recorded at Westonbirt (8.2°C). Cheltenham had a variation of 5.8°C for minimum and 5.2°C maximum air temperatures. For eight of the ten years, Cheltenham recorded the highest maximum air temperatures (Table 4.1); in 1992 and 1997 Pershore recorded the highest maximum air temperatures. The coldest records were shown to be held by Little Rissington from 1990 to 2000. In contrast to this. Little Rissington recorded the lowest maximum temperature of 21.80°C in 1995.

The main pattern that can be extrapolated from Table 4.1 is that there are three periods of significant warming among the sites in 1990, 1995 and 2000. Evaluating this further, using averages calculated from each station, maximum air temperatures from 1990 to 1994 decrease on average by 5.7°C before increasing again in 1995 by around 3.7°C for the region. A similar pattern occurs between 1996 to 2000.

Temperatures decline again by around 2.5°C before increasing again in 2000 by roughly 0.5°C.

**Table 4.1:** Maximum and minimum annual air temperatures for each weather station from 1990 – 2000.

		Year										
		1990	1991	1992	1993	1994	1995	1996	1997	1998	1999	2000
<b>Cheltenham Maximum Air Temperature (°C)</b>	<b>Maximum</b>	37.10	28.30	29.30	27.90	32.20	34.60	32.00	31.60	28.20	31.60	31.90
<b>Cheltenham Minimum Air Temperature (°C)</b>	<b>Minimum</b>	-4.30	-10.10	-8.30	-5.60	-6.80	-7.60	-5.30	-7.60	-6.20	-8.90	-9.40
<b>Cirencester Maximum Air Temperature (°C)</b>	<b>Maximum</b>	25.30	27.20	29.00	25.60	29.50	33.50	32.00	29.50	27.50	29.90	27.80
<b>Cirencester Minimum Air Temperature (°C)</b>	<b>Minimum</b>	-5.20	-10.60	-7.50	-6.60	-9.50	-8.00	-6.40	-7.00	-5.50	-10.90	-9.50
<b>Little Rissington Maximum Air Temperature (°C)</b>	<b>Maximum</b>	33.40	25.90	25.90	24.40	29.80	21.80	30.30	29.00	27.40	29.60	28.40
<b>Little Rissington Minimum Air Temperature (°C)</b>	<b>Minimum</b>	-4.50	-8.90	-7.50	-5.20	-5.60	-7.10	-7.60	-8.80	-4.90	-8.00	-8.40
<b>Pershore Maximum Air Temperature (°C)</b>	<b>Maximum</b>	34.80	27.20	29.80	25.60	30.40	31.30	31.80	31.90	28.00	30.10	28.30
<b>Pershore Minimum Air Temperature (°C)</b>	<b>Minimum</b>	-7.00	-12.40	-8.70	-5.40	-6.30	-7.50	-8.60	-7.30	-6.30	-8.60	-12.40
<b>Pershore College Maximum Air Temperature (°C)</b>	<b>Maximum</b>	34.90	28.10	29.20	26.60	33.00	32.30	31.30	32.10	23.80	30.10	29.20
<b>Pershore College Minimum Air Temperature (°C)</b>	<b>Minimum</b>	-5.20	-9.00	-6.70	-4.90	-5.90	-6.60	-5.30	-7.50	-2.60	-9.20	-10.40
<b>Randwick Maximum Air Temperature (°C)</b>	<b>Maximum</b>	34.00	26.10	29.50	24.90	28.30	34.40	29.90	29.50	25.50	30.10	28.10
<b>Randwick Minimum Air Temperature (°C)</b>	<b>Minimum</b>	-5.70	-9.70	-7.00	-5.30	-5.10	-6.90	-5.50	-7.20	-4.50	-6.20	-5.10
<b>Westonbirt Maximum Air Temperature (°C)</b>	<b>Maximum</b>	34.00	26.20	28.90	25.60	27.90	32.60	29.60	29.10	26.60	24.90	29.20
<b>Westonbirt Minimum Air Temperature (°C)</b>	<b>Minimum</b>	-6.00	-10.70	-7.60	-9.00	-10.70	-8.20	-6.50	-6.70	-4.20	-5.90	-12.40

To discover the climate for each locality a 10-year running average for each site was produced (Table 4.2). This shows that Cheltenham holds the highest maximum decadal average temperatures of 31.34°C when compared against other sites. The lowest maximum decadal air temperature is Little Rissington (27.81°C). The differences between urban and rural temperatures show that maximum air temperatures are higher in built-up environments when compared to their rural counterparts. Westonbirt recorded the lowest minimum air temperature with -7.99°C.

The warmest site for minimum air temperatures is Randwick with  $-6.20^{\circ}\text{C}$ , which is warmer than its urban counterpart Cheltenham.

**Table 4.2:** Running 10-year average maximum and minimum air temperature for each weather station.

	Air Temperature ( $^{\circ}\text{C}$ )	
	Maximum	Minimum
Cheltenham	31.34	-7.28
Cirencester	28.80	-7.88
Little Rissington	27.81	-6.95
Pershore College	30.05	-6.66
Pershore	29.93	-8.23
Randwick	29.12	-6.20
Westonbirt	28.60	-7.99

A regional air temperature profile was also calculated (Table 4.3). When comparing the regional data to the 10-year averages for each site (Table 4.2) Cheltenham has an increased temperature of  $1.96^{\circ}\text{C}$  above the regional maximum mean. Similarly, Pershore ( $0.55^{\circ}\text{C}$ ) and Pershore college ( $0.67^{\circ}\text{C}$ ) show an increase above the regional average. Against regional minimum air temperatures, Cheltenham records lower temperatures by  $0.03^{\circ}\text{C}$ . The greatest difference in regional minimum and decadal average is Pershore ( $0.92^{\circ}\text{C}$  warmer than the regional average), and Pershore College also records the warmest minimum air temperatures for the area varying by  $0.65^{\circ}\text{C}$  against regional averages.

**Table 4.3:** Regional air temperature profile calculated from averaging 10-year air temperature data from each weather station.

Regional Average Air Temperature (°C)	
Maximum	29.38
Minimum	-7.31

#### 4.1.2 Daily and Monthly Mean Air Temperature

Figure 4.1 describes changes in air temperature over time for each site, the time-series shows the directional increase or decrease in air temperature over time for each site. All data follow a sinewave, which is representative of the fluctuations in air temperature collected from each site. The wave-like nature is the direct result of temperature change through monthly, seasonal and yearly fluctuations in temperature over time. Analysis of the trends in temperature can be categorized into three categories: sites which demonstrate (1) significant warming, (2) slight warming, and (3) no significant warming. These categories can be interpreted through the means of visual analysis and the implementation of deductive reasoning based on mean values and trends established in the time-series in figure 4.1.

Three sites show a strong increase in air temperature over time; Cirencester (Figure 4.1b), Little Rissington (Figure 4.1c) and Westonbirt (Figure 4.1g). Cirencester shows a strong increase in air temperature from 1990 to 2000, increasing from 9°C to 11.5°C based on mean values. Although some data are missing from this dataset the results have not been omitted nor interpolated to fill in gaps in data. Therefore, this could potentially affect the overall trend in the data; however, the majority of the dataset is complete. From 1990 to 1996 Cirencester shows a strong increase in daily temperature before levelling off for the later part of the decade. The maximum

temperature recorded from the data for mean air temperature in Cirencester is around 25°C and the lowest recorded temperature is around -6°C. Similarly, Westonbirt (Figure 4.1g) shows a strong increase in mean daily air temperature over time when compared to other sites however statistical analysis should be implemented to establish a directional relationship between temperature change over time and further quantify this relationship. There are multiple outliers within the dataset which can be noted with extreme high and low air temperatures. The maximum air temperatures can be seen to average around 25°C for 1990 and 1996 and extreme low temperatures around -9°C for 1991, 1995 and 2000 respectively. Little Rissington (Figure 4.1c) has an incomplete record of temperature data through 1995. With this in consideration, the overall trend of air temperature can be seen to increase over time rising by 1°C over the 10-year period. There is a greater number of outliers within this dataset, which can be seen predominantly in 1991 demonstrating both the highest and lowest recorded temperatures for the area. Ignoring the outliers within the data, summertime air temperatures can be seen to rise over time throughout this dataset.

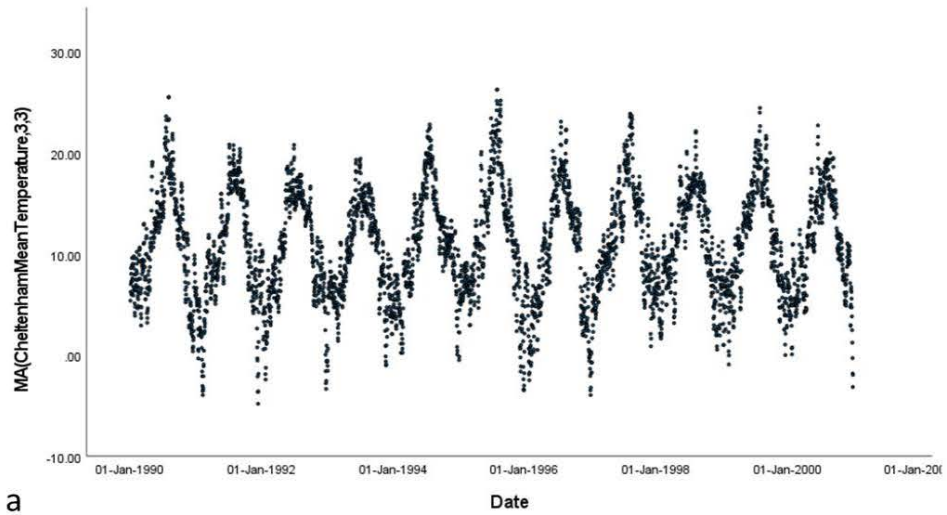
Two sites demonstrate a slight increase in air temperature over time these sites are Cheltenham (Figure 4.1a) and Pershore (Figure 4.1d). The average temperature for Cheltenham does not fluctuate much between 10°C and 11°C from 1990 to 2000 based on mean temperature values taken from figure 4.1. The main outlier can be seen mid-way through 1990 with a maximum mean daily temperature of around 28°C. Maximum temperatures from this point can be seen to dip to around 18°C in following years before rising again over the second half of the decade. There are two main outliers for this data set, the first is recorded at 30°C, which can be attributed to the heatwave present during 1990, which contributed to the British Maximum



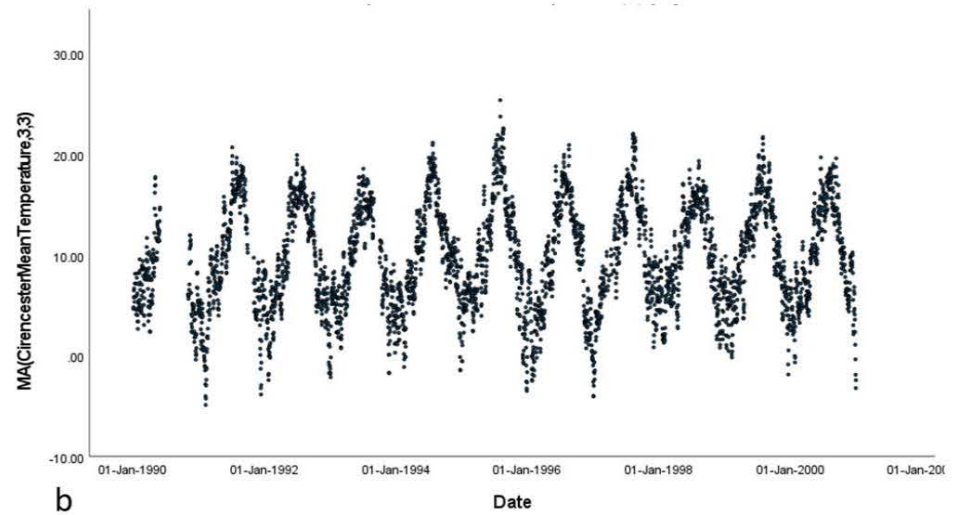
temperature for this site. The second outlier to note is present in mid-1995 which records temperatures of  $\sim 28^{\circ}\text{C}$ , this too can be attributed to the heatwave event during 1995 which induced high air temperatures. Pershore (Figure 4.1d) shows a slight trend in warming in daily air temperature over the 10-year period which fluctuates between  $10^{\circ}\text{C}$  and  $10.5^{\circ}\text{C}$  according to the mean temperature values. Higher air temperatures can be seen present in 1990 which corresponds to the 1990 heatwave. There is a slight decrease in lower temperatures for the majority of the data showing slight warming before dropping at the end of 2000, dropping to around  $-8^{\circ}\text{C}$ .

Two sites demonstrate no general trends in regard to a decrease or increase in air temperature over time; Pershore College (Figure 4.1e) and Randwick (Figure 4.1f). The cyclical nature of air temperature throughout stays consistent. All summer and winter air temperatures stay within a  $3^{\circ}\text{C}$  variance. Despite missing some data for early 1999, summer air temperatures for this year are the lowest recorded for this area at  $18^{\circ}\text{C}$  when compared to the average  $22^{\circ}\text{C}$  for the subsequent years.

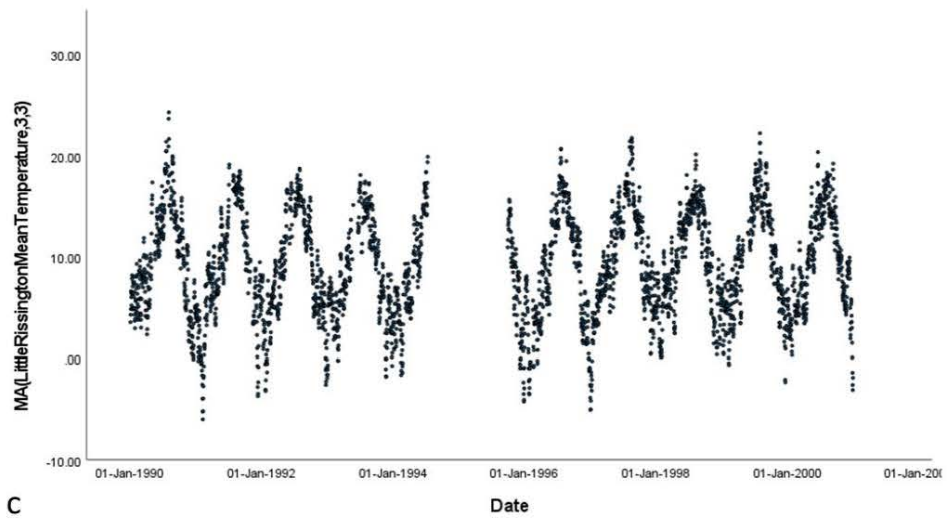
Pershore college shows no deviations outside of  $10^{\circ}\text{C}$ . Randwick (Figure 4.1f) stays constant and level throughout in regard to temperature over time. It has relatively high summer air temperatures which stay consistent between  $26^{\circ}\text{C}$  and  $21^{\circ}\text{C}$ . A presumption for this consistency within the dataset may be accredited towards the site being a rural area and therefore lacking changes in population or land change over time.



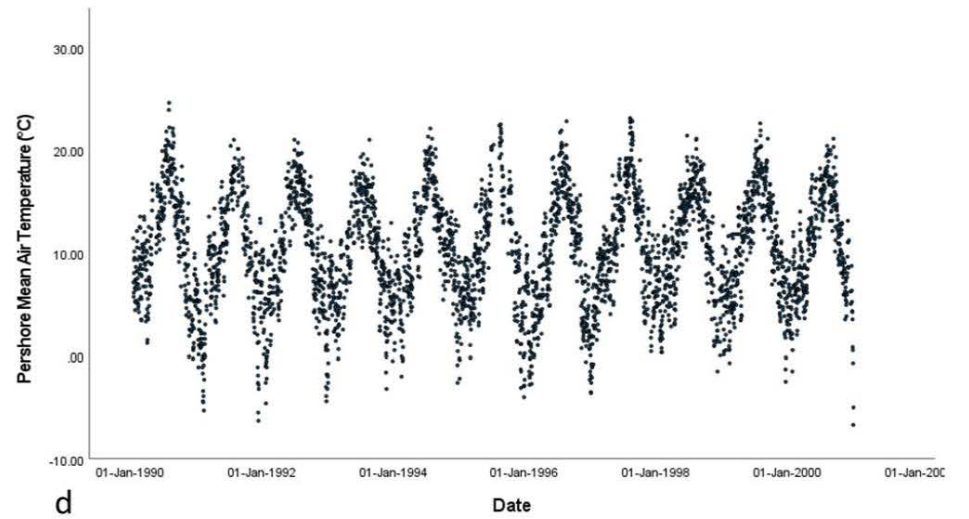
a



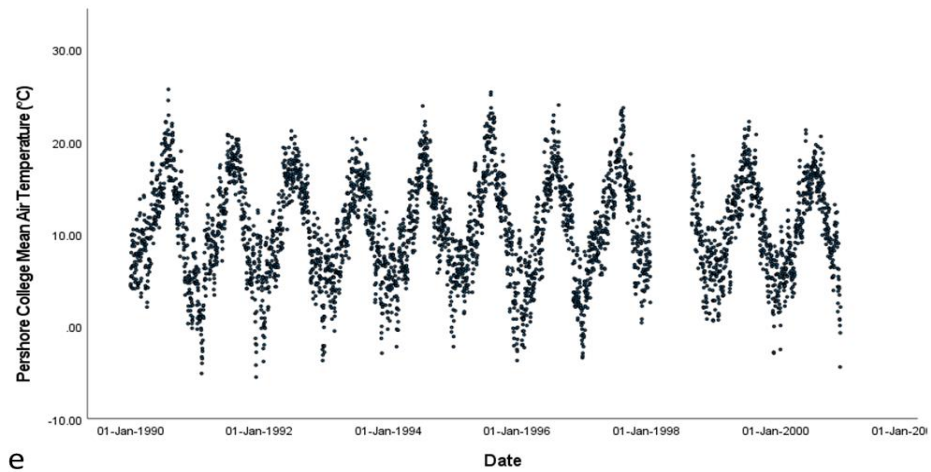
b



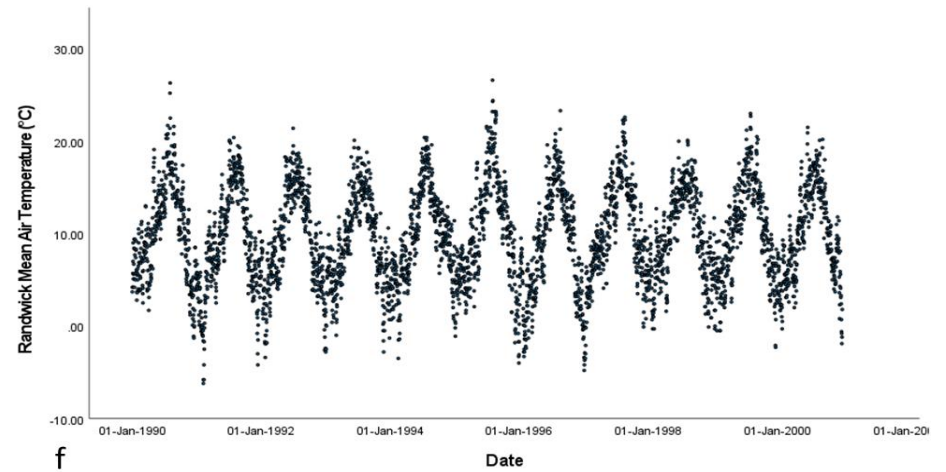
c



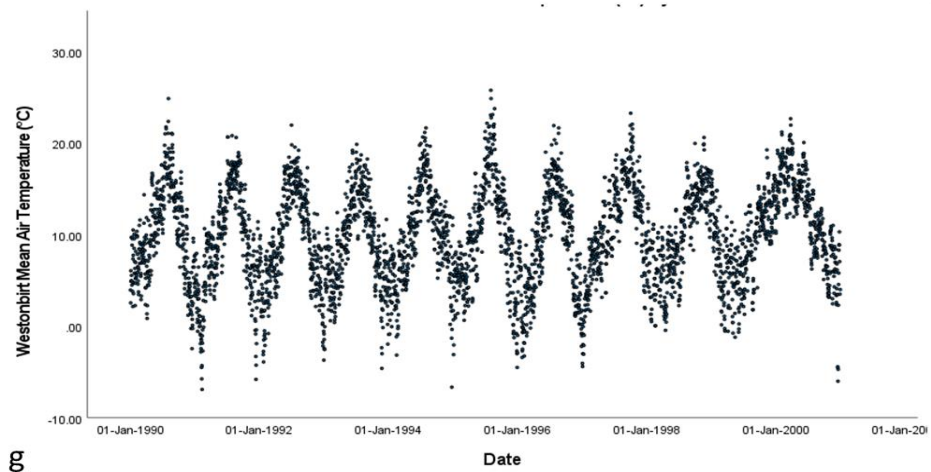
d



e



f



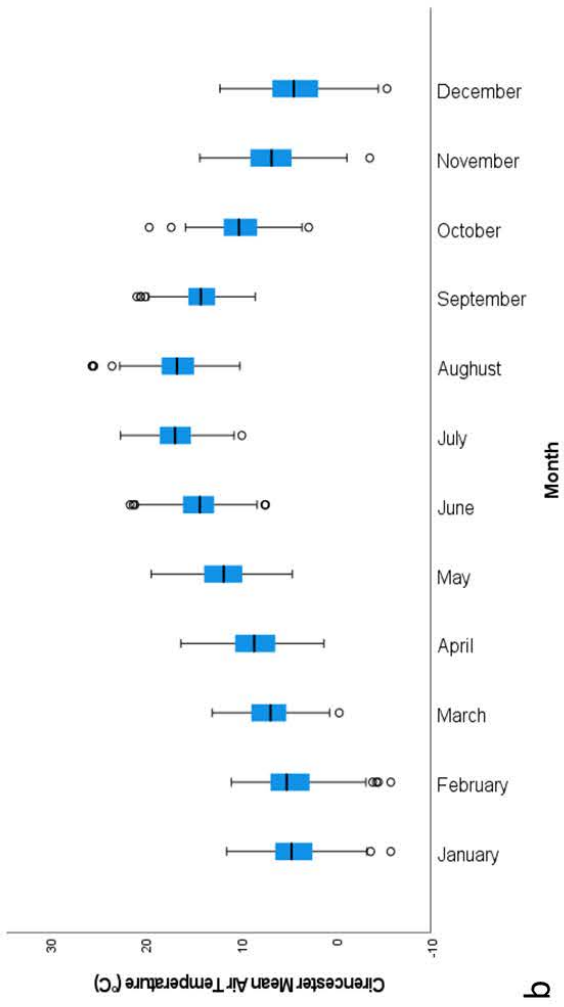
g

**Figure 4.1:** Three month moving average of mean daily air temperature for each weather station from 1990 – 2000. Stations a – i: (a) Cheltenham, (b) Cirencester, (c) Little Rissington, (d) Pershore, (e) Pershore College, (f) Randwick, (g) Westonbirt.

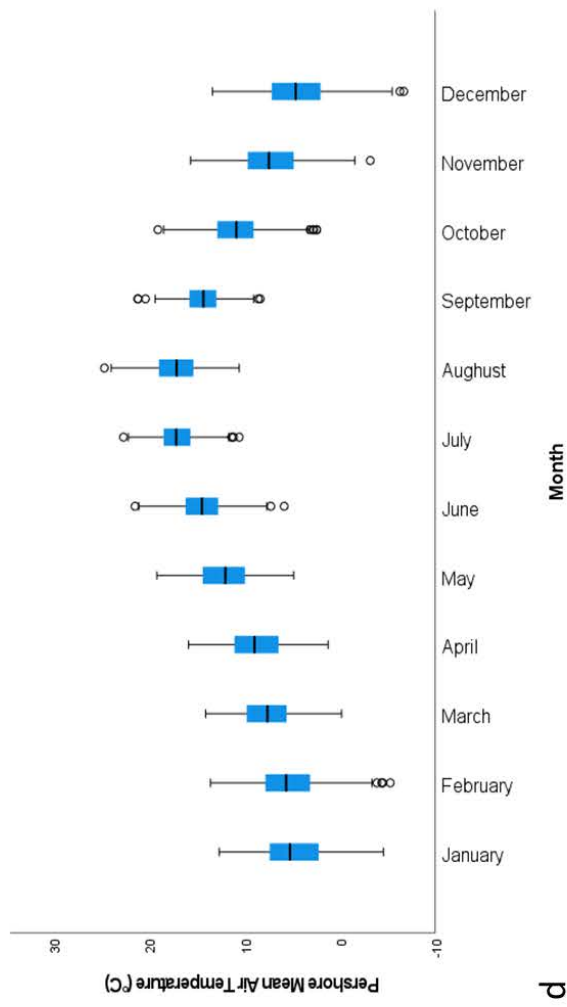
Monthly mean average air temperature profiles were generated by compiling daily mean air temperatures from each station and grouped by month between 1990 and 2000 (Figure 4.2). Westonbirt (Figure 4.2g) has the greatest variance in air temperature of all locations studied. The spread of the data varies extensively through the year with maximum and minimum air temperatures ranging between -3 to 22°C  $\pm$ 3°C. The data contains many outliers occurring with maximum values extending to maximum air temperature values reaching 22°C in March and minimum air temperature values reaching -1°C in June. The maximum temperature recorded is August with temperatures reaching 22°C and minimum temperatures reaching -5°C in February. The distribution of median air temperature values ranges between 4°C to 14°C from January to December. Conversely, Little Rissington (Figure 4.2f) shows the least variation in the distribution of monthly air temperatures. The distribution of maximum air temperatures occurs mainly from July to September ranging between 20°C – 22°C. Minimum temperatures occur predominantly between December to February with temperatures varying between -5°C to -6°C. The distribution of median air temperature from January to December ranges from 4°C to 15°C.

Evaluating the distribution of the temperature data, Cheltenham (Figure 4.2a) records the highest temperatures across all the sites evaluated. Monthly mean air temperature for Cheltenham shows increased temperatures from June to August, with maximum mean temperatures varying between 21°C to 25°C, with outliers in August extending to 28°C. Cooler temperatures occur typically between December to February with minimum temperatures of -2°C to -5°C. The distribution of median temperature varies between 5°C and 18°C.

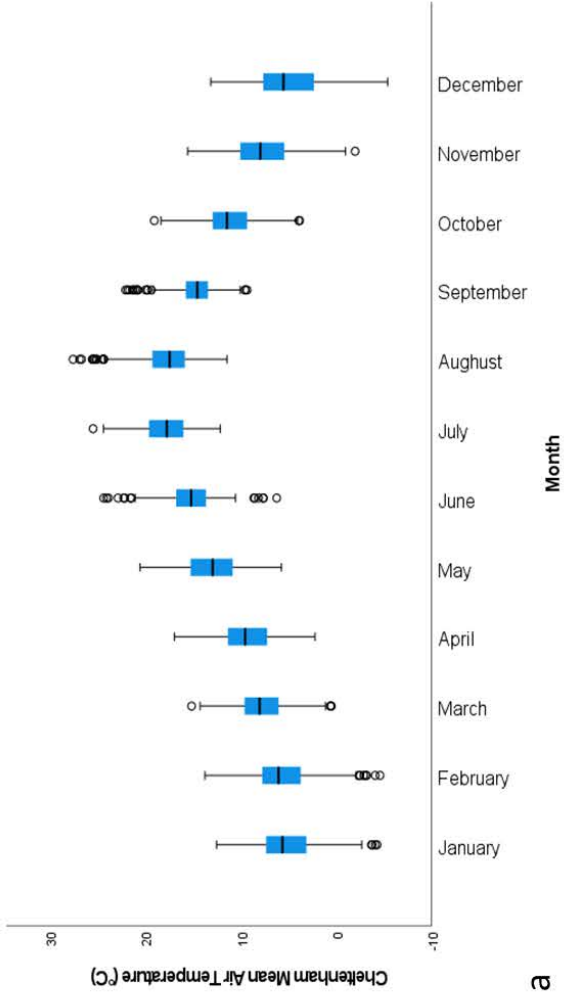
The second warmest locations are Cirencester (4.2b) and Pershore (Figure 4.2d). Both sites show that June to September are the warmest months, with temperatures ranging typically between 20°C to 23°C. Similarly, coldest temperatures occur from December to February, ranging between -2°C to -5°C. Median monthly values for both sites vary between 5°C to 17°C ( $\pm 1^\circ\text{C}$ ). Pershore College (Figure 4.2e) and Randwick (Figure 4.2f) show similar distributions in monthly temperature. Maximum temperatures typically vary between 19°C to 22°C between June and August. Pershore College shows increased warming with outliers recording up to 25°C maximum monthly air temperatures. December to February record the lowest temperatures for both sites ranging between -2°C to -6°C, with colder temperatures pertaining to Randwick with outliers recording up to -7°C in February. The temperature variance for median monthly values ranges between 5°C to 18°C ( $\pm 1^\circ\text{C}$ ).



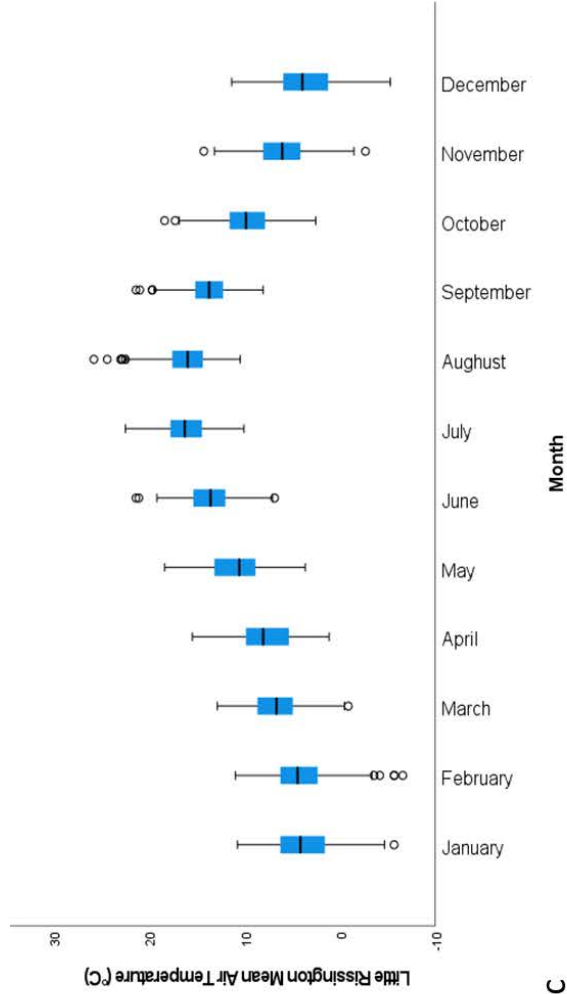
**b**



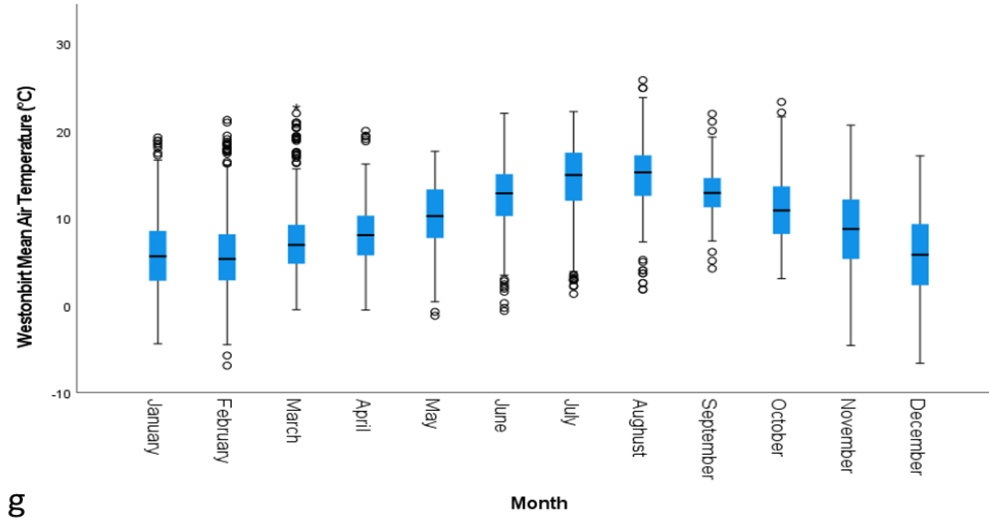
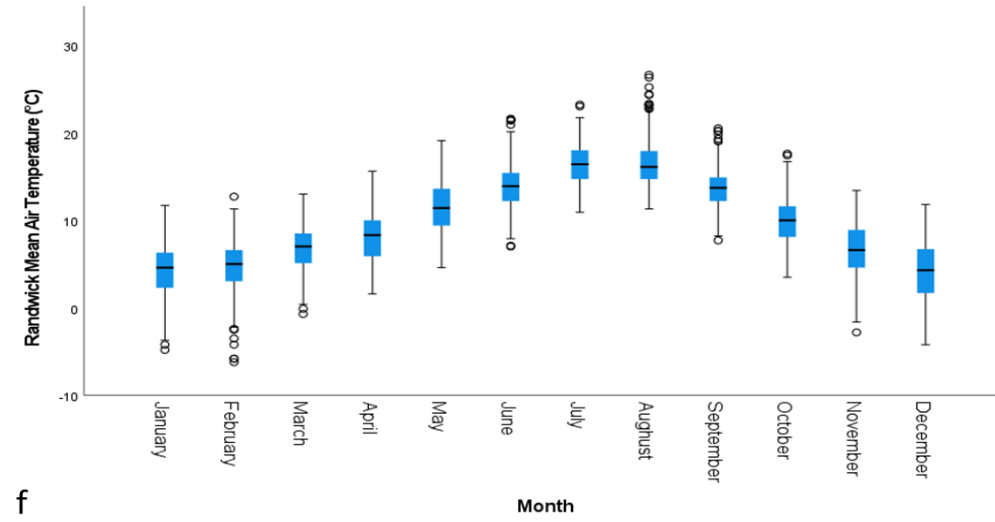
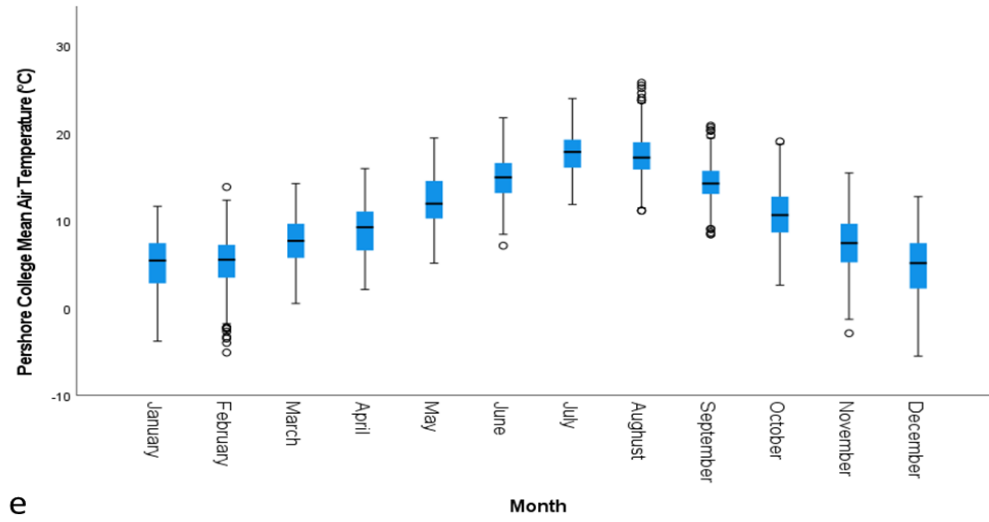
**d**



**a**



**c**

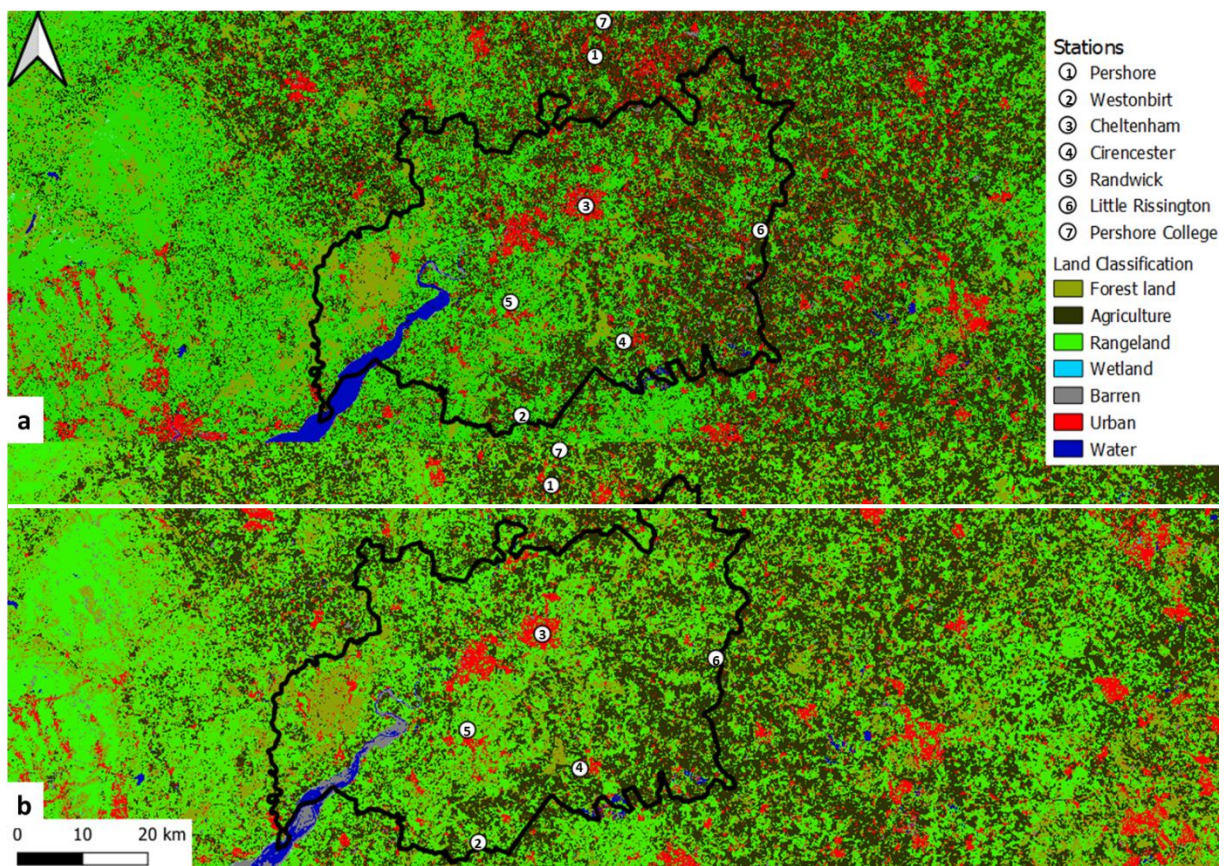


**Figure 4.2:** Mean monthly air temperature profiles at each station for using aggregated data from 1990 to 2000. Stations a – i: (a) Cheltenham, (b) Cirencester, (c) Little Rissington, (d) Pershore, (e) Pershore College, (f) Randwick, (g) Westonbirt.



## 4.2 Land Classification

The land classification between 1990 and 2000 (Figure 4.3) shows the variation in land cover classifications across the region, the area of each of these, as well as percentage change between the two dates, is provided in Table 4.4. There is an increase in forest (43%) and barren (80%) land cover from 1990 to 2000. Urban land cover declined by 8%, which is atypical of population growth over time; although evaluating each site in detail Cheltenham does demonstrate significant urban growth, extending by 3.5 km<sup>2</sup> in area, (Figure 4.5). The proportion of water (-73%) and wetland (-43%) land cover declined through the decade. Although, agriculture appears to show a small growth from 1990 to 2000 with an increase of 4%.



**Figure 4.3:** Land classification map of Gloucestershire for 1990 (a) and 2000 (bottom), using reclassified land classification values. Land Cover Map 2000 and 1990: Based upon LCM1990 © UKCEH; LCM2000 © UKCEH; Contains OS data © Crown copyright and database right 2022.



**Table 4.4:** Land Classification area and percent change for Gloucestershire from 1990 to 2000.

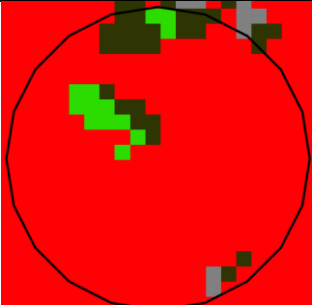
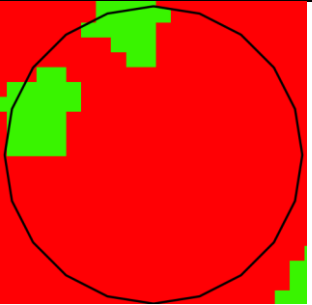
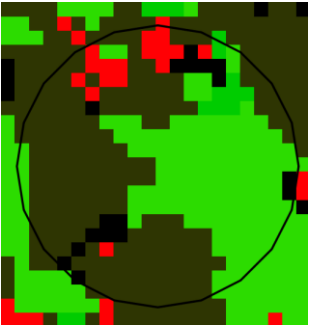
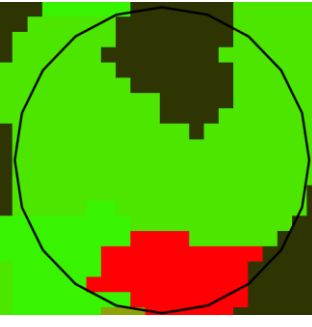

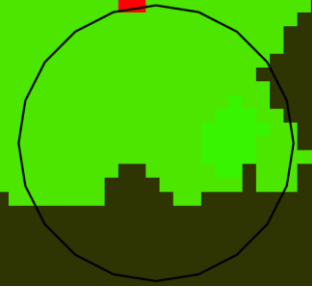
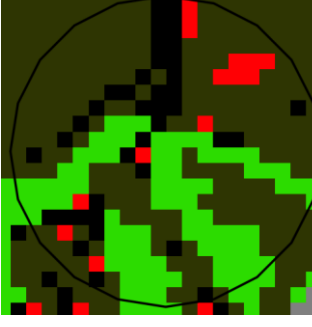

<b>Land Classification</b>	<b>1990 km<sup>2</sup></b>	<b>2000 km<sup>2</sup></b>	<b>% Change</b>
Water	607.75	161.07	-73%
Barren	219.55	394.36	80%
Wetland	21.97	12.63	-43%
Rangeland	10523.73	10106.77	-4%
Agriculture	7653.66	7926.72	4%
Urban	2437.78	2259.85	-7%
Forest	2119.99	3025.96	43%

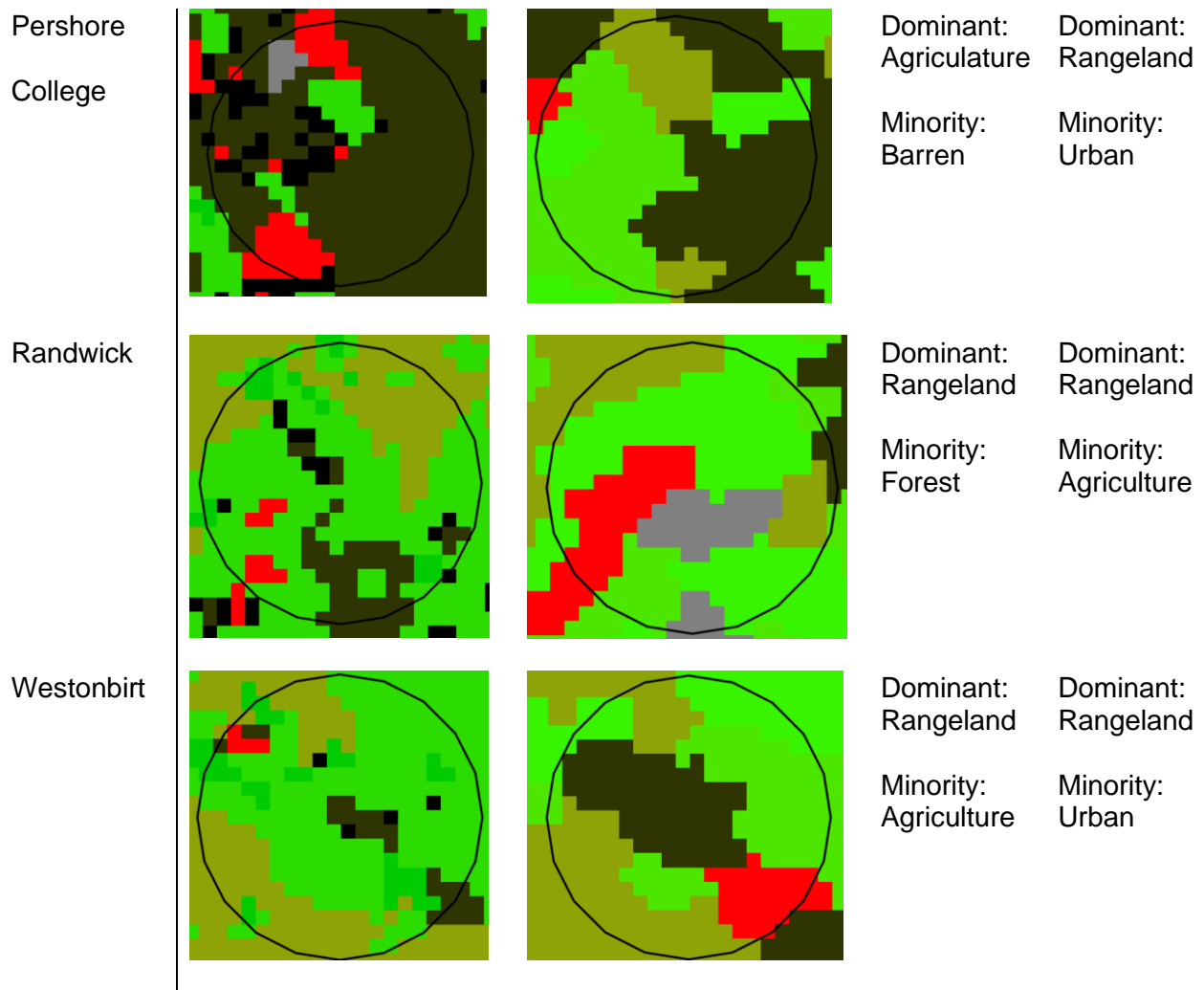
Evaluating land classification locally, land classifications for each site are shown in Table 4.5. Three sites show little or no change in dominant land classifications from 1990 to 2000 (Cheltenham, Randwick and Westonbirt).

The largest variance in land cover classification was in Pershore, Little Rissington, Cirencester and Pershore College. Cirencester shows a significant decline in agriculture, with a significant increase in rangeland as well as a transition towards urban land classifications; with fragments of urban land class towards the north in 1990, contrasting to the high concentration of urban land class pertaining to the south edge of the circle of influence in 2000. Similarly, Pershore had a significant decline in agriculture and a significant increase in both rangeland and urban land classes. Little Rissington had a removal of urban and barren land classifications and a high increase in rangeland and decrease in agriculture. Pershore College shows a major decline in urban, barren and agriculture land classes. These prevalent land

classes for 2000 are primarily forest and rangeland with a small concentration of urban land class towards the north-west of the circle of influence.

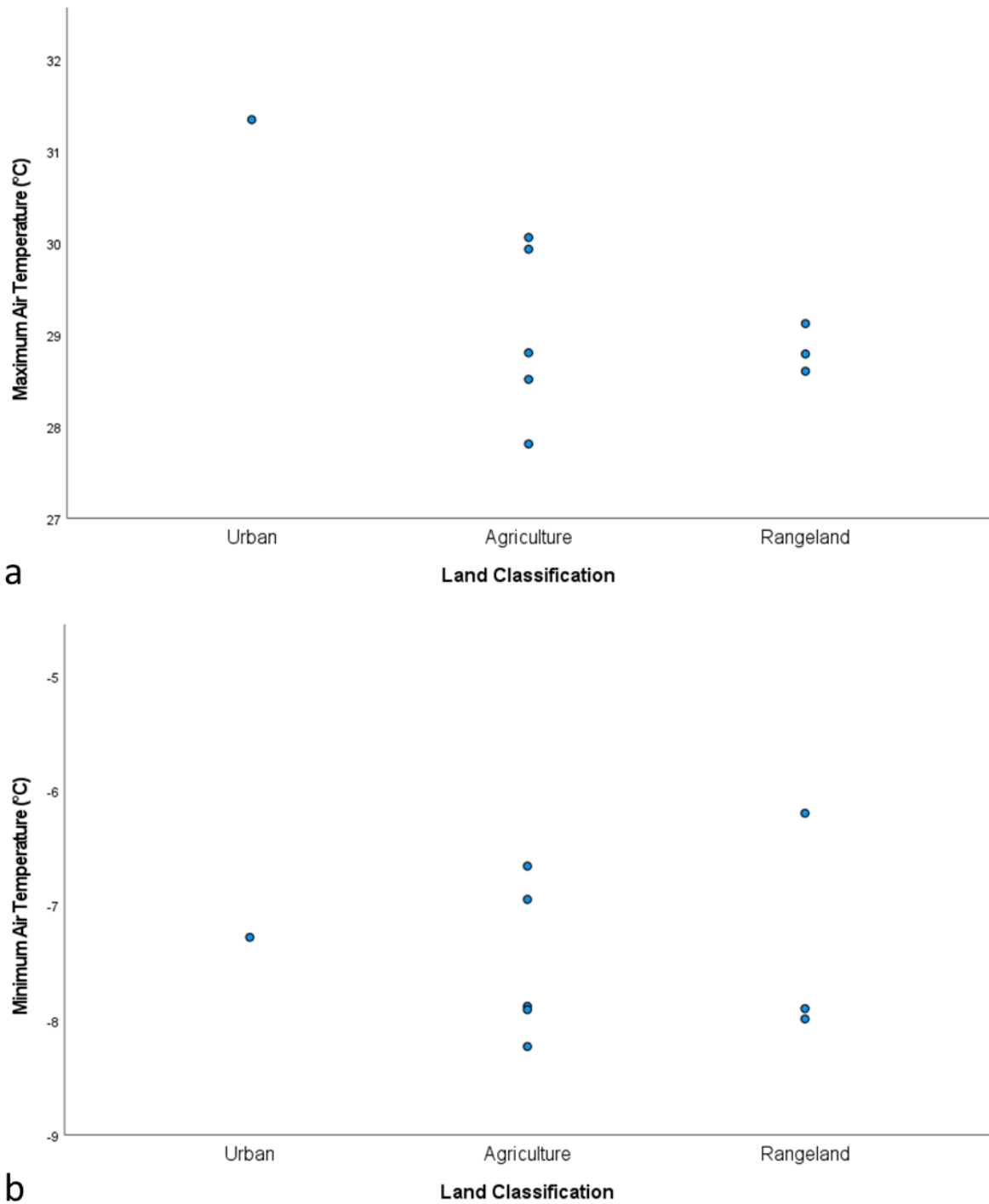
**Table 4.5:** Reclassified land cover classifications produced using LaGro (2005) homogenous land classification methods for each site in 1990 and 2000. Unclassified (Black), Water (Blue), Barren (Grey), Wetlands (Light Blue), Rangeland (Green), Agriculture (Dark Green), Forest Land (Olive Green), Urban (Red). Based upon LCM1990 © UKCEH; Based upon LCM2000 © UKCEH.

Station	1990 Circle of Influence	2000 Circle of Influence	Land cover 1990	Land cover 2000
Cheltenham			Dominant: Urban Minority: Barren	Dominant: Urban Minority: Rangeland
Cirencester			Dominant: Agriculture Minority: Rangeland	Dominant: Rangeland Minority: Urban
Little Rissington			Dominant: Agriculture Minority: Barren	Dominant: Rangeland Minority: Forest
Pershore			Dominant: Agriculture Minority: Rangeland	Dominant: Rangeland Minority: Barren



The effects of land cover classification on temperature were plotted to show the variation in temperature for each dominant land classification recorded (Figure 4.4). This shows that urban land cover classifications demonstrate higher maximum air temperatures when compared against other dominant land classifications; this is 31.2°C. Air temperature for agriculture land classifications varies between 1°C to 3°C. In comparison, rangeland shows less variation in air temperature recording between 1°C to 1.5°C. In comparison, minimum air temperatures are higher in rangeland classifications, when compared with urban these are 1.5°C higher. However, rangeland has the highest variance between values with a difference of 2°C. Agriculture is the second coldest land classification with temperatures varying

between  $-7.5^{\circ}\text{C}$  and  $-8.2^{\circ}\text{C}$ . Urban land classes are the second warmest with temperatures of  $-7.2^{\circ}\text{C}$ .



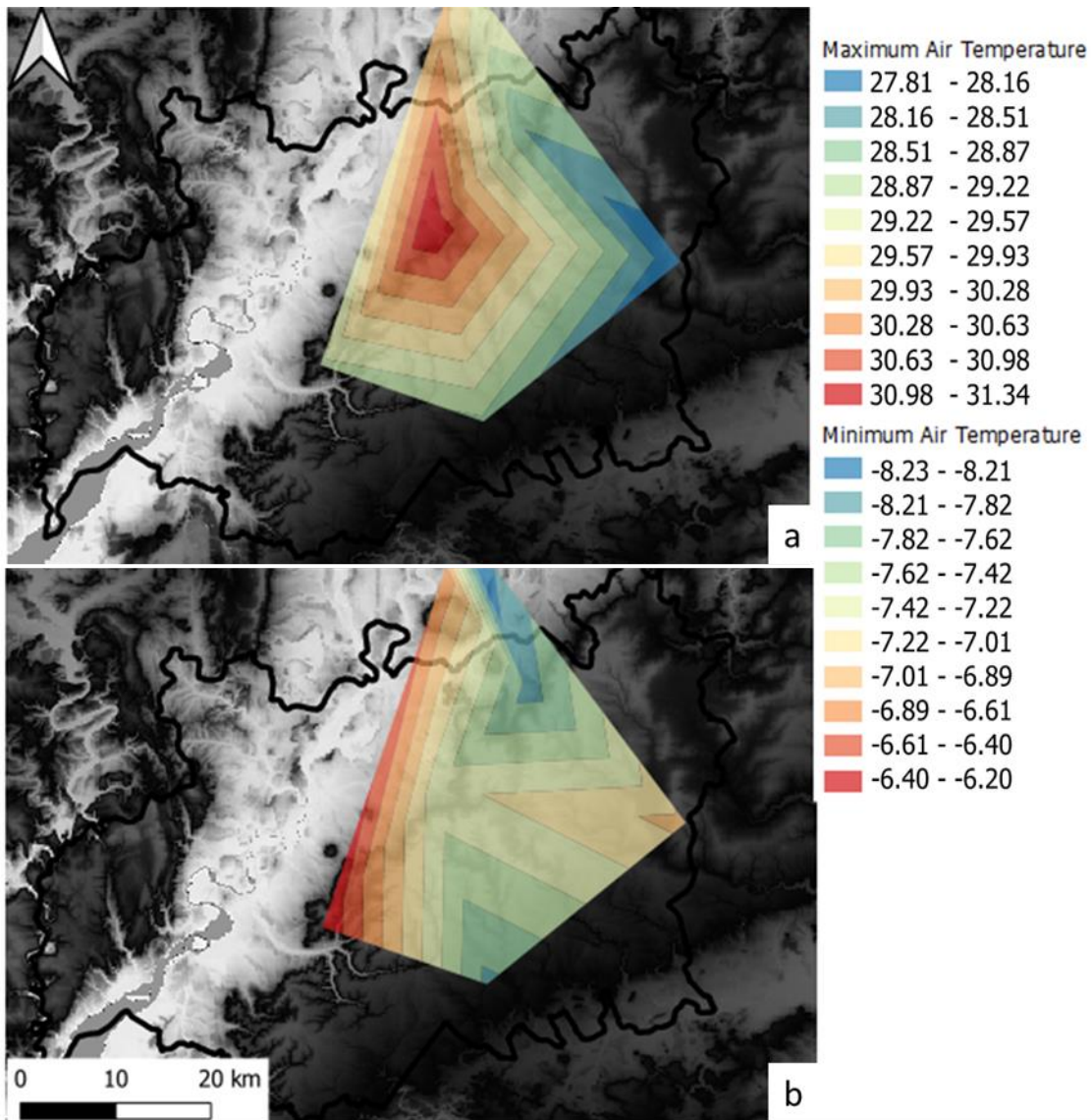
**Figure 4.4:** Dominant land cover classifications plotted against (a) maximum and (b) minimum air temperature. The air temperature values are extracted from interpolated air temperature values and plotted against each site, according to their land classification.

### 4.3 Heat Maps

To visually investigate the regional air temperature profile for the study area, the regional air temperature data (Table 4.2) was plotted, and these data were interpolated for both minimum and maximum air temperature, producing a regional air temperature profile (Figure 4,5).

The interpolated decadal average air temperatures show the magnitude and formation of the UHI in Gloucestershire. The maximum regional air temperature (Figure 4.5a), clearly defines Cheltenham as a hotspot for increased air temperatures, with air temperatures over 30°C-31°C. The magnitude of maximum air temperature dissipates outwards reaching 28°C to the outer limits, with extreme values of 27°C on the outer, eastern perimeters. Typically, high-temperature values occur at lower elevations as depicted by the digital elevation model, in which the heatmap is overlaid, with temperature decreasing as elevation increases.

Conversely, the minimum air temperature heatmap (Figure 4.5b) shows increased warming south-westerly of Cheltenham. Although higher temperatures are recorded around Cheltenham, ranging around -7°C, warmer temperatures of ~6°C can be noted south-westerly, following the low elevation patterns depicted by the digital elevation model. Lower elevations are defined in white, with higher elevations defined as darker colours. Unlike maximum air temperature, warmer temperatures occur at higher elevations, with the coolest temperatures prevailing towards the northern and southern extents of the heatmap around -8°C.

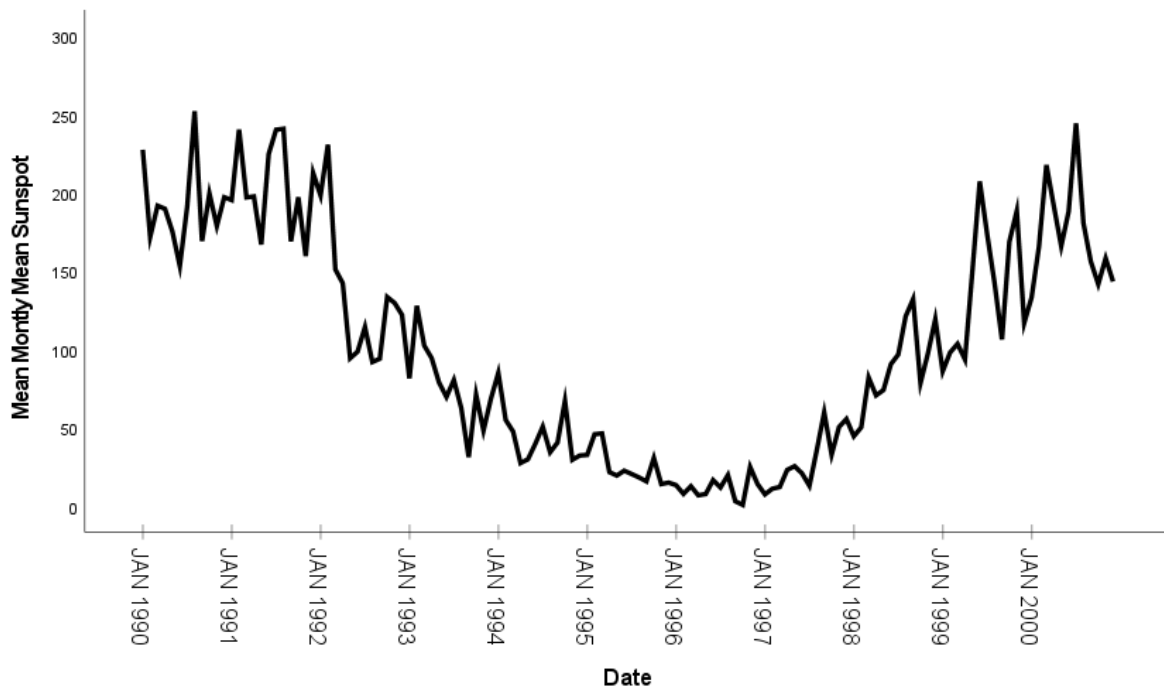


**Figure 4.5:** Heatmap of regional (a) maximum and (b) minimum air temperature. Interpolated from running 10-year average data. Heatmap is overlaid on OS Terrain 5 Digital Terrain Model. © Crown copyright and database rights 2022 Ordnance Survey (100025252).

## 4.4 Weather Variables and Extra-Terrestrial Influences

### 4.4.1 Sunspot Cycle

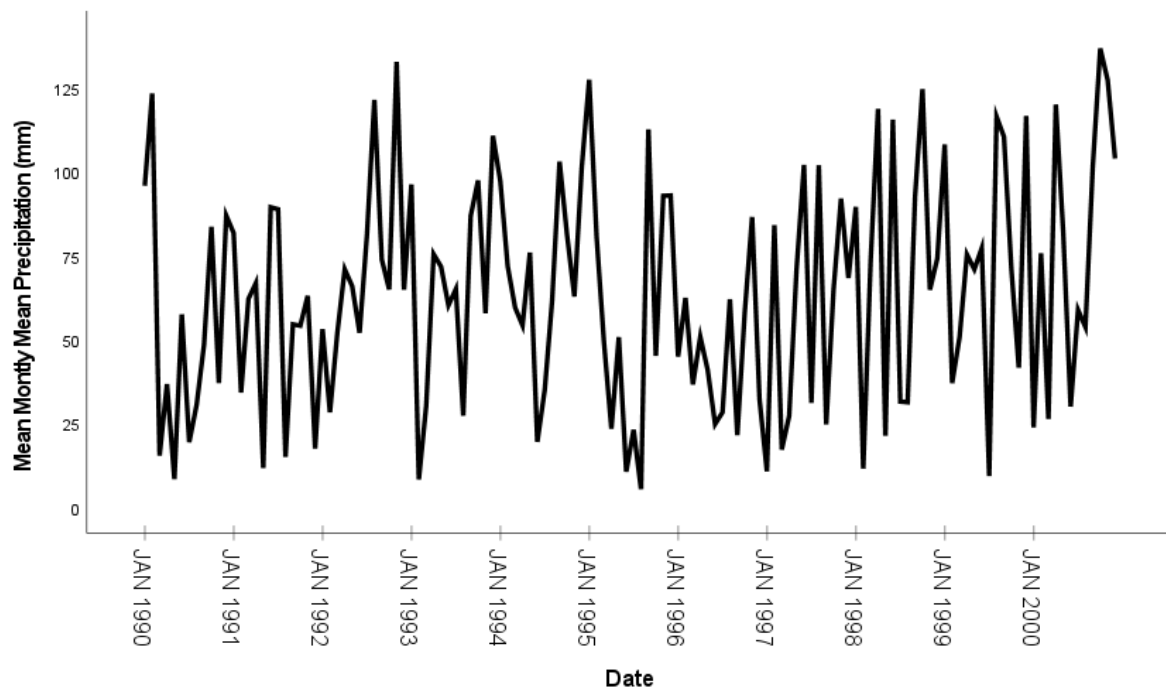
Sunspot cycle data from 1990 to 2000 is shown in Figure 4.6. Two peaks in sunspot cycle occur, the first occurring between 1990 to 1992, fluctuating between 225 and 250. The second observation occurred from 1999 to mid-2000 which fluctuates between 215 and 250. The maximum number of sunspots is 250 which occurs in mid-1990. The minimum sunspot number of 0.7 can be noted in late 1996 and the median of 100 observed sunspot number.



**Figure 4.6:** Monthly mean number of observed sunspot cycles from 1990 to 2000 adapted from WDC-SILSO (2021). Values are taken Royal Observatory of Belgium, but values are reflective of UK observations.

#### 4.4.2 Precipitation

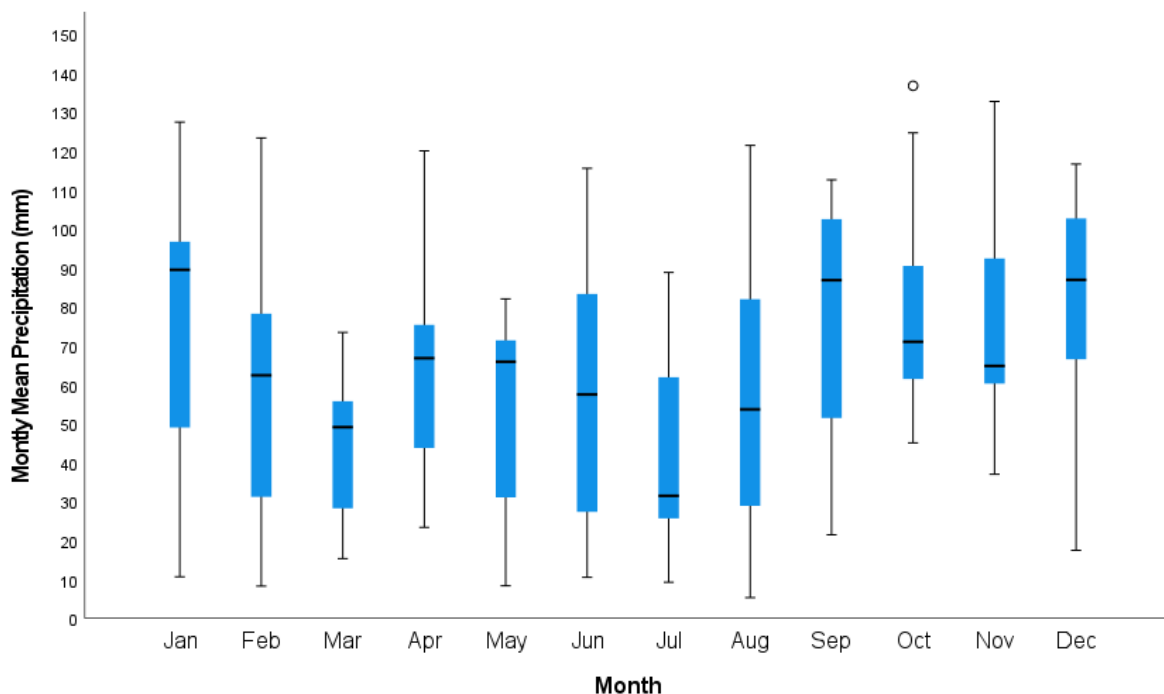
Figure 4.7 shows the mean monthly precipitation from 1990 to 2000 in Gloucestershire. The variability in precipitation changes rapidly over time, varying by 120mm from peak (130mm) rainfall to minimum (10mm) rainfall through the decade. There are four major peaks in maximum precipitation, the highest precipitation occurs in late 1992 and late 2000 with maximum precipitation of ~130mm. the next highest precipitation occurs in 1990 and late 1994 with high precipitation of ~125mm. Similarly, the lowest rainfall also occurs during these years, with minimum precipitation occurring in both late 1993 and 1995 with lows of ~10mm. Average rainfall for the decade is 63mm with highest average precipitation of 78mm in 2000, conversely, the lowest average rainfall is 46mm in 1996.



**Figure 4.7:** Monthly mean precipitation (mm) for Gloucestershire from 1990 to 2000. Data derived from CEDA archive (Harris et al., 2020).



Average monthly precipitation between 1990 and 2000 is shown in Figure 4.8. An overview of the median values for precipitation show that rainfall typically varies from 90 to 35mm with higher precipitation occurring in January and lower precipitation occurring in July. The largest variability in precipitation is in January varying by 117mm. This is followed closely by August which has the second highest variability of 116mm and June with 105mm variability in precipitation. In contrast, the lowest variability for precipitation is March with 58mm with the average monthly variability calculated as 95mm. Three months show high measurements of precipitation. The highest precipitation values occur in January (127mm), February (123mm) and October, with an outlier of 137mm. Conversely, the lowest precipitation can be observed over four months, between May and August with minimum precipitation varying between 5.3mm to 10.5mm

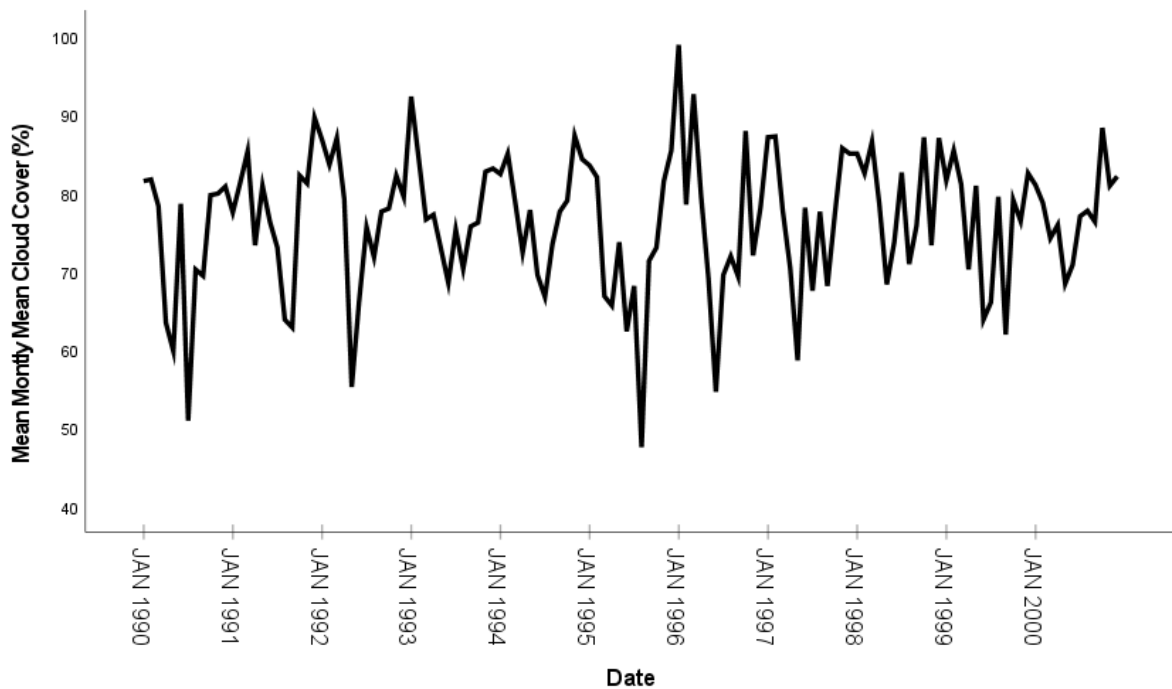


**Figure 4.8:** Average monthly precipitation data for Gloucestershire between 1990 and 2000. Derived from CEDA archive (Harris et al., 2020).

### 4.4.3 Cloud Cover

Figure 4.9 shows the variability of cloud cover for Gloucestershire. Cloud cover typically appears lower within summer months (June - August). Cloud cover is cyclical in nature with peaks in winter months (December - February) and reduced cover in summer months. Cloud cover within Gloucestershire typically varies between 85% and 55% from 1990 to 2000.

The average cloud cover percentage varies between 71 and 78% from 1990 to 2000. Trends from the figure show that the highest cloud cover percentage ranges from 90% to 99% with the highest cloud cover in January 1995 (99%) and March 1995 (93%) and the third highest in December 1991 (90%). In contrast, the minimum cloud cover percentage varies between 48% to 65% typically occurring between May and August with the lowest cloud cover percentage recorded in 1995 (48%) and 1990 (51%).

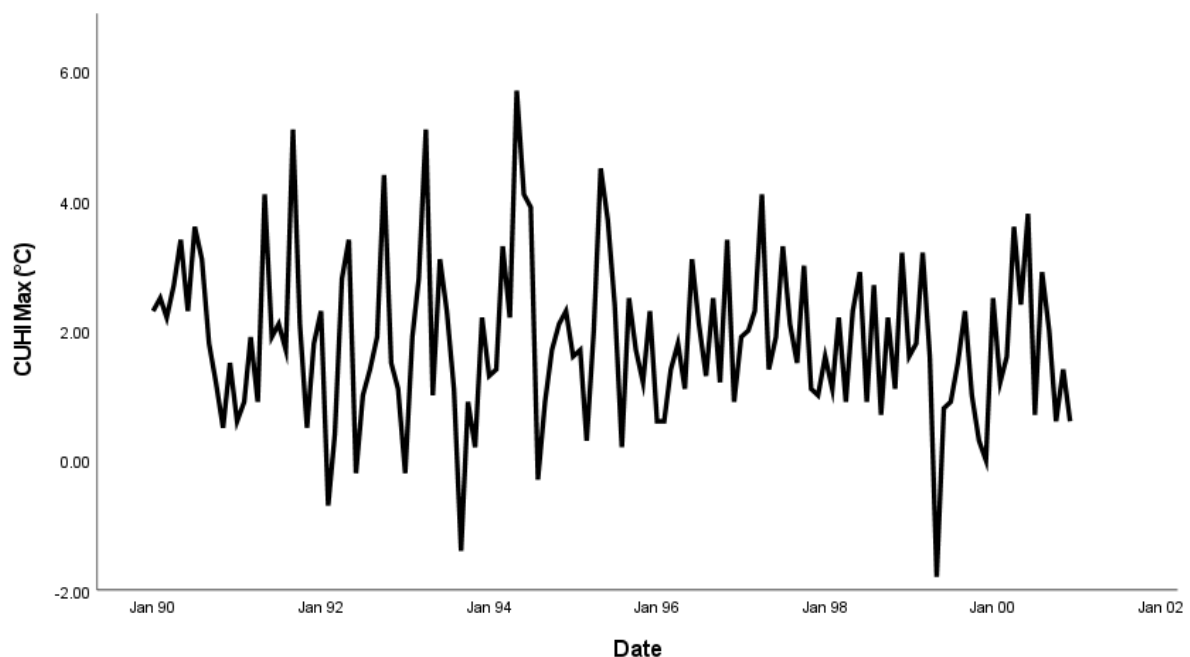


**Figure 4.9:** Monthly mean cloud cover (%) for Gloucestershire from 1990 to 2000. Derived from CEDA archive (Harris et al., 2020).

#### 4.5 Urban Heat Island (UHI) Intensity

Both CUHI maximum and minimum have been calculated to show the fluctuations in both maximum and minimum air temperatures between Cheltenham (urban) and Randwick (rural).

CUHI maximum typically varies between 1°C and 3.8°C between 1990 and 2000 (Figure 4.10). The data show how CUHI varies over time, the overall trend in CUHI maximum shows a significant increase over time from 1990 to 1995 with an increase of 2.2°C in temperatures. The temperature trends decline and stabilize from 1996 to 1999, with minor variation or fluctuation in CUHI maximum values. CUHI maximum declines significantly in mid-late 1999 before increasing and stabilizing in 2000.

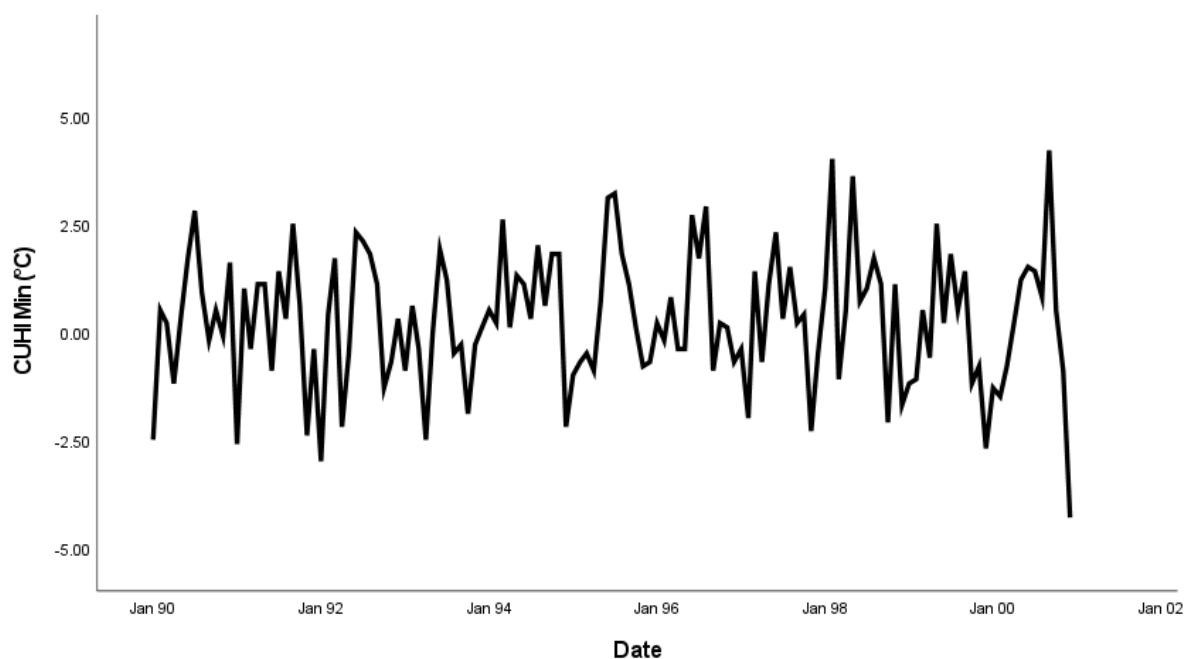


**Figure 4.10:** Maximum canopy urban heat island (CUHI) intensity from 1990 to 2000.

From Figure 4.10 there are five key outliers which have been detected: (1) mid-1990 with peak CUHI of 3.8°C; (2) in 1991 which records peak CUHI of 5.5°C, a significant period of warming occurring during the summer period; (3) late 1993, which shows a significant period of cooling with CUHI reaching -1.5°C; (4) 1995 with a CUHI of 6°C;

(5) late 1999 has a period of significant cooling,  $-1.8^{\circ}\text{C}$ . this is greater than the cooling in 1993 by  $\sim 0.3^{\circ}\text{C}$ . In comparison the average cooler CUHI temperatures, the variance between the average and maximum cold temperatures differs by  $\sim 1.5^{\circ}\text{C}$  throughout the decade.

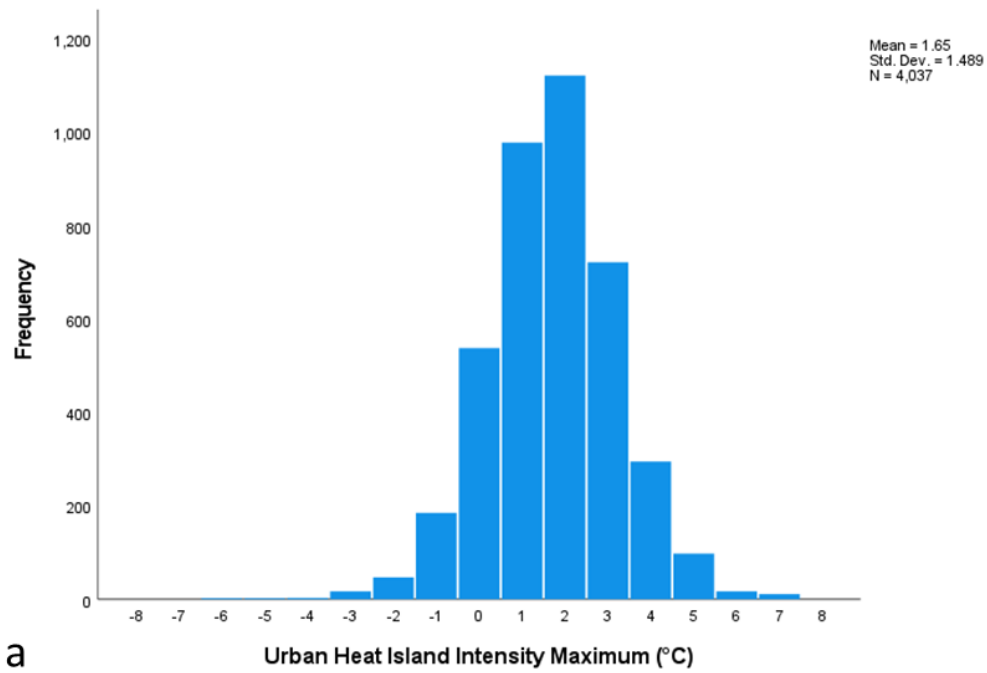
The average CUHI minimum varies between  $-2.5$  and  $2.5^{\circ}\text{C}$  through the decade (Figure 4.11). Overall trends in CUHI minimum show an increase or warming in CUHI temperatures over time, increasing by  $\sim 1^{\circ}\text{C}$  from 1990 to 2000. Negative temperature trends within this data show little or no change ( $\sim 0.3^{\circ}\text{C}$  variation) in trends except for the sharp decline in temperatures occurring in late 2000. From Figure 4.11 four key outliers can be noted: (1) late 1995 shows a significant increase in CUHI minimum temperatures, reaching  $3^{\circ}\text{C}$ ; (2) 1998 with temperatures exceeding  $3^{\circ}\text{C}$ ; (3) mid-2000 with the CUHI minimum exceeding  $3.5^{\circ}\text{C}$ ; and (4) a significant period of cooling in late 2000 with CUHI minimum plummeting down to  $-3.5^{\circ}\text{C}$ .



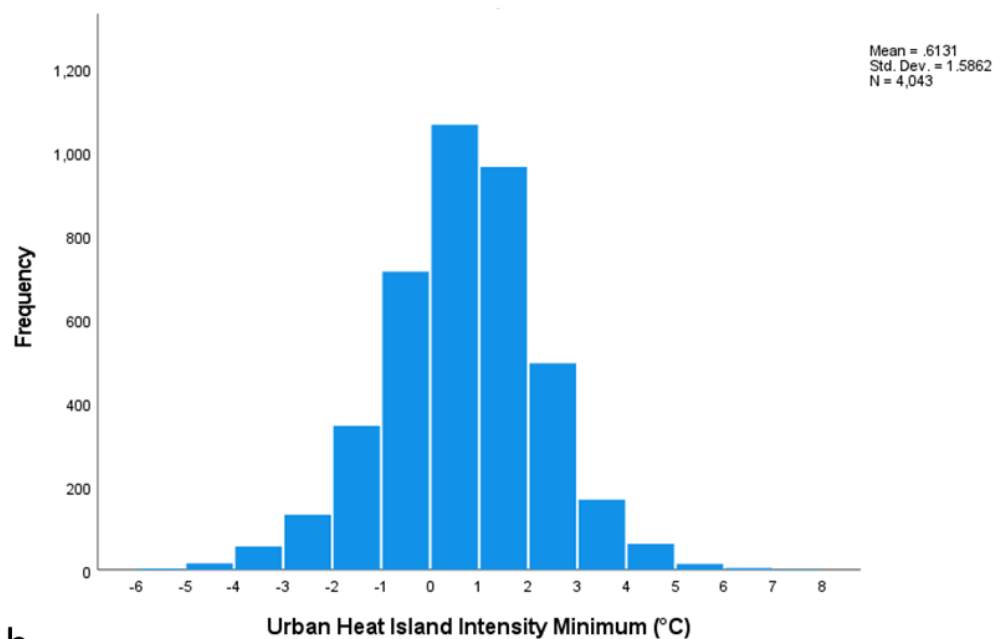
**Figure 4.11:** Minimum canopy urban heat island intensity (CUHI) from 1990 to 2000.

Daily CUHI frequency plots were produced for minimum and maximum UHI intensity (Figure 4.12). These show that there were 1122 days in the temperature record with a maximum intensity exceeding 2°C, and 125 days when this exceeded 5°C (Figure 4.12a). There were 256 days of the record temperature of -1°C or less, and only 5 days recording -4°C or less; which demonstrates periods of urban cooling, to which urban areas present cooler air temperatures when compared with their rural counterpart. Although there is high frequency in UHI intensity exceeding 1°C or more, 978 cases are recorded in the data with no variation in UHI intensity. A summary of the data is provided, where the mean CUHI maximum is 1.65°C with a standard deviation of 1.49°C.

An evaluation of the UHI intensity minimum frequency (Figure 4.12b) shows high frequency in warming with UHI intensity reaching up to 8°C. 966 cases record a UHI of 1°C with a further 495 cases recording an UHI intensity in excess of 2°C. Although there is a large spread (2,821 days) of positive UHI intensity, 560 cases of net cooling in the UHI intensity reaching below 0°C; three of these cases are an extreme value of -6°C. Despite the variation in frequencies and range of values, the highest frequency value is 0°C for CUHI minimum, with over 1067 cases recorded. A summary of the mean CUHI minimum is 0.61°C with a standard deviation of 1.59°C.



a



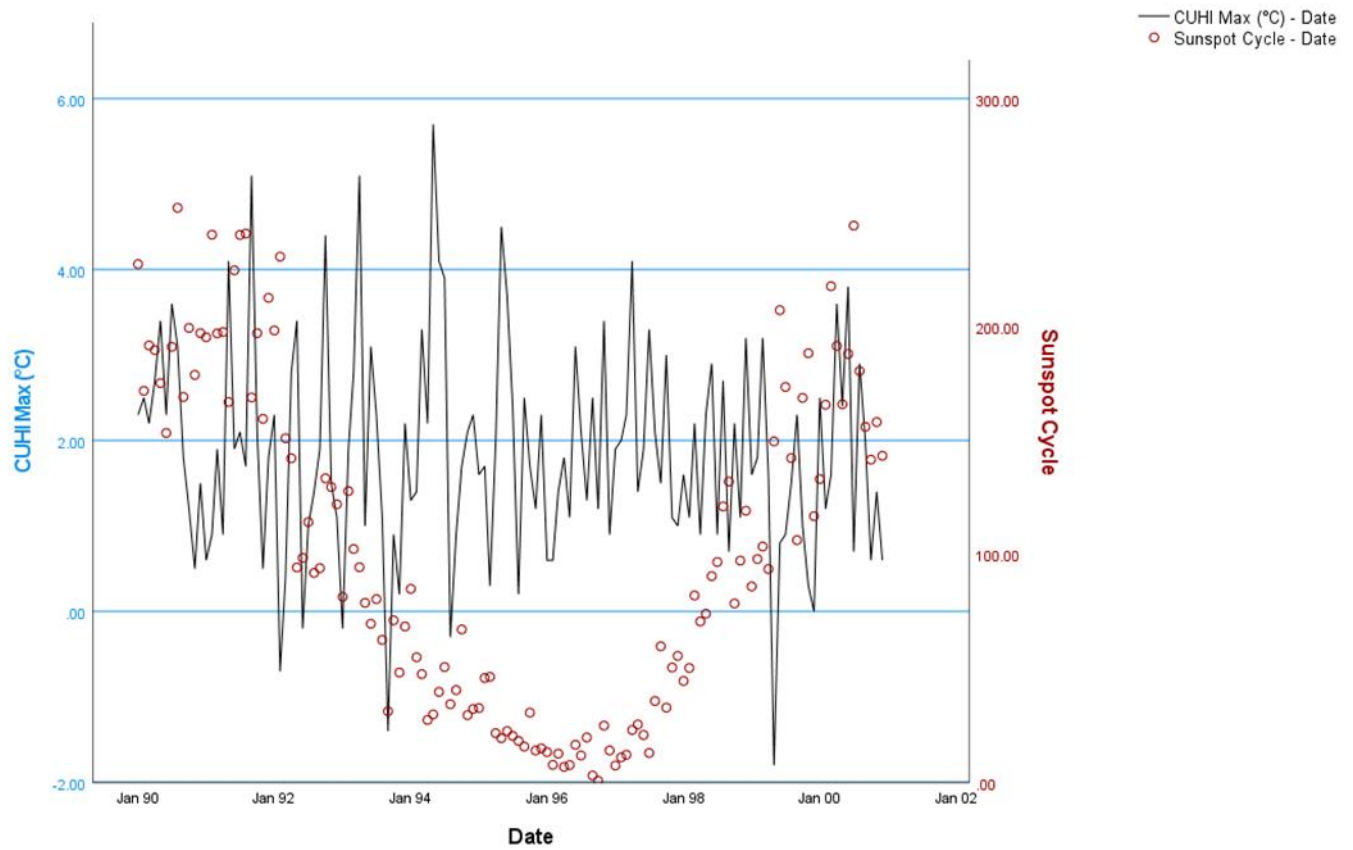
b

**Figure 4.12:** Frequency plots of daily mean urban heat island (UHI) intensity values, for (a) maximum and (b) minimum UHI Intensity.

#### 4.6 Sunspot Cycles and Urban Heat Island (UHI) Intensity

Figure 4.13 shows UHI maximum and sunspot cycle. In 1990 the peak sunspot cycle corresponds to increased temperatures. CUHI decreases in intensity as Sunspot cycle declines over time. CUHI increases again in 2000 corresponding to the

increase in sunspot cycle. A key outlier within the data is from 1994 to 1995 as CUHI increases significantly at a point of Sunspot minima.



**Figure 4.13:** A dual-axis plot of CUHI maximum and Sunspot Cycle.

## 4.7 Analysis of relationships

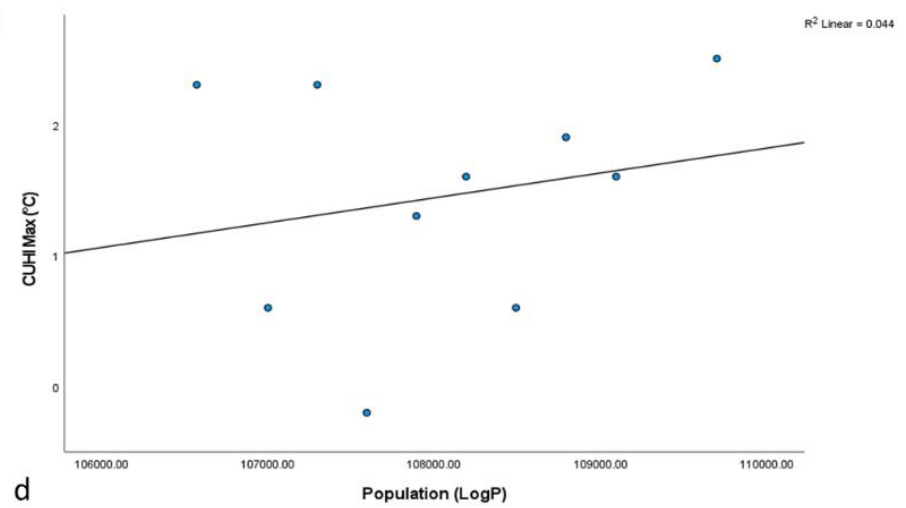
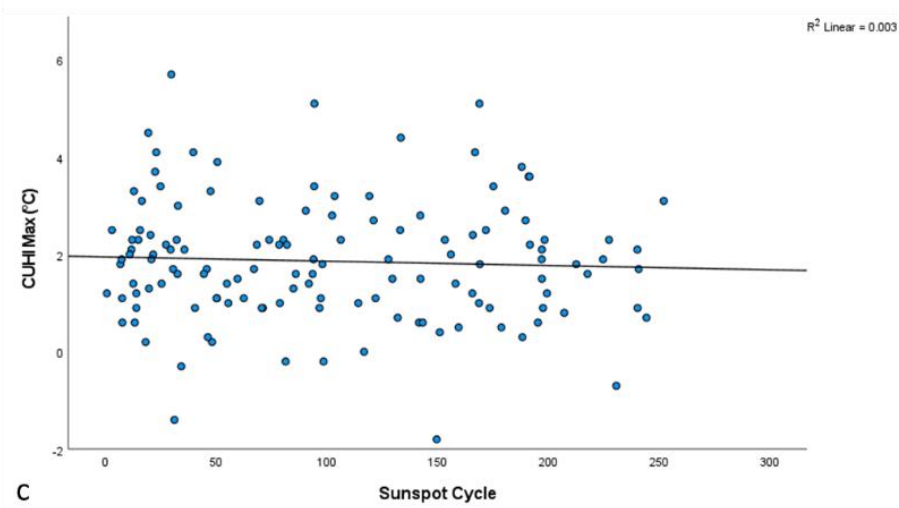
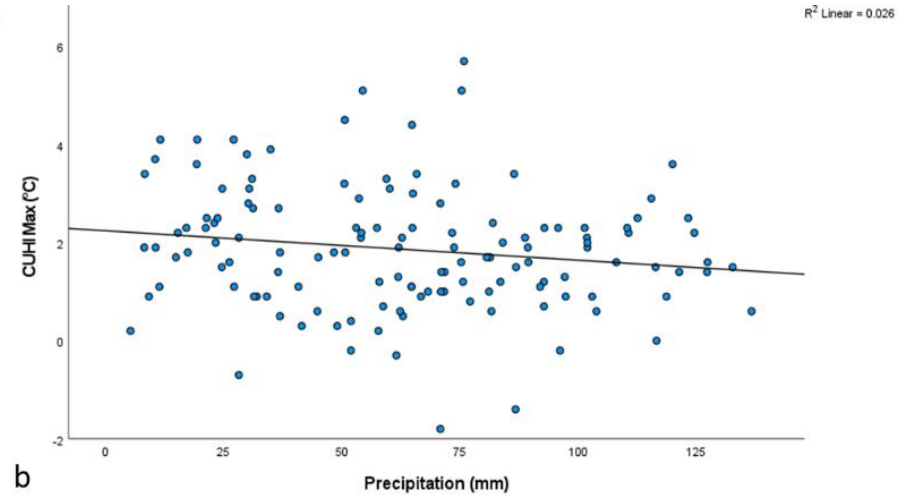
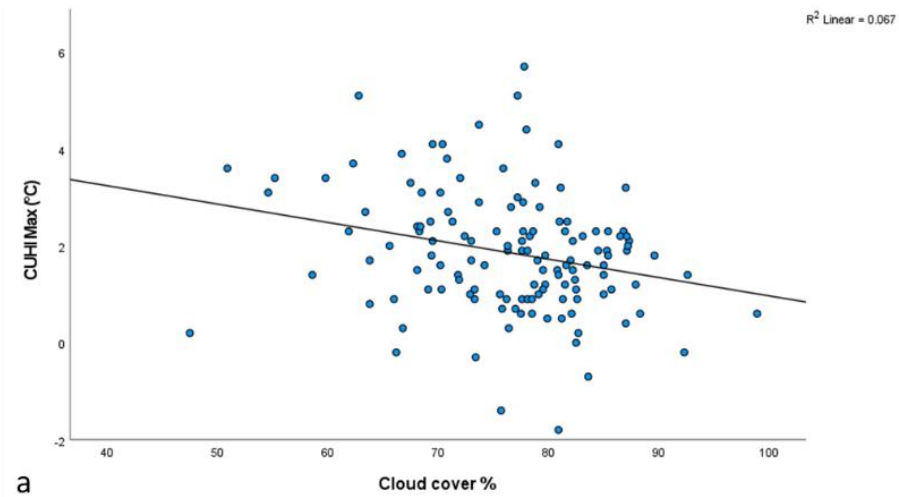
### 4.7.1 Correlation and Regression Analysis of maximum CUHI

There was a significant, weak negative correlation between maximum CUHI and cloud cover (Figure 4.14a and Table 4.6:  $r = -0.248$ ,  $n = 132$ ,  $p = 0.003$ ). A negative correlation was found between precipitation (Figure 4.14b and Table 4.6:  $r = -0.160$ ,  $n = 132$ ,  $p = 0.067$ , and sunspot cycles (Figure 4.14c and Table 4.6:  $r = -0.051$ ,  $n = 132$ ,  $p = 0.563$ ), however, this was not found to be significant. A positive correlation was found between maximum CUHI and population, but again this was not found to be significant (Figure 4.14d and Table 4.6:  $r = -0.211$ ,  $n = 132$ ,  $p = 0.559$ ).

**Table 4.6:** Pearson's correlation analysis between maximum CUHI and Cloud Cover (%), Precipitation (mm), Sunspot Cycles, and Population. \*\*. Correlation is significant at 0.01 level (2-tailed).

		Cloud cover %	Precipitation (mm)	Sunspot Cycle	Population (LogP)
<b>CUHI Max (°C)</b>	Pearson	-.258**	-.160	-.051	.211
	Correlation				
	Sig. (2-tailed)	.003	.067	.563	.559
	N	132	132	132	10
	R	.258	.16	.051	.211
	R <sup>2</sup>	.067	.026	.003	.044





**Figure 4.14:** Relationship between maximum CUHI and (a) cloud cover (%), (b) precipitation (mm), (c) sunspot cycles, and (d) population

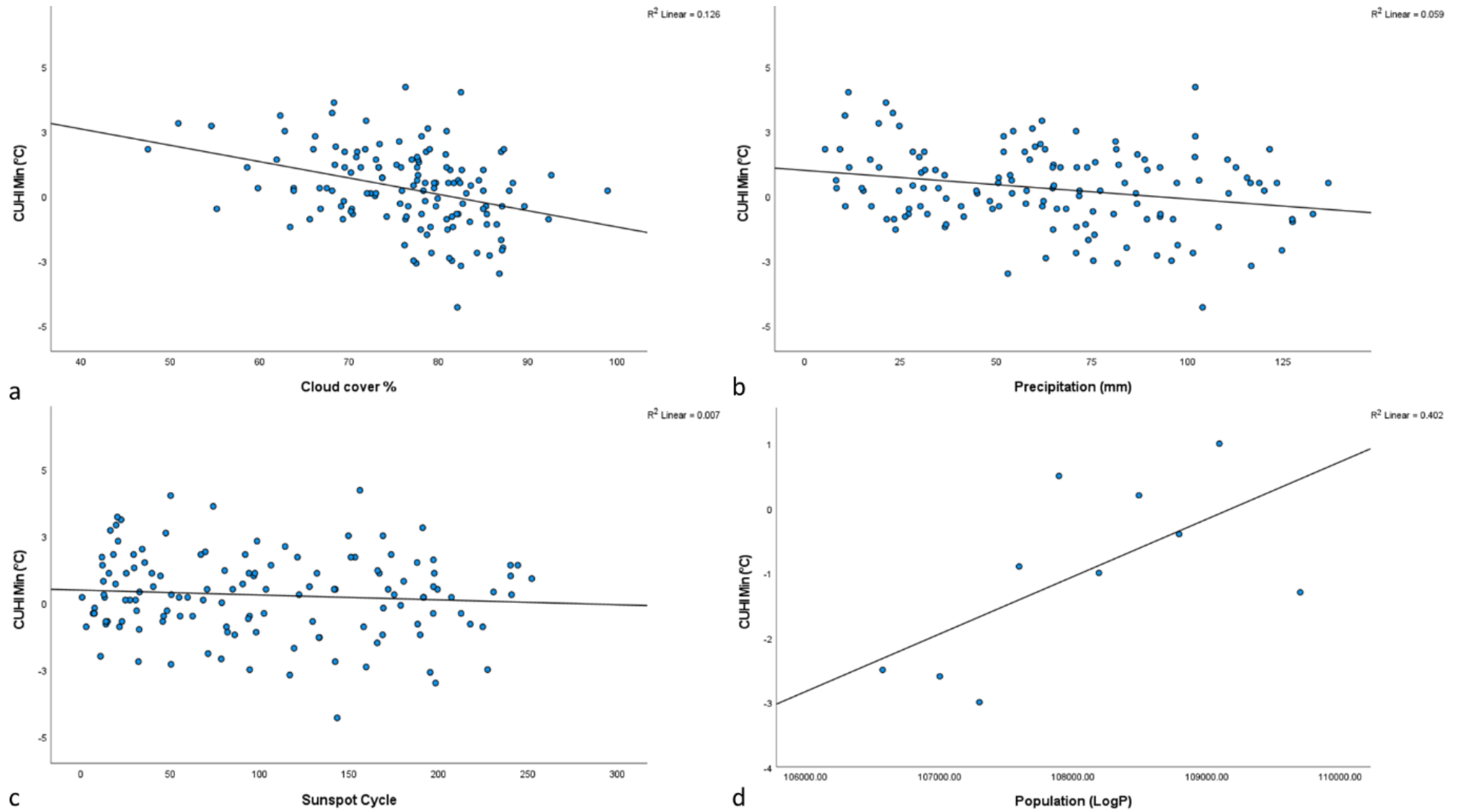
#### 4.7.2 Correlation and Regression Analysis CUHI Minimum

A significant, strong positive correlation was found between minimum CUHI and population (Figure 4.15d and Table 4.7:  $r = -0.634$ ,  $n = 132$ ,  $p = 0.049$ ). There was a significant, moderate negative correlation between minimum CUHI and cloud cover (Figure 4.15a and Table 4.7:  $r = -0.355$ ,  $n = 132$ ,  $p = 0.000$ ). Minimum CUHI and precipitation showed a significant, weak correlation (Figure 4.15b and Table 4.7:  $r = -0.243$ ,  $n = 132$ ,  $p = 0.005$ ). A weak, negative correlation was found between minimum CUHI and sunspot cycles (Figure 4.14c and Table 4.7:  $r = -0.051$ ,  $n = 132$ ,  $p = 0.563$ ), however, this was not found to be significant.

**Table 4.7:** Pearson's correlation analysis between minimum CUHI and Cloud Cover (%), Precipitation (mm), Sunspot Cycles, and Population. \*\*. Correlation is significant at the 0.01 level (2-tailed).

\*. Correlation is significant at the 0.05 level (2-tailed).

		Cloud cover	Precipitation	Sunspot	Population
		%	(mm)	Cycle	(LogP)
CUHI Min (°C)	Pearson	-.355**	-.243**	-.086	.634*
	Correlation				
	Sig. (2-tailed)	.000	.005	.325	.049
	N	132	132	132	10
	R	.355	.243	.086	.634
	R <sup>2</sup>	.126	.059	.007	.402



**Figure 4.15:** Relationship between minimum CUHI and (a) cloud cover (%), (b) precipitation (mm), (c) sunspot cycles, and (d) population

## 5. Discussion

### 5.1 Air Temperature Trends

Ten-year average air temperature trends fluctuate over time, decreasing and increasing from 1990 to 2000. A strong increase in air temperature occurred around 1990, 1995 and 2000 for all sites within Gloucestershire. Significant increases in temperature variations were detected of around  $\sim 2^{\circ}\text{C}$  on average before and after 1995. This increase in air temperature is an anomaly that justifies investigation. This study originally postulated that fluctuations in the energy balance equation would result in changes in both air temperature and UHI intensity. Changes in incoming solar radiation have a profound effect on the energy balance. As a substitute for solar radiation, sunspot cycles were used as a surrogate measure.

A running 10-year average (Table 4.1) was calculated for the region to generate a background decadal temperature profile. The regional average air temperature profile for Gloucestershire has been calculated as  $29.38^{\circ}\text{C}$  for maximum air temperature and  $-7.31^{\circ}\text{C}$  for minimum air temperature.

Comparing this to Cheltenham's 10-year average air temperature profile,  $31.34^{\circ}\text{C}$  maximum and  $-7.28^{\circ}\text{C}$  minimum average for the site it. A  $1.96^{\circ}\text{C}$  temperature difference in maximum air temperature and  $0.03^{\circ}\text{C}$  difference in minimum air temperature can be calculated. This difference shows the markedly higher temperatures that Cheltenham records when compared to the background regional air temperatures. This indicates that there is trend of warming in Cheltenham when compared with its surroundings. Furthermore, when comparing this average to that of the 30-year average from 1981 – 2010 produced by the Met Office (2017), Cheltenham's maximum average air temperature has been calculated as  $14.69^{\circ}$  and

6.8°C for minimum average air temperature. The 10-year average calculated within this study shows a stark difference in recordings when compared against each other. This may be owing to the Met Office using a larger sample and their handling of said data. Smoothing the 30-year average of air temperature data removes outliers within data sets and larger samples produce differences in mean air temperature outputs.

Although the stark difference, the analysis of data used in this study is representative of the location within the constraints of the spatio-temporal analysis. By this, the results for Cheltenham and the regional background air temperature profiles are reflective and representative of the 10-year collation of air temperature used within this study and reflect fluctuations in air temperature data from 1990 to 2000.

Furthermore, this study is caveated by its limitation of available data for the area and by its spatial extent. Although this can be considered a case-study, these results from this study cannot be confidently extrapolated as a real-world example. By this, this study is limited by its temporal and spatial extent. However, this study does provide context for the UHI effect within small towns and cities.

The 10-year running average temperature figures for Cheltenham are 31.34°C (Maximum) and -7.28°C (Minimum). In comparison to other locations within the study area, these are significantly higher, by 3.43°C (maximum) and 0.95°C (minimum), than its neighboring urban and rural neighbors. Therefore, this provides a key indication of the magnitude of the UHI in Cheltenham, which is 1.96°C (maximum) and 0.03°C (minimum) higher when compared to its regional background temperature profile and surrounding conurbations.

Upon closer analysis, monthly averages break down the temporal variability of air temperature for each location within the study area. Temporal patterns follow a

cyclical nature, typical of temperature data over time. These cyclical patterns show increases in air temperature during warmer, summer periods and decreases in air temperature during cooler, winter periods. Thus, the seasonal variability of the air temperature profile for each location is revealed. However, a stronger method for establishing the significance of this is needed. This study is caveated by its limitations in statistical analysis and can only be interpreted based on what the data shows. Figures 4.2a through 4.2g display this trend through the use of time-series. Scrutiny needs to be applied to the interpretation and analysis to some locations as noted in Table 4.2, as Stewart and Mills (2021) state that interpretation and analysis should only be applied where complete data are existent. Although some locations are missing data and attempts to interpolate and handle missing data have been avoided to reduce bias and forcing of data values, this conclusion may be drawn. Data are untampered and un-interpolated to infill missing values, the data are still representative of each site for the points in time that data exist and therefore despite incompleteness, are still valuable owing to their metadata collected at each weather station. For the sake of the study and the importance metadata hold to the investigation and evaluation of temperature profiles, background climate and UHI studies (Stewart and Mills, 2021; Oke, 2017) alike, they have been included for these reasons.

## 5.2 Impact of Weather and Population on the CUHI

### 5.2.1 Impact of Cloud Cover

Atmospheric processes have a direct effect on both weather and climate as energy is transferred between the Earth's surface and atmosphere through conduction, convection and radiation (Oke, 2017; Stewart and Mills, 2021). This study found that increased cloud cover has a profound inverse effect on CUHI intensity in Cheltenham. It is known that UHI intensity is most pronounced under clear, anticyclonic conditions (Oke, 1998) and that meteorological characteristics affect UHI intensity (Lee et al., 2014).

A correlation analysis was performed to evaluate the impact of cloud cover on the CUHI. The results from Table 4.6 show that there was a statistically significant, weak negative correlation between CUHI maximum and cloud cover percentage,  $r(130) = .258, p = .003$ . The results of the correlation show that cloud cover increases, CUHI decreases. Similarly, a correlation analysis was performed to test the relationship between CUHI minimum and cloud cover. The results from Table 4.8 show that there was a statistically significant, weak, negative correlation between CUHI minimum and cloud cover percentage  $r(130), = .355, p = .000$ . This relationship shows that as cloud cover increases, CUHI minimum decreases. From this, this study confirms that Cheltenham's CUHI intensity is conditioned by fluctuation in cloud cover. It can be stated that an inverse relationship exists between these two variables; where an increase in cloud cover presents decreases in CUHI intensity.

The statistical relation between cloud cover and CUHI are universally known, such that cloud cover demonstrates negative correlations (Stewart and Mills, 2021). However, the results from this study only show weak correlations, whereas Stewart and Mills (2021) state that strongly negative correlations are common. To explain

this within the constraints of this study, a town or city's location, size, shape and function have confounding effects on air temperature and the surrounding atmospheric processes including the effects of cloud cover for a given location. Typical studies as defined by Stewart and Mills (2021) focus largely on larger cities and mega-cities, with larger quantities of data supporting the relationship between cloud cover and UHI intensity. Therefore, a reduction in sample size and transition from cities to small towns would provide reasons to explain the smaller correlations. In contrast to the typical studies performed, as described by Stewart and Mills (2021),

Cheltenham is a small town, situated within the confounds of the Cotswold's. Its location and size, as defined by population, ranges from 107,102 to 116,043 between 1990 and 2020 (ONS, 2018; Inform Gloucestershire, 2020). Secondly, its population density is lesser than larger cities or mega-cities in comparison.

Furthermore, its size and shape, as defined by area only covers 46.62km<sup>2</sup> (ONS, 2016). In comparison, London is the most populous city in the UK with a city population of around 8 million and a metropolitan area population of 12 – 14 million, therefore making it a megacity (Hacker et al., 2010) which has increased land area, continuous urban land classifications and larger shape and size by comparison to Cheltenham. An analysis of cloud cover on the London UHI, Hacker et al., (2010) show that the variation in UHI intensity decreases with increased cloud cover.

Furthermore, a study into the frequency of UHI frequency against weather phenomena by Wang et al., (2015), shows that UHI frequency increases with lower cloud cover. These studies further support the relationships shown within this study into the relationship between cloud cover and UHI. However, links have been made in extensive long-term analysis of persistent cloud cover on the UHI in megacities



(London and Paris) showed associations between persisting cloud cover to prolonged surface heating and convection over megacities (Theeuwes et al., 2019).

To compare this with a study, which similarly investigates UHI intensity in small towns. Pinho and Orgaz (2000) investigated the UHI in Aveiro, a small coastal town in Portugal. Their results found a significant negative correlation between cloud cover and UHI. The reduction in UHI intensity in relation to cloud cover are associated with low-pressure (cyclonic) conditions. Within the context of the energy balance, clouds reduce the reception and release of radiation which moderates UHI intensities (Hidore & Oliver, 2010). However, the location of Aveiro, being a coastal town, and the influence of water-bodies were not accounted for. According to Oke et al., (2006), corrections of air temperature near water-bodies must be accounted for. The only data treatment used by Pinho and Orgaz (2000), was to account for time lags between mobile transects in collecting air temperature data.

A further explanation into the weak correlation between CUHI maximum and minimum against cloud cover is that according to Morris et al., (2000), most UHI studies are usually limited to the atypical conditions thought to be optimal for its development. This is to say that previous studies typically focus on the development of the UHI under stable anticyclonic events with clear skies and calm conditions. However, this study follows a holistic approach using a range of decadal data from weather stations situated within Gloucestershire to investigate the UHI under a wider climatological spectrum (Taeslar, 1986). In sum, this study uses normal, broader range of typical weather conditions within the normal daily to annual cycle of weather events as described by Morris et al., (2000).

Few studies have analysed datasets which have both high temporal resolution and have covered an extended period of time (Morris et al., 2000). Morris et al., (2000) elaborates on this by stating that using long, historical data, studies allow for more putative explanations to the variability of the physical processes that influence UHI magnitude. The use of high temporal resolution data used within this study, using atypical conditions, which other studies follow provides insight into the natural variations of the CUHI over time. However, the spatial limitation of this study cannot conclude the variation of UHI and cloud cover over spatial scales. Therefore, an investigation into the spatial variation of CUHI and cloud cover would be recommended for further analysis.

Explanations to this relationship can be explained through changes in pressure, which lead to the formation of cyclones and anti-cyclones. These pressure systems relate to weather and climate at both local and regional scales (Burt, 1992).

Therefore, it is possible to assume that weather variables such as precipitation and cloud cover have an adverse effect on CUHI. It is known that UHI intensity is most pronounced under clear, anticyclonic conditions (Oke, 1998) and moreover, that meteorological characteristics affect UHI intensity (Lee et al., 2014). Under these anticyclonic conditions, the UHI can be seen to increase. Calm, clear conditions with low or no cloud cover can be shown in Figure 4.14a and 4.15a which shows the relationship between low cloud cover and high CUHI maximum and minimum.

The correlation shows that with increased cloud cover percentage, the intensity of the UHI decreases in temperature. Cloud cover percentage, therefore, affect flows of radiation by reflecting some, absorbing part and transmitting the remainder of incoming incident radiation from the Sun. Typically, under ideal conditions, clouds tend to warm the Earth by radiating sky radiation to the ground and by preventing the

loss of terrestrial radiation to space. On the contrary, increased cloud cover causes cooling on the whole by reflecting solar radiation away from the Earth, back into space (Linacre and Geerts 1997). In summary, increased cloud cover reduces overall maximum and minimum both CUHI minimum and maximum temperatures by reflecting solar radiation away from the Earth, resulting in cooler temperatures. Although the typical studies across the literature focus on cloud cover fraction and cloud type, the theory remains the same, cloud fraction and cover are linked to the sign of incoming radiation and its interaction with temperature and atmospheric processes (Karlický et al., 2020). Overall, the analysis shows that increases in cloud cover percentage result in decreases in the UHI magnitude. However, its causality cannot be determined, and caution must be applied when extrapolating patterns in magnitudes or differences in urban-rural temperature in relation to cloudy or non-cloudy conditions (Kidder and Essenwanger, 1995).

### **5.2.2 Relationship of Precipitation and CUHI**

A correlation analysis was performed to test the relationship between CUHI maximum (Table 4.6). The results show that there was no significant relationship between CUHI maximum and precipitation,  $r(130) = -.160$ ,  $p = .067$ . Despite no significant relationship between the two variables, the trend still shows a weak, negative correlation between CUHI maximum and precipitation. Therefore, the results of this analysis cannot be extrapolated. The cause of the insignificant relationship can be explained by Stewart (2011) and Lowry (1977), who states researchers passively control weather to reduce the risk on confounding 'real' heat islands with 'fictitious' ones. To explain this, it is to say that sampling designs must be decisive in their approach to investigating the effects of weather on the UHI effect. This is the argument on using steady or unsteady weather as a metric to test against

CUHI intensity. In this study, atypical data were used to evaluate the CUHI of Cheltenham from 1990 to 2000, however through using atypical data in the form of continuous, long-term, historical data, as opposed to the optimal conditions used in typical studies this introduces a confounding effect on the statistical relationship between CUHI maximum and precipitation (Lowry, 1977; Stewart, 2011). In sum, the use of continuous weather data, which is homogenous to the study area, introduced extraneous effects which have produced insignificant relationships. Therefore, to rectify this for future study, it would be advised to either use select, typical data to reperform the analysis to investigate the true relationship between precipitation and CUHI maximum. Or, to find new methods to correct for the extraneous effects of weather on the CUHI magnitude.

In contrast to this, a correlation analysis between CUHI minimum and precipitation was performed Table 4.8. The results showed a significant, weak, negative correlation between CUHI minimum and precipitation.  $r(130) = -.243$ ,  $p = .005$ . The results of this analysis show that as precipitation increases, CUHI minimum decreases. The implications of this suggest that CUHI minimum is more adversely affected by increased precipitation than CUHI maximum. This relationship is supported by Arifwidodo and Chandrasiri, (2015) who state that precipitation is found to be inversely proportional to the UHI magnitude.

According to (He, 2018), it is widely evidenced that precipitation reduces urban temperature. Furthermore, the reduction in urban temperature consequently reduces the temperature difference between urban and rural areas, thus, lowering CUHI intensity (He, 2018). The reduction in CUHI minimum can be explained through the association with lower intake of shortwave radiation, as a consequence of cloud covering (Jin, 2012). This interaction between precipitation and increased cloud

cover impacts the amount of incoming solar radiation to Cheltenham, thus reducing the CUHI intensity. Placing this in a wider context, it can be stated that incident radiation is reduced in urban areas owing to increased diffusion and reflection of solar radiation through increased cloud cover owing to precipitation. Furthermore, increased precipitation alters the emissive and reflective properties of urban environments (Doughty et al., 2012). Direct receipt of radiation at surface level is reflected further and dissipated owing to increased albedo properties (Doughty et al., 2012) Focusing solely on the principle of increased precipitation, increased wet surfaces allow for cooling effects in urban areas owing to evapotranspirative processes. This would therefore increase specific heat capacity of surfaces and reduce latent heat (Oke et al., 2017)

Although the relationship is small between the two variables, the results show that CUHI minimum decreases marginally as precipitation increases. Contextualizing this relationship within the literature, it is possible to reason that increased rainfall increases soil moisture, which in turn affects surface temperatures and transmission of heat. Put simply, a larger amount of energy is required to induce warming. Therefore, as precipitation increases, CUHI minimum decreases as a result of both sensible and latent heat fluxes. It is important to note that the process of precipitation cannot be isolated on its own or reduced to simple terms. It is commonly recognized that increased cloud coverage precursors precipitation (Yu et al., 2009; He, 2018). Increased cloud cover has been shown to have a correlation with decreases in CUHI within this study. As cloud cover and precipitation are associated variables, both increases in cloud cover and precipitation have a negative correlation with CUHI temperatures. Furthermore, evaporation after precipitation interacts with both urban sensible and latent heat (Li et al., 2011). Evaporation as a process removes latent

heat within urban environments. Overall, the analysis of the impacts of precipitation on CUHI intensity indicate that CUHI intensity is far greater under stable meteorological conditions (Gonçalves et al., 2018).

### **5.2.3 Population Growth and CUHI**

Population density and growth have been strongly associated with UHI intensity (Oke, 1967; Rauf et al., 2020). The relationship between population (LogP) and CUHI maximum was explored. The results from Table 4.6 show no statistically significant correlation between population and CUHI maximum,  $r(8) = .211$ ,  $p = .559$ .

Many studies show a significant relationship between population and the UHI. A study based on 67 cities in North America found strong positive correlations between UHI population (Zhao et al., 2014). Furthermore, Oke (1967), shows a positive correlation between average UHI and population growth for European settlements, including London. However, the results from this study show that CUHI maximum and population show no significant relationship. Despite this relationship, the trend shows a weak, positive correlation between the two variables, which is supported by the literature. Despite this, interpretation and extrapolation of this relationship is therefore limited. The results for this can be attributed to Cheltenham having a smaller population size. Although relationships between population and CUHI have shown strong relationships (Zhao et al., 2014), these cities typically have larger population size, density and larger samples. The small samples of data used within this study both reduce the effect size and significance of the relationship between the two variables. In contrast to this study, Levermore and Parkinson (2015) investigated UHI intensity in Manchester, which has a population of 2.8 million. The results showed that Manchester demonstrated high UHI intensity, comparable to London. Although their study did not directly investigate the effect of population on the UHI

effect, their study implies that higher population has a proportional effect on UHI intensity and frequency and therefore a greater effect.

A further criticism into the use of population as a metric for establishing relationships with CUHI is that population growth is commonly associated with urbanization (Arifwidodo and Chandrasiri, 2015). The urban infrastructure of Cheltenham is composed of both Regency period and modern buildings, although it has developed rapidly over time, the area is still relatively small when compared to other studies such as Manchester (Levermore and Parkinson, 2015) and London (Hacker et al., 2010). Therefore, with regard to population as a metric of urbanization, the degree of CUHI intensity is not going to establish itself as a significant relationship. The urban metabolism, in comparison to cities and mega-cities, is lesser for Cheltenham, as there is no dependant need for the exchange of materials and energy for urbanization (Marx, 1981).

Conversely, the relationship between population (LogP) and CUHI minimum was explored. The results from Table 4.8 show a strong, positive, statistically significant correlation between CUHI minimum and population,  $r(8) = .634$ ,  $p = .049$ .

The relationship between population and CUHI minimum indicates a strong relationship between population growth over time and increase in CUHI minimum. Anthropogenic activities such as population growth have been considered a key driving mechanism of UHI intensity. The increase in population growth extends outwards, contributing towards increased CO<sub>2</sub> emissions, urban expansion and urban sprawl and alterations to the natural landscape (Oke, 2017; Stewart and Mills, 2021, Nuruzzaman, 2015; Marx, 1981). The increase in CUHI maximum and minimum are reflective of these anthropogenic activities and support the literature

and field of study they relate to. A key focus on the increase in CUHI minimum is important to note as it shows increased minimum temperatures over time. This process of warming shows the increase in the CUHI magnitude over time. Although Cheltenham is a small town, in comparison to other studies investigating larger cities (Peng et al., 2019) it shows that even smaller towns and cities have prevalent UHI and are key areas to study further. This study does not suggest that only Cheltenham is unique for having an UHI effect. Instead, this study supports, and is supported by surrounding literature regarding smaller towns and cities having urban heat islands. This study is limited owing to its nature of being a case-study and therefore cannot be confidently validated without further research to quantify the urban heat island effect within Cheltenham.

### **5.3 Relationship Between Sunspot Cycles and CUHI**

This study originally postulated that fluctuations in the energy balance equation would result in changes in both air temperature and UHI intensity. Changes in incoming solar radiation have a profound effect on the energy balance. As a substitute for solar radiation, sunspot cycles were used as a surrogate measure.

The relationship between sunspot cycle and CUHI maximum was investigated (Table 4.6). The results show that there was no statistically significant relationship between sunspot cycle and CUHI maximum,  $r(130) = -.051$ ,  $p = .563$ .

Similarly, the relationship between CUHI minimum and sunspot cycle was investigated (Table 4.8). The results showed no statistically significant relationship between CUHI minimum and sunspot cycle,  $r(130) = -.086$ ,  $p = .325$ .

A sunspot is a relatively dark area on the Sun occupying up to 0.2% of the sun's visible surface area; they can reach temperatures of up to ~3000 degrees Kelvin



(Linacre and Gerts, 1997). Sunspots alter the solar constant by 0.3% but are associated with slight increases in ultraviolet radiation and solar winds (Linacre and Geerts, 1997). This increase in radiative output from the Sun, based on the concept of the energy balance should show markedly higher temperatures and a strong correlation between CUHI and sunspot cycle. However, the results of the analysis contradict this claim. Henson (2002), states that even at smaller scales, the eleven-year cycles can trigger variations in global temperatures and result in a slight warming of Earth's temperatures (Linacre and Geerts, 1997). Although the data do not support this, it is potentially possible that at smaller scales, within the context of this study, that the relationship is not significant nor detectable. However, within the context of Burt (1992), higher solar radiative outputs and zenith angles are more detectable within a regional or national context.

Sunspot cycles were used as an experimental surrogate measure for solar intensity which, as explored by the literature show that increased incoming net radiation have a profound effect on both air temperature and UHI intensities (Burt, 1992; Harmon et al., 2004). The analysis showed no correlation between CUHI and sunspot cycle. (Nazari-Sharabian and Karakouzian, 2020) conclude that sunspot activities should not be translated directly into climate but are likely an influence. the study used nine locations in Iran, which represented the climatic conditions of the country. Analysis from sunspot numbers and their effect on weather phenomena suggest that there are more factors which affect this relationship such as human-driven changes, changes in land use and classification and the UHI effect. Within the context of this study, the correlation between sunspot cycle and CUHI can be inferred through this. Moreover, the peaks in air temperature and CUHI maximum for 1990, 1995 and

2000 correspond more putatively toward extreme weather events in the form of heatwaves.

### **5.3.1 Isolating Sunspot Cycle and CUHI**

Although no relationship was found, visual analysis between air temperature trends and sunspot cycles, there appears to be an inverse relationship between sunspot data and air temperature trends for 1995 when compared with the relationship between air temperature and sunspot data for both 1990 and 2000 (Figure 4.13).

Peaks in sunspot cycles correspond to both higher temperatures reported in 1990 and 2000 and further correspond to the British maxima recorded in 1990 and 2003.

To elaborate, Cheltenham recorded the British maximum of 37.1°C in 1990, this event corresponds with a peak in maximum sunspot observations which too, occurred in 1990. Furthermore, this event corresponds with a peak in the CUHI maximum values (Figure 4.13). Cheltenham lost the record for British maximum temperature in 2003 to Faversham, Kent, which also occurred after peak sunspot cycle, between 2000 and 2003. However, increased temperatures in 1995 within Gloucestershire are unaccounted for during a period of sunspot minima. Maximum air temperatures for sites within Gloucestershire recorded between 31°C and 35°C in 1995, ~4°C higher than the previous three years.

Similarly, to this, in 2019, Cambridge Botanic Gardens achieved the new British maximum, however, this occurred during a period of sunspot minimum. Therefore, other systems must be at work to influence peaks in air temperature at this scale. In comparative studies, Friss-Kristenson and Lassen (1991) and Solheim et al., (2012) account for this discrepancy. According to their observations, they indicate there is a time lag between solar activity and air temperature in the northern hemisphere. This

time lag shows that there is a delay between peak sunspot activity and air temperature response. Reichal et al., (2001); Solheim et al., (2012) indicate the duration of time lag is ~2 years. Furthermore, they conclude that in accordance with this, the length of one solar cycle can indicate the temperature trends of that in the next cycle (Solheim et al., 2012).

Richards et al., (2009), state that the typical sunspot cycle is  $10.80 \pm 0.50$  years. Continuing on from Solheim et al., (2012), shorter cycles indicate higher solar output and therefore, potentially higher temperatures on Earth owing to increased incident radiation at the Earth's surface, increasing revived net radiative energy. The length of cycle 22, which corresponds to the 1990 heatwave and increased air temperatures in Cheltenham lasted around 9.9 years, relatively shorter than the length outlined by Richards et al., (2009). Cycle 23 which followed this, lasting from 1996 to 2008 (12.3 years) corresponds with increased air temperatures recorded in the later years of the study time frame.

A two-year time lag between peak sunspot cycle and the temperature would account for the delayed response to increased air temperature recorded in 1995 and 2003. Both of which proceed around 2 – 3 years after peak sunspot cycle activity. In both 1995 and 2003, the UK experience heatwave events which coincide with the increase air temperatures recorded in the UK. Similarly, these increased air temperatures reflect within the CUHI time series analysis produced in Figure 4.13. However, attributing the rise in air temperature and CUHI maximum to a sole variable is reductionist. Although this is not to say that sunspot cycles do not have a confounding effect or influence on air temperatures of the magnitude of the CUHI, it is more possible that high-pressure systems and extreme weather events have a

more confounding effect at local scale and sunspot cycles have a confounding effect at a larger scale.

However, upon statistical analysis of sunspot cycles and their relationship to CUHI, no relationship was found. The potential to explore relationships between the UHI and the influence of sunspot observations if both CUHI and sunspot data were smoothed to remove outliers within the datasets, which may result in potential relationships (Friss-Kristenson and Lassen, 1991). Although, a more putative explanation may be that the product of sunspot data may only be significant at larger scales (regional/ national) and may be difficult to observe direct relationships and effects at smaller, localized scales. This explanation is grounded within the context of Burt (1992), to which the effects of the 1990 heatwave were most observable directly at regional and national scales. Furthermore, at local scales, the effects of weather interactions, landscape, topography and background climate conditions are extraneous variables which are difficult to separate from air temperature data (Oke, 2017). Therefore, it is possible at smaller scales, the interactions of extraneous variables may create issues in detecting such phenomena as the effects of sunspot cycles on localized air temperature profiles which can be reflected from the results of this study.

### **5.3.2 Examination of Sunspot Cycles on Weather and Temperature**

The isolation of sunspot cycles on temperature is reductionist and evidence suggests that sunspot cycles as a singular variable, does not have a confounding effect on temperature and the CUHI within this study.

The Earth-atmospheric system is driven primarily by solar radiation and its energy budget (Trenberth et al., 2000; Liang et al., 2019). These interactions influence

weather and climate at both global and local scales. Therefore, a combined effect of solar variation through sunspot cycles on weather and climate may provide evidence for an indirect relationship between sunspot cycles on temperature and CUHI. Results from spectral analysis of cloud cover anomalies over the United States shows a statistically significant relationship between sunspot number and cloud cover (Udelhofen and Cess, 2001). However, this research is limited to the geographic restrictions of eastern part of the United States and cannot directly be extrapolated to the UK or this study. Despite this, the relationship is established, and trends can be inferred. Further supporting this, a decadal analysis into the relationship between sunspot number and cloud cover percentage for Earth was examined by Pallé Bagó and Butler (2000). The results of the analysis showed a strong negative correlation of  $-0.82$  that lower sunspot observations are associated with increased cloud cover. As discussed earlier, the relationship between cloud cover and precipitation is synonymous. Nazari-Sharabian and Karakouzian (2020) show that precipitation also increases with the decline in sunspot number. Therefore, the implication of the data within this study is limited to the analysis of CUHI, however, the influence on sunspot cycles on weather and climate may, by extension show a stronger relationship and prediction for fluctuations in CUHI.

Placing this in context of the energy balance, decreased cloud cover and precipitation result in increased temperature and CUHI, as evidenced by the correlation between cloud cover and precipitation on CUHI minimum. The interactions of both cloud cover and precipitation result in increased reflection of short-wave radiation back into space away from the Earth's surface as well as increased mixing of turbulent air through evaporation which further reduces temperature and CUHI. It can therefore be inferred those interactions between

sunspot cycle and weather have a putative effect on temperature and CUHI intensity. However, to support this claim, further correlation and regression analysis would be advised to assess this relationship and assess if changes in these variables can predict fluctuations in temperature.

#### **5.4 An Evaluation of the CUHI in Cheltenham**

A numerical analysis of the CUHI between the urban and rural stations was investigated. The canopy layer UHI fluctuates over time, there are two main notable points in relation to UHI max which shows two peaks in intensity over time. Firstly, the peak in late 1990 can be related directly to the synoptic weather conditions explored by Burt (1991). Secondly is a maximum peak in mid-1994 which reports a CUHI of +5.7°C. An explanation for this is owing to high cloud cover. Although research shows a correlation between high cloud cover and lower temperatures, the results of the temperature data taken from the weather stations is recorded at a min/max daily value, not hourly. Therefore, diurnal variation cannot be accounted for. A potential explanation for this is that the CUHI intensity is the result of nocturnal temperature recordings in which energy stored in the specific heat capacity of the building is released, resulting in temperature inversion (Oke, 1982). High cloud cover during daytime results in lower air temperatures owing to radiation blocking, however, during nighttime high cloud cover and latent heat escaping result in higher CUHI intensity. Although this explanation may provide an insight to why the CUHI peaks in 1994, it is merely speculation and a resultant limitation of this study.

Changes in synoptic weather conditions and urban form and function affect the UHI intensity and magnitude. Cloud cover limits the amount of shortwave radiation reaching the surface during the day and absorbs longwave radiation at night therefore resulting in a decrease in UHI intensity. Comparing this to Figure 4.9 and

4.10, peaks in CUHI maximum correspond to decreases in cloud cover, although the statistical relationship of this is non-significant, the continued trend in comparison to cloud cover and CUHI minimum (Figure 4.11) further show similar trends to peaks in CUHI minimum with declines in cloud cover, which produced a significant, weak correlation. This is supported by research by Yow and Carbone (1996), who show that an increase in cloud cover and changes to synoptic weather conditions directly affect and share a relationship with UHI intensity through an energetic basis (Oke, 2017). Although their research is based on hourly figures and not monthly averages, changes in the energetic balance of an area, local or regional, result in alterations to the energetic basis of the UHI and its magnitude. An explanation for the increase in CUHI minimum temperatures can be explained by (Wuebbles et al., 2017) who state that overall, minimum temperatures increase at a higher rate than average maximum temperatures.

The CUHI is defined as the difference in the equivalent temperatures of an urban environment and the surrounding natural area (Stewart and Mills., 2021) and is calculated by subtracting the air temperature at a rural reference station from an urban weather station (Stewart, 2011). The canopy layer is defined as the near-surface air temperatures, measured below roof height and the heat island is measured using fixed weather stations, recording air temperatures at screen level ~2m above surface (screen level).

The results from Figure 4.5 support the concepts first proposed by Howard (1833), to which the built-up environment is warmer than its rural counterpart and further follows the concept of forming a dome over an urban environment (Oke, 2017). Cheltenham displays higher temperatures for both minimum and maximum air temperatures. On average, Cheltenham is ~2.1°C warmer than surrounding areas,

with extreme differences of  $\sim 3^{\circ}\text{C}$  for maximum air temperatures (Figure 4.5a).

Furthermore, minimum air temperatures show Cheltenham to be on average  $\sim 1^{\circ}\text{C}$  warmer than the surrounding area and  $\sim 2^{\circ}\text{C}$  for extreme minimum temperatures.

The results produced in Table 4.2 which show the 10-year running average minimum and maximum air temperature for each locality were assigned their respective coordinates and processed through QGIS for interpolation. A heatmap was produced through interpolated values derived from the data produced in Table 4.2. The heatmap was then overlaid both the over-simplified land classification imagery for 2000 and the elevation contour data derived from digital elevation models from Edina Digimaps. Two outputs were created, mapping the interpolated values for the minimum and maximum air temperature values from 1990 to 2000 (Figure 4.16 and Figure 4.17).

Figure 4.5a shows the maximum air temperature shows the highest temperatures ( $31.16^{\circ}\text{C}$ ) emanating from Cheltenham outwards. Maximum air temperature decreases both outwards in area and with increased elevation. There is a small increase in temperature averaging around  $30^{\circ}\text{C}$  towards built-up, urban environments towards the north, east and southeast of Gloucestershire.

Temperature typically decreases outwards, especially in less populous and built-up environments.

In contrast, Figure 4.5b shows minimum air temperatures concentrating adjacent to Cheltenham. A vein of higher temperatures running south easterly through the lower elevations. Similarly, to Figure 4.16, temperature decreases with elevation and deviation from populous, built-up environments.



The data show the clear spatial extent and magnitude of the CUHI in Cheltenham, relative to the study area (Figure 4.5a). Although the heat maps produced use maximum and minimum air temperatures, the interpolation of air temperature defines the UHI spatially. A study by Szymanowski and Kryza (2011) interpolates air temperature to show spatial distribution of the UHI effect. The results from their study show that urbanized areas record higher air temperatures before dissipating outwards (Szymanowski and Kryza, 2011). In context of this study, the maximum air temperature gradient clearly shows higher air temperatures forming a dome (Tursilowati et al., 2018) over Cheltenham before decreasing in values outwards and increasing elevation. Furthermore, UHI (maximum) corresponds with the built-up outline (Oke, 2017) of Cheltenham.

Figure 4.5 shows maximum and minimum air temperatures overlaid on a digital elevation model. From the results, the distribution of higher air temperatures follows the ridge of escarpments that surrounds Cheltenham to the east-side. Higher temperatures follow a spatial pattern which extends to the north and southwest of the lower elevations, with increased elevations recording lower temperatures. An explanation to the difference in air temperature between Cheltenham and Little Rissington (Figure 4.5) which shows signs of warming of  $\sim 3^{\circ}\text{C}$  is that the natural landscape induces higher temperatures at lower elevations. Differences in elevation favour the development of an anticyclonic foehn effect towards Cheltenham (Martin, 2005). These strong downslope winds introduce warmer air to lower elevations on the lee side of mountains or escarpments. This study proposes that the natural landscape surrounding Cheltenham may have exacerbated the effects of the anticyclonic systems in 1990 by capping the south-easterly movement of air through the 'anticyclonic canyon effect' or 'natural canyon effect'. However, the results from

this study do not have the means to deduce this association, a further in-depth analysis between elevation and temperature must be adopted to establish this relationship.

This definition is crudely adopted from the urban canyon effect (Oke et al., 2017) which proposes that in place of tall buildings or urban canyons reducing the potential for heat to dissipate, the natural landscape, surface roughness and increases in elevation have the potential to trap heat and inflate localized temperatures.

This study provides an explanation owing to the intrinsic and extrinsic controls that influence the energetic basis of the UHI. These intrinsic and extrinsic controls influence the surface energy balance for a location. Extrinsic controls can force and influence the general climate of a location. This study proposes that the biophysical properties of the surrounding escarpments around Cheltenham influence the internal dynamics of the weather in the study area (Oke, 2017). In conjunction with the solar geometry of a place and its prevailing synoptic weather a positive feedback loop of net radiation and by increased temperatures can be witnessed. In order to cement this claim, an analysis of the UHI in relation to the Normalized Difference Vegetation Index (NDVI) could be used to establish the rate at which the surrounding escarpments and biophysical processes have on the urban heat island intensity.

The intrinsic controls of a town or city are governed by the fabric, form and properties of the urban environment (Oke, 1982; Stewart and Mills, 2021; Oke; 2017). These intrinsic controls affect the surrounding atmosphere and affect the processes that transport and dissipate heat (Oke, 2017). Alterations to natural and artificial landscape change the properties of albedo and emissivity for each facet and surface. On these principles, lower albedos exist within the built-up environments, contrasting the higher albedo of the surrounding escarpments around Cheltenham.

The increased albedo reflects longwave radiation towards Cheltenham or within the basin that surrounds Cheltenham. The steep variation in elevation between Cheltenham (60m) and Little Rissington (223m), derived from digital elevation model in Figure 4.5. This net radiation is either re-emitted to space or contained within the specific heat capacity of the natural or built-up environment. Hao et al., (2018) states that when terrain is relatively flat, albedo increases with higher solar zenith angle. With more rugged terrain, albedo first increases, then decreases with an increase in solar zenith angle. Further analysis would be advised to investigate if increased surface roughness of the surrounding escarpments can therefore trap and redirect radiation towards Cheltenham to provide a key understanding on the effects of surface roughness and topography on temperature trends. This net radiation is then stored within the fabric of both the natural and artificial environment, which is later re-emitted as latent heat, thus resulting in generally higher temperatures for Cheltenham when compared with its surrounding conurbations.

Although the results do not provide the foundation for this proposal, this study suggests that the topography of the study area contributes to increased temperatures for Cheltenham owing to the processes of advection and capping of high-pressure systems may provide putative explanations for increased temperatures and CUHI for Cheltenham. This process of advection and capping of high-pressure forces warmer air back down towards lower elevations, therefore, resulting in localized net warming of Cheltenham. Areas around Cheltenham display significantly lower temperatures as both surrounding topography and elevation change.

#### **5.4 Topography, Land Classification and CUHI**

Visual examination of the imagery shows a degree of urban metabolism, growth and urban sprawl, a natural function of population growth over time (Marx, 1981; Oke, 1987; Voogt, 2004).

In regard to Figure 4.3a which presents land classifications for 1990. Centrally present in the imagery is Cheltenham and to the southwest of which is Gloucester. Sprawling outwards from these built environments are high concentrations of rangeland and agriculture, specifically to the east of Cheltenham. Westwards of this, there are increased densities of forest land, markedly the Forest of Dean, eastwards of the River Severn. Towards the south, there are present urban bodies and built-up environments.

In regard to Figure 4.3b which presents land classifications for 2000. Centrally present is Cheltenham and Pershore, there are clear increases in urban expansion, specifically regarding Cheltenham which shows a sprawl northward connecting into surrounding conurbations around the town. Furthermore, there is increased density in urban classification for Cheltenham and Pershore, however, this is to a smaller degree than standard studies with cities and mega-cities (Peng et al., 2017).

Interestingly, there are changes in land use in the east/southeast showing a change in predominantly agricultural use towards rangeland. Westwards shows increased growth in built-up environments in the Forest of Dean and a small increase in the density of forest land within this area.

Table 4.4 quantifies the degree of land classification change from 1990 to 2000 for Gloucestershire. At a regional scale, there is a decline of 7% in urban classifications, which is atypical for the process of urbanization and land classification over time.

Considering that typical values for annual urban growth between 1990 to 2000 show an average net increase of 0.6% in urban population for the UK (World Bank, 2021). Population growth is a metric commonly associated with urbanization (Oke et al., 2017). The results from this study do not support the general trend in urbanization when placed in context to urbanization for the UK.

Instead, the trend for increased land classification is attributed to barren (80%) and forest (43%). An explanation for this increase in barren land classification may be owing to anomalies in the processing and reclassification of land classification for 1990 and 2000 land classification data. Therefore, attributing the increased growth in barren land classifications would support the increase in urbanization and urban land classifications, however stricter methods of analysis would be required to significantly investigate and test this hypothesis. Furthermore, this would explain the continuous decline in other land classifications for the region between 1990 and 2000. A key insight into the percentages may result from errors in following LaGro (2005) methods, to which, homogenizing land classification data may introduce unforeseen errors in precise and accurate land classification outputs. However, the majority of the land classification types appear to decline over time, with only two instances increasing, barren and forest. Barren land classification refers to beaches, sandy areas bare exposed rock, mines and quarries (LaGro, 2005). It is through this that, errors of land classifications may be introduced, barren lands in regard to urban, suburban and rural development may be mis-interpolated as bare exposed rock when homogenizing land classification types. Albeit speculation, the land cover changes clearly define a sharp increase in natural land classification types and show small declines in urban growth.

To summarize the results of the land classification analysis, there are signs of continuous growth in both urban sprawl and development in Cheltenham and surrounding built-up environments throughout the study area from 1990 to 2000. A significant change from agriculture to rangeland in the east of Gloucestershire can be inferred from the imagery (Figure 4.3). However, a degree of scrutiny may need to be applied in the interpretation and inference of the data present though. As noted in the methods chapter prior, the changes in resolution of the imagery from 1990 to 2000 and the methods used for land classifications and creating homogenous or uniform classifications create problems.

The differences in resolution and pixilation of the imagery from 1990 and 2000, despite pre-processing and post-processing methods (Aremu et al., 2019; LaGro, 2005) create disparities in band classification and by extension the ability to distinguish one land type from another. This can be seen present in 2000 imagery, to which barren land classification is dominant in the River Severn water land classification. Further issues arrive in the sub-categorization of land classifications from 25 to 5 or 7 homogenous classifications. As mentioned above, the ability to distinguish one band or land class from another becomes hindered and the reductions or oversimplification of land use types reduces accuracy and analysis. Although the use of this imagery is to provide visual analysis over statistical analysis, the blurring of bands and land uses can become a problem under closer inspection. The outlined method of investigation for sky view factor and land climate zone (Oke, 2004; Sakakibara and Matsui, 2005; Sui and Hart, 2012) analysis, has been omitted owing to pixilation and reduced accuracy of imagery at closer scales. Thus, localized analysis or focus on changes in and around weather stations present in-situ cannot be obtained using data collected from this time period, nor within the timeframe of

this study. This, however, would be a key area of investigation in future analyses and a definite focal point to develop within the field of study.

## Chapter 6: Conclusion

This study aimed to evaluate the CUHI in Cheltenham from 1990 to 2000 by investigating and providing putative explanations as to why Cheltenham was ranked the hottest town in the UK between 1990 and 2000. Furthermore, it evaluated the effects of weather, sunspot cycles, population and changes in natural and artificial land use have on the CUHI. The main objectives for this study are to describe the temperature trends for each weather station by year as well as providing a 10-year average to produce a temperature profile for each locality and the region.

Through the evaluation of temperature profiles, the CUHI in Cheltenham and the effects of weather, sunspot cycles, population and changes in landscape between 1990 and 2000, several key conclusions can be derived from this study.

It can be concluded that five locations show significant to slight increase in temperature trends between 1990 to 2000. Cirencester, Little Rissington and Westonbirt show the highest degree of warming over time with temperatures increasing by an average of 2.5°C from 1990 to 2000. Cheltenham and Pershore show slight increases in air temperature over time with an average fluctuation of 1°C despite having higher concentrations of urban land classifications when compared with other sites. Finally, 10-year running average temperature figures for Cheltenham can be calculated as 31.34 (maximum) and -7.28°C (minimum). These results place Cheltenham as the hottest town in Gloucestershire with temperatures exceeding surrounding sites by 3.43°C (maximum) and 0.95°C minimum.

Comparing the decadal temperature profiles to regional background temperatures, as produced within this study. Decadal analysis of air temperature show Cheltenham has significantly higher temperatures than the regional maximum mean (1.96°C).



Furthermore, significantly higher maximum air temperatures when compared against other weather stations within Gloucestershire (between 1.29°C and 3.54°C higher than lowest and highest maximum decadal averages).

Further evaluation of the decadal temperature profiles shows three periods of significant warming, occurring in 1990, 1995 and 2000 respectively. These findings can be concluded to be the result of extreme weather events through the form of heatwaves (Burt, 1992; Burt, 1994), which are shown to exacerbate regional and local temperatures for Gloucestershire. Another key finding of this study shows two of the peaks in annual temperature appear to be synonymous with fluctuations in sunspot maxima in 1990 and 2000. However, statistical analysis between sunspot cycle and CUHI maximum and minimum, it can be concluded from the results that there is no significant relationship between these two variables. However, this is not to assume that sunspot cycles do not influence temperature and CUHI intensity but may be related through indirect means as an extrinsic control, affecting intrinsic Earth-Atmosphere systems which affect atmospheric processes and weather (Oke, 1982; Stewart and Mills, 2021). To confine these conclusions to this study, the results are only limited to this geographical location and time point. There is a definite need to carry out further research to quantify this relationship and establish a strong foundation to make grounded conclusions.

Secondly, is to analyze the relationships between UHI intensity and other meteorological variables collected from automated weather stations within the study area. Through the analysis of CUHI intensity against weather, sunspot cycles and population, it can be concluded that weather has a significant effect on both CUHI maximum and minimum. The results of the analysis support this showing a weak, negative correlation between CUHI maximum and cloud cover percentage. This

shows that increased cloud cover percentage has a weak, but significant negative effect on CUHI maximum. Furthermore, it can be concluded that CUHI minimum is more adversely affected by changes in weather conditions. Changes in the variation of cloud cover and precipitation reflect alterations to the energy balance at local scales (Schmittner, 2018; Le Treut et al., 2021) which provide putative explanations to decreases in CUHI intensity. This is supported by the results which show a weak to medium negative correlation between CUHI minimum, cloud cover and precipitation respectively.

The effect of population showed no significant relationship with CUHI maximum; however, this study reports a strong correlation between population increase and increase in CUHI minimum. These changes only partially reflect the literature, population size have been attributed as anthropogenic driving mechanisms to the CUHI formation and magnitude (Oke, 1973; Oke, 1995). In context of this study, population is shown to solely affect CUHI minimum.

This study originally postulated that sunspot cycles may have a statistically significant confounding effect on the CUHI. Sunspot cycles were used as an experimental surrogate for solar intensity; however, the results show no significant correlation between sunspot cycle and CUHI intensity. This study therefore postulates that sunspot cycle may be inadvertently related to variations in the CUHI however further statistical analysis would be required to test the associations between sunspot cycles on cloud cover, precipitations and by extension its indirect effect on CUHI intensity.

This study utilizes a wide range of data using weather data which is not limited to the typical conditions preferred for investigation. Morris et al., (2000) states that most

studies focus on UHI analysis using atypical conditions thought to be optimal for its development. This may provide explanations as to why there were non-significant correlations between UHI maximum, precipitation, sunspot cycle and population.

Thirdly, is to use GIS to explore the relationship between geography and temperature an evaluation of land cover change in Gloucestershire between 1990 and 2000 show that the largest decreases in land cover classifications are water (-73%) and wetland (-43%) land classifications for the region. Furthermore, small decreases in urban (-7%) and rangeland (-4%) land classifications have been detected too, with significant increases in barren (80%) and forest (43%) land classifications. These trends appear to be atypical when compared against World Bank (2021) statistics which show a 0.6% increase in urban population for the UK between 1990 and 2000. Population size is associated with the process of urbanization (Oke, 1973) and by extension urban sprawl (Voogt, 2004). The results from this study do not support these associations in population and urbanization. Limitations from these results would permit further analysis to confirm these relationships and extensively quantify land classification and population growth over time.

Further evaluation at local scales, using the 250 m circle of influence around each weather station shows significant variance in land classification for four of the sites used. Two of these sites (Cirencester and Pershore), show increases in small increases in urban land classifications. Conclusions can be drawn to show that when compared with decadal temperature trends, there are slight increases in air temperatures respective for these sites. Although further analysis in regard to quantifying this relationship are required. Conversely, Little Rissington and Pershore College show little variation in air temperature trends over time which correspond to

increases in rangeland and agriculture land classifications, therefore supporting the concept that rural areas show lesser degrees of heating compared to urban areas (Oke 1997; Cardoso et al., 2017). In regard to Cheltenham, concluding remarks shows no significant change in land classification, with a minor exchange in barren land classifications for increased urban concentrations and rangeland. The exploration of dominant land classifications against air temperature show that urban land classifications record higher air temperatures when compared against agriculture and rangeland. It can therefore be inferred that urban land classifications demonstrate higher air temperatures when compared with their rural surroundings (Oke, 1997; Tursilowati et al., 2018).

Finally, is to draw out conclusions on the data and compose putative explanations to the formation and extent of the UHI in Cheltenham from 1990 to 2000. Synthesizing the conclusions from this study, it would appear that the primary attribute associated with extreme maximum temperatures in Cheltenham and Gloucestershire can be associated with heatwave events. These events provide putative explanations for elevated temperatures through the region in 1990 and 1995. Evaluated temperatures for both cases resulted from high-pressure systems that exerted themselves over the UK (Burt, 1992; Burt, 1994) which resulted in clear, calm conditions. These conditions resulted in low precipitation and cloud cover which have been shown to be statistically significant in the increase of CUHI within Cheltenham.

The topography and land cover may also explain the formation and magnitude of the CUHI. The effects of the natural and artificial landscape can provide putative explanations towards increased temperatures in Cheltenham. It has been noted from the results and literature that anthropogenic activity and urban landscapes display significantly higher temperatures than their rural surroundings (Oke, 1984; Oke et al.,

2017; Voogt, 2004, Stewart and Mills, 2021). However, the natural landscape and topography of Gloucestershire predisposes Cheltenham to the foehn effect, the meteorological effects of which, are dry adiabatically heating on the downwind side.

This results in warm, dry wind on the downward side, towards Cheltenham.

Therefore, warmer temperatures at lower elevations induce further warming in and around Cheltenham. However, this postulated concept has not been proven and therefore, is a tenuous link between geography and temperature.

In summary, this study concludes even small towns and cities have UHI akin to populous and mega-cities (Peng et al., 2019). Through the analysis of both the literature and exploration of weather, temperature, sunspot and population data this study has provided putative explanations as to why Cheltenham was ranked the hottest town in the UK between 1990 and 2000. Furthermore, the use and analysis of secondary data has shown that increases in precipitation, cloud cover and population have significant relationships with the CUHI, specifically regarding increases in CUHI minimum. Placing this within the wider context of the study, the proportion of net incoming solar radiation and high solar azimuth increases the proportion of received solar radiation (Burt, 1992; Oke et al., 2017) absorbed in both natural and artificial surfaces. In tandem with low cloud cover and precipitation, increase absorption and emissivity of radiation is available as latent heat (Burt, 1992; Trenberth et al., 2000). If the balance is altered, by changes in solar radiation the Earth will respond by either warming or cooling until a new balance is achieved (Hill et al., 2010). Increased anthropogenic activity has resulted changes to the natural landscape which result in changes the energy balance of the urban and natural landscape, these alterations change the radiative properties of the surface and affect the energy balance on both local and global scales (Oke, 2017; Schmittner, 2018; Le

Treut et al., 2021). These factors have been considered a putative driving mechanism of UHIs owing to direct and diffuse radiation and the interactions with the radiative properties of the urban environment (Liang et al., 2019; Oke, 2017; Stewart and Mills, 2021).

### **6.1 Limitations to the Study**

A significant limitation to this study relates to the accessibility and quality of secondary data used within this study. As Perez-Sindin (2017) outlined there is a miscommunication in the methods of how data were collected and processed, unless effective metadata is provided the metadata for MIDAS weather stations are not readily available and are scattered amongst several different archives and limited by permissions required to view, use and analyse data. Therefore, this makes it difficult to assess the reliability of data used and the methods used to collect, archive and quality control data.

Another significant limitation for this study is the small sample size in MIDAS weather stations that contain data and cases of missing data regarding air temperature. There are a total of 232 weather stations listed on the CEDA archives that exist within Gloucestershire, with records extending between 1843 to present day. Of these stations, only 16 stations out of 232 contain any meteorological data. Within the confines of 1990 to 2000, only 11 weather stations exist within Gloucestershire that contain meteorological data. Concerning missing data, the number of usable weather stations within this research were limited to 5 stations containing any continuous, long-term records of air temperature. Although there are methods to deal with interpolating missing values, this increases the risk of introducing bias where large values of data are missing. Two supplementary stations were incorporated; Pershore and Pershore College, which were used to increase spatial distribution of

weather stations. These stations were specifically used to assist in the production of interpolated air temperature heatmaps. However, a criticism of these two supplementary stations, although existing within the 25-mile confines established, exist outside of the Gloucestershire boundary.

The reduction in this data size reduces the reliability of the results. An increase in or denser network of weather stations containing long-term, continuous air temperature data would allow for a greater analysis of the CUHI formation, spatial extent and magnitude.

Another limitation of this study is through the use of only using data from 1990 to 2000. The result of this means that no long-term comparisons can be made, owing to the temporal restrictions of this study. Furthermore, this reduces the ability to make quantifiable comparisons or references to other periods of time which would aid in showing the change in both air temperature trends over longer periods and shifts in the CUHI over longer periods of time. In continuation, a caveat to the analysis of the decadal data would have provided a foundation for exploring the strength and direction of trends in air temperature over time for each site and the region as a whole. The incorporation of Fourier analysis would have allowed for the proper analysis of cyclical data in place of using data derived from mean values from the figures and overall, strengthened the analysis of this section.

A more focused methodology into investigating the effect of radiation, land cover and anthropogenic influences on the CUHI would have provided better analysis and allowed for more putative explanations into the effect of the CUHI in Cheltenham. Surface radiation data would permit the analysis of the reflective properties of urban and rural areas, therefore allowing further analysis into the properties of surface

reflectance and the emissive properties of urban and rural land classifications. As the energy balance is a crucial dynamic in urban climates, the effect of albedo and cross-comparisons to surface UHI could be investigated.

Further limitations of this study relate to the quantification towards the sensitivity of the CUHI minimum and maximum values. Although it has been stated that CUHI minimum was more affected by changes in cloud cover and precipitation, the sensitivity or explanation towards this has not been provided. Changes in cloud cover and precipitation, respectively affect UHI intensity owing to processes of evapotranspiration, alterations in specific and latent heat capacity of materials and furthermore, their albedo. This in turn provides the basis to explain why CUHI intensity changes in relation to these variables. However, quantification towards the sensitivity of CUHI intensity for both minimum and maximum should be investigated as a recommendation for future research. This will allow for further discussion as to why CUHI minimum correlated more with independent variables than CUHI maximum. Conversely, the discussion will open up opportunities to explore and discuss why CUHI maximum is less variable to changes in relation to the independent variables.

Although there are many limitations and caveats within this study, the study provides an initial investigation into quantification of temperature trends within Gloucestershire and the CUHI within Cheltenham. With these limitations outlined, it is therefore possible to make recommendations for future studies.



## 6.2 Suggestions for Future Research

Owing to the limited sample size and the restrictions in the timeframe the study was carried out, it would be advised to produce a contemporary analysis of the CUHI from 2000 onwards. Although limitations in the availability of temperature data collected by MIDAS weather stations and the number of readily available weather stations containing useful data for analysis from 2000 onwards. It would be of use to utilize new readily available sources of data, such as using a network of independent, professional and hobbyist weather stations. The implication of this would allow for a far denser network of weather stations to calculate temperature and CUHI trends for Cheltenham and throughout Gloucestershire. Alternatively, high-resolution satellite observations would provide a key investigation into the surface UHI derived. A study of this kind would provide key explanations and examination of the spatial and temporal dynamics of the UHI effect.

Factors relating to the sensitivity of UHI minimum should be investigated in further research. The results of this study demonstrated that UHI minimum values were affected more than UHI maximum values. The limitations of this study does not offer an in-depth analysis into the causality of this. However, the conduction of a sensitivity analysis may yield some results. An evaluation into the effects of urban morphology and the energetic basis of the UHI has the potential to quantify the sensitivity of the urban heat island, for both minimum and maximum values. From a theoretical perspective, the trapping and emission of heat from urban fabrics and morphology into the surrounding atmosphere allows for the transmission energy. This energy in the form of heat, would provide context for the increase in UHI intensity, especially concerning UHI minimum. In sum, an analysis into the relationship between incoming and outgoing heat transfer from both the built-up and

natural environment may provide a scientific basis for quantifying the sensitivity of both UHI minimum and maximum.

A key area for further research as presented by the limitations within this study is the relationship between sunspot activity and air temperature. Although this method of examination was experimental within this study, interactions between air temperature, sunspot cycles and other confounding variables are difficult to separate. Therefore, with regards to further research, this study would propose a systematic investigation to detect correlations between these two variables.

Specifically, areas for future research should implement the use for Fourier analysis to detect signals within both air temperature and sunspot data. As both datasets contain cyclical data, Fourier analysis would allow for the detection of signals within cyclical data. Therefore, from isolating signals present within the data, correlation analysis could be performed to establish if there is any cross-correlation between the both datasets. Alternatively, an adjusted correlation analysis could be performed to try and isolate factors between the two datasets in order to establish a relationship. Further research should be continued into this field to determine the extent both temporally and spatially the effects of sunspot cycles on air temperature and UHI intensity at different locations through the UK for towns, cities and mega-cities. Furthermore, research should be carried out to establish the effects of sunspot cycles on these factors across different latitudes to account for changes in the reception of solar radiation and sunspot intensity.

Another suggestion for future studies would be to perform further analysis into the anthropogenic influences on the CUHI. Although population was used as a metric for city size and population growth, there are far more anthropogenic contributors to the UHI effect as outlined by Nuruzzaman (2015) and Ningrum (2018).

A key feature for future studies within this field should, in two parts, focus more on the dynamics of the UHI at different scales (surface, canopy, boundary layer UHI), but more importantly, demonstrate a key focus on the UHI effect on smaller towns and cities. The observations of the UHI island effect primarily focus on larger populous and mega-cities (Peng et al., 2019). However, this study has contributed to the wider field of research showing that smaller towns and cities, such as Cheltenham, have UHI's. Therefore, future research should focus on building knowledge in this field at sites which are atypical from the norm.

## References

- Ackerman, B. (1985) Temporal March Of The Chicago Heat Island, *Journal of Climate and Applied Meteorology* 24 (6): 547-554
- Ackerman, S. & Knox, J. (2015) *Meteorology: Understanding The Atmosphere*, Burlington, Ma: Jones Bartlett Learning
- Akbari, H., Pomerantz, M. & Taha, H. (2001) Cool Surfaces And Shade Trees To Reduce Energy Use And Improve Air Quality In Urban Areas, *Solar Energy* 70 (3): 295-310
- Andrei, N. And Liviu, A., 2016. Central European Blocking Anticyclones And The Influences Imprint Over The Romania's Climate. *Present Environment And Sustainable Development*, 10(2), Pp.235-248.
- Aremu, O., Bello, E., Aremu, P., Aganbi, B. & Machoko, J. (2017) Monitoring And Analysis Of Urban Heat Island Using Remote Sensing Data – A Case Study Of Akure, Ondo State, Nigeria, *International Journal Of Environmental Sciences & Natural Resources* 4 (5)
- Arifwidodo, S. And Chandrasiri, O., 2015. Urban Heat Island And Household Energy Consumption In Bangkok, Thailand. *Energy Procedia*, 79, Pp.189-194.
- Arnfield, A. (2003) Two Decades Of Urban Climate Research: A Review Of Turbulence, Exchanges Of Energy And Water, And The Urban Heat Island, *International Journal of Climatology* 23 (1): 1-26
- Atkinson, B., 1998. *Modelling Weather And Climate*. *Geography*, 83(2), Pp.147-62.
- Ayoola, M., Sunmonu, L., Bashiru, M. & Jegede, O. (2014) Measurements Of Net All-Wave Radiation At A Tropical Location, Ile-Ife, Nigeria, *Atmósfera* 27 (3): 305-315

Baldwin, J., Dessy, J., Vecchi, G. And Oppenheimer, M., 2019. Temporally Compound Heat Wave Events And Global Warming: An Emerging Hazard. *Earth's Future*, 7(4), Pp.411-427.

Bassett, R., Cai, X., Chapman, L., Heaviside, C. And Thornes, J. (2017). Methodology To Separate Urban From Regional Heat Advection By Use Of The Weather Research And Forecasting Mesoscale Model. *Quarterly Journal Of The Royal Meteorological Society*, 143(705), Pp.2016-2024.

Beckett, A. And Sanderson, M., 2021. Analysis Of Historical Heatwaves In The United Kingdom Using Gridded Temperature Data. *International Journal Of Climatology*,.

Bennett, D., 2001. How Can I Deal With Missing Data In My Study?. *Australian And New Zealand Journal Of Public Health*, 25(5), Pp.464-469.

Bottyan, Z. & Unger, J. (2003) A Multiple Linear Statistical Model For Estimating The Mean Maximum Urban Heat Island, *Theoretical and Applied Climatology* 75 (3-4): 233-243

Bouyer, J., Huang, Y., Athamena, K. & Musy, M. (2022) Mitigating Urban Heat Island Effect By Urban Design: Forms And Materials, In: Hoorng, D., Freire, M., Lee, M., Bhada-Tata, P. & tuen, B. *Cities and Climate Change : Responding to an Urgent Agenda.*, World Bank, pp.161-181

Brugge, R., 1991. Two Remarkably Sunny Years In Southern Britain-1989 And 1990. *Weather*, 46(12), Pp.384-390.

Brunetti, M., 2003. Solar Signals In Instrumental Historical Series Of Meteorological Parameters. *Societa Atronomica Italiana*, 74.

Burt, S. (1992) The Exceptional Hot Spell Of Early August 1990 In The United Kingdom, *International Journal Of Climatology* 12 (6): 547-567.

Burt, S. (2004) The August 2003 Heatwave In The United Kingdom: Part 1 ? Maximum Temperatures And Historical Precedents, *Weather* 59 (8): 199-208

Busato, F., Lazzarin, R. & Noro, M. (2014) Three Years Of Study Of The Urban Heat Island In Padua: Experimental Results, *Sustainable Cities and Society* 10: 251-258

Cardoso, R., Dorigon, L., Teixeira, D. And Amorim, M. (2017). Assessment Of Urban Heat Islands In Small- And Mid-Sized Cities In Brazil. *Climate*, 5(1), P.14.

Cheltenham Council, 2021. From The Middle Ages To The 19th Century | Historic Cheltenham | Cheltenham Borough Council. [Online] Cheltenham.Gov.Uk. Available At:

<[https://www.cheltenham.gov.uk/info/37/local\\_history\\_and\\_heritage/272/historic\\_cheltenham/2#:~:Text=Cheltenham's%20heyday%20as%20a%20spa,Had%20serv ed%20in%20the%20empire.](https://www.cheltenham.gov.uk/info/37/local_history_and_heritage/272/historic_cheltenham/2#:~:Text=Cheltenham's%20heyday%20as%20a%20spa,Had%20serv ed%20in%20the%20empire.)> [Accessed 22 December 2021].

Collins, K., 2007. Permeable Pavement Research. [Ebook] North Carolina: North Carolina State University. Available At: <<http://www.bae.ncsu.edu/info/permeable-pavement/>> [Accessed 2 January 2022].

Doughty, C., Loarie, S. & Field, C. (2012) Theoretical Impact Of Changing Albedo On Precipitation At The Southernmost Boundary Of The ITCZ In South America, *Earth Interactions* 16 (8): 1-14

EEA, 2013. Energy Related Greenhouse Gas Emissions. [Ebook] European Environment Agency, Pp.1-10. Available At: <<https://www.eea.europa.eu/data-and-maps/indicators/en01-energy-related-greenhouse-gas->

Emissions/En01#:~:Text=Energy%2drelated%20fugitive%20emissions%20include,O  
f%20the%20energy%20production%20sector.> [Accessed 3 January 2022].

Effat, H. & Hassan, O. (2014) Change Detection Of Urban Heat Islands And Some Related Parameters Using Multi-Temporal Landsat Images; A Case Study For Cairo City, Egypt, Urban Climate 10: 171-188

El-Hattab, M., S.M., A. & G.E., L. (2018) Monitoring And Assessment Of Urban Heat Islands Over The Southern Region Of Cairo Governorate, Egypt, The Egyptian Journal of Remote Sensing and Space Science 21 (3): 311-323

Elvidge, A. And Renfrew, I., 2016. The Causes Of Foehn Warming In The Lee Of Mountains. Bulletin Of The American Meteorological Society, 97(3), Pp.455-466.

EPA. (2008) Reducing Urban Heat Islands: Compendium Of Strategies. Urban Heat Island Basics., Available From: <https://www.epa.gov/heat-islands/heat-island-compendium/> [Accessed: 12 March 2018].

Fabrizi, R., De Santis, A. & Gomez, A. (2011) Satellite And Ground-Based Sensors For The Urban Heat Island Analysis In The City Of Madrid, 2011 Joint Urban Remote Sensing Event

Ferguson, G. & Woodbury, A. (2007) Urban Heat Island In The Subsurface, Geophysical Research Letters 34 (23)

Friss-Christensen, E. And Lassen, K., 1991. Length Of The Solar Cycle: An Indicator Of Solar Activity Closely Associated With Climate. Science, 254(5032), Pp.698-700.

Gobo, A., 2004. Mainstreaming Climate Change Adaptation And Mitigation Issues Into Development Planning In Rivers State. Us Open Climate Change Journal, 1.

Gonçalves, A., Ornellas, G., Castro Ribeiro, A., Maia, F., Rocha, A. & Feliciano, M. (2018) Urban Cold And Heat Island In The City Of Bragança (Portugal), *Climate* 6 (3): 70

Hacker, J., Belcher, S. And Yau, R., 2010. Climate Scenarios For Urban Design: A Case Study Of The London Urban Heat Island. [Ebook] London: Arup, Pp.1-12.

Available At:

[Http://Www.Hkccf.Org/Download/Iccc2007/30may/S3a/Jake%20hacker/Climate%20scenarios%20for%20urban%20design%20-%20a%20case%20study%20of%20the%20london%20urban%20heat%20island.Pdf](http://www.hkccf.org/download/icc2007/30may/S3a/Jake%20hacker/Climate%20scenarios%20for%20urban%20design%20-%20a%20case%20study%20of%20the%20london%20urban%20heat%20island.pdf)  
> [Accessed 19 December 2021].

Hajat, S., Vardoulakis, S., Heaviside, C. & Eggen, B. (2014) Climate Change Effects On Human Health: Projections Of Temperature-Related Mortality For The Uk During The 2020s, 2050s And 2080s, *Journal Of Epidemiology And Community Health* 68 (7): 641-648

Harris, I., Osborn, T., Jones, P. & Lister, D. (2020) Version 4 Of The Cru Ts Monthly High-Resolution Gridded Multivariate Climate Dataset, *Scientific Data* 7 (1)

Hartmann, D., 2009. The Global Energy Balance. *Global Physical Climatology*, Pp.18-39.

Hathaway, D.H., Wilson, R.M. & Reichmann, E.J. The Shape Of The Sunspot Cycle. *Sol Phys* 151, 177–190 (1994). <https://doi.org/10.1007/Bf00654090>

He, B., 2018. Potentials Of Meteorological Characteristics And Synoptic Conditions To Mitigate Urban Heat Island Effects. *Urban Climate*, 24, Pp.26-33.



Heaton, J. (2008) Secondary Analysis Of Qualitative Data: An Overview, *Historical Social Research* 33 (3): 33-45

Henson, R., 2006. *The Rough Guide To Climate Change*. London: Rough Guides.

Hibbard, K., Hoffman, F., Huntzinger, D. And West, T., 2017. Changes In Land Cover And Terrestrial Biogeochemistry. In: D. Wuebbles, D. Fahey, K. Hibbard, D. Dokken, B. Stewart And T. Maycock, Ed., *Climate Science Special Report: Fourth National Climate Assessment*. Washington: U.S. Global Change Research Program, Pp.277-302.

Hidore, J. & Oliver, J. (2010) *Climatology*, New York: Prentice Hall

Hill, J., Wyatt, H. And Peters, J., 2010. The Importance Of Energy Balance. *European Endocrinology*, 9(2), P.111.

Holden, J., 2017. *An Introduction To Physical Geography And The Environment*. 4th Ed. Harlow: Pearson.

Holden, J., 2018. *An Introduction To Physical Geography And The Environment*. Harlow, United Kingdom: Pearson Education Canada.

Hollis, D., Mccarthy, M., Kendon, M., Legg, T. And Simpson, I., 2019. Haduk-Grid— A New Uk Dataset Of Gridded Climate Observations. *Geoscience Data Journal*, 6(2), Pp.151-159.

Houghton, J., Meiro Filho, L., Callander, B., Harris, N., Kattenburg, A. And Maskell, K., 1996. *Climate Change 1995*. Cambridge: Cambridge University Press For The Intergovernmental Panel On Climate Change.

Howard, L., 1833. The Climate Of London. [Online] Urban-Climate.Org. Available At: <[https://www.urban-climate.org/documents/lukehoward\\_climate-of-london-v1.pdf](https://www.urban-climate.org/documents/lukehoward_climate-of-london-v1.pdf)> [Accessed 9 May 2021].

Inform Gloucestershire, 2020. Mid 2020 Population Estimates. [Ebook] Gloucestershire: Inform Gloucestershire. Available At: <<https://inform.gloucestershire.gov.uk/media/2108954/mid-2020-population-estimates-final.pdf>> [Accessed 13 November 2021].

Johnston, M. (2012) Connecting Teacher Librarians For Technology Integration Leadership., *School Libraries Worldwide* 18 (1): 18-33

Johnston, M. (2014) Secondary Data Analysis: A Method Of Which The Time Has Come, *Qualitative And Quantitative Methods In Libraries* 3 (1): 619-626

Karlický, J., Huszár, P., Nováková, T., Belda, M., Švábik, F., Ďoubalová, J. And Halenka, T., 2020. The “Urban Meteorology Island”: A Multi-Model Ensemble Analysis. *Atmospheric Chemistry And Physics*, 20(23), Pp.15061-15077.

Kendon, M., Mccarthy, M., Jevrejeva, S., Matthews, A., Sparks, T. And Garforth, J., 2020. State Of The Uk Climate 2019. *International Journal Of Climatology*, 40(S1), Pp.1-69.

Kennedy, D., Parker, T., Woollings, T., Harvey, B. And Shaffrey, L. (2016). The Response Of High-Impact Blocking Weather Systems To Climate Change. *Geophysical Research Letters*, 43(13), Pp.7250-7258.

Kennedy, M., 2013. *Introducing Geographic Information Systems With Arcgis®*. 3rd Ed. New Jersey: Wiley.

Kidder, S. And Essenwanger, O., 1995. The Effect Of Clouds And Wind On The Difference In Nocturnal Cooling Rates Between Urban And Rural Areas. *Journal Of Applied Meteorology*, 34(11), Pp.2440-2448.

Kirtman, B., Power, S., Adedoyin, J., Boer, G., Bojariu, R. & Camilloni, L. (2013) Near-Term Climate Change: Projection And Predictability, In: Stoker, T., Qin, D., Plattner, G., Tignor, M.,

Lagro, J. (2005) Land-Use Classification, *Encyclopedia Of Soils In The Environment*: 321-328

Lavoie, C. And Lachance, D., 2006. A New Herbarium-Based Method For Reconstructing The Phenology Of Plant Species Across Large Areas. *American Journal Of Botany*, 93(4), Pp.512-516.

Le Treut, H., Somerville, H., Cubasch, U., Ding, Y., Mauritzen, C., Mokssit, A., Peterson, T. And Prather, M., 2021. Historical Overview Of Climate Change Science. In: S. Solomon, D. Qin, M. Manning, Z. Chen, M. Marquis, K. Averyt, M. Tignor And H. Miller, Ed., *Climate Change 2007: The Physical Science Basis. Contribution Of Working Group I To The Fourth Assessment Report Of The Intergovernmental Panel On Climate Change*, 1st Ed. Cambridge: Cambridge University Press, Pp.95-122.

Lee, J., Lewis, A., Monks, P., Jacob, M., Hamilton, J., Hopkins, J., Watson, N., Saxton, J., Ennis, C. And Carpenter, L., 2006. Ozone Photochemistry And Elevated Isoprene During The Uk Heatwave Of August 2003. *Atmospheric Environment*, 40(39), Pp.7598-7613.

Lee, T., Choi, H. And Lee, J., 2014. Generalized Scaling Of Urban Heat Island Effect And Its Applications For Energy Consumption And Renewable Energy. *Advances In Meteorology*, 2014, Pp.1-5.

Levermore, G. & Parkinson, J. (2015) The Manchester Urban Heat Island And Adjustments For The Chartered Institution Of Building Services Engineer Calculations, *Building Services Engineering Research And Technology* 37 (2): 128-135

Liang, S., Wang, D., He, T. And Yu, Y., 2019. Remote Sensing Of Earth's Energy Budget: Synthesis And Review. *International Journal Of Digital Earth*, 12(7), Pp.737-780.

Lim, T., Rajabifard, A., Khoo, V., Sabri, S. & Chen, Y. (2021) The Smart City In Singapore: How Environmental And Geospatial Innovation Lead To Urban Livability And Environmental Sustainability, *Smart Cities for Technological and Social Innovation*: 29-49

Linacre, E. (2004) *Climate Data And Resources*, London: Routledge

Lohmann, U. (1992) *The Köppen Climate Classification As A Diagnostic Tool For General Circulation Models*, Hamburg, Germany: Max-Planck-Institut Für Meteorologie

Lowe, J., Walker, M. And Porter, S., 2013. Introduction | Understanding Quaternary Climatic Change. *Encyclopedia Of Quaternary Science*, Pp.26-35.

Macintyre, H. (2017) *Urban Heat Islands Workshop Report*, [Accessed: 26 April 2018].

Madley-Dowd, P., Hughes, R., Tilling, K. And Heron, J., 2019. The Proportion Of Missing Data Should Not Be Used To Guide Decisions On Multiple Imputation. *Journal Of Clinical Epidemiology*, 110, Pp.63-73.

Manoli, G., Fatichi, S., Schläpfer, M., Yu, K., Crowther, T., Meili, N., Burlando, P., Katul, G. And Bou-Zeid, E., 2019. Magnitude Of Urban Heat Islands Largely Explained By Climate And Population. *Nature*, 573(7772), Pp.55-60.

Martin, E., 2005. The August 1990 Heatwave. *Weather*, 60(3), Pp.83-83.

Martinez-Gracia, A., Arauzo, I. And Uche, J., 2019. Solar Energy Availability. *Solar Hydrogen Production*, Pp.113-149.

Marx, K. (1981) *Capital: Critique Of Political Economy. Volume 3.*, London: Penguin Books Ltd.

Masson, V. (2005) *Urban Surface Modeling And The Meso-Scale Impact Of Cities*, *Theoretical and Applied Climatology* 84 (1-3): 35-45

Matzinger, N., Andretta, M., van Gorsel, E., Vogt, R., Ohmura, A. & Rotach, M. (2003) *Surface Radiation Budget In An Alpine Valley*, *Quarterly Journal of the Royal Meteorological Society* 129 (588): 877-895

Mccarthy, M., Armstrong, L. And Armstrong, N., 2019. A New Heatwave Definition For The Uk. *Weather*, 74(11), Pp.382-387.

Mcgrane, S., 2016. *Impacts Of Urbanisation On Hydrological And Water Quality Dynamics, And Urban Water Management: A Review*. *Hydrological Sciences Journal*, 61(13), Pp.2295-2311.

Menberg, K., Bayer, P., Zosseder, K., Rumohr, S. And Blum, P. (2013). *Subsurface Urban Heat Islands In German Cities*. *Science Of The Total Environment*, 442, Pp.123-133.

Menke, K., 2019. *Discover Qgis 3.X*. Locate Press.

Met Office (2012). Hot Spell August 1990. [Online] Met Office. Available At:  
<https://www.metoffice.gov.uk/climate/uk/interesting/aug1990/> [Accessed 8 Nov. 2017].

Met Office (2017). Cheltenham Climate Information - Met Office. [Online] Metoffice.gov.uk. Available At:  
<https://www.metoffice.gov.uk/public/weather/climate/gcnx0z9e5> [Accessed 21 Nov. 2017].

Met Office (2019) Cheltenham (Gloucestershire) Uk Climate Averages, Available From: <<https://www.metoffice.gov.uk/research/climate/maps-and-data/uk-climate-averages/gcnx0z9e5>> [Accessed: 17 June 2019]

Met Office (2021) Past Weather Events, Available From:  
<<https://www.metoffice.gov.uk/weather/learn-about/past-uk-weather-events>> [Accessed: 18 September 2021]

Met Office, (2017) Monthly Ranked Hadcet Mean. [Online] Metoffice.gov.uk. Available At:  
<[https://www.metoffice.gov.uk/hadobs/hadcet/mly\\_cet\\_mean\\_sort.txt](https://www.metoffice.gov.uk/hadobs/hadcet/mly_cet_mean_sort.txt)> [Accessed 26 December 2021].

Met Office, 2019. New Official Highest Temperature In Uk Confirmed. [Online] Met Office. Available At: <<https://www.metoffice.gov.uk/about-us/press-office/news/weather-and-climate/2019/new-official-highest-temperature-in-uk-confirmed>> [Accessed 22 December 2021].

Met Office, 2019. Record Breaking Heat-Wave July 2019. [Ebook] Met Office. Available At:  
<<https://www.metoffice.gov.uk/binaries/content/assets/metofficegovuk/pdf/weathe>

r/Learn-About/Uk-Past-Events/Interesting/2019/2019\_007\_July\_Heatwave.Pdf>

[Accessed 26 December 2021].

Met Office, 2021. Uk Climate Averages. [Online] Met Office. Available At:

<<https://www.metoffice.gov.uk/research/climate/maps-and-data/uk-climate-averages#?tab=climateanomalies>> [Accessed 26 December 2021].

Min, M., Lin, C., Duan, X., Jin, Z. & Zhang, L. (2019) Spatial Distribution And Driving Force Analysis Of Urban Heat Island Effect Based On Raster Data: A Case Study Of The Nanjing Metropolitan Area, China, *Sustainable Cities and Society* 50: 101637

Mitas, L. & Mitasova, H. (2005) Spatial Interpolation, In: Longley, P. *Geographical Information Systems: Principles, Techniques, Management And Applications*, Abridged, New Jersey: Wiley

Mitas, L. And Mitasova, H., (1999). Spatial Interpolation. In: P. Longley, M. Goodchild, D. Maguire And D. Rhind, Ed., *Geographical Information Systems: Principles, Techniques, Management And Applications*. Wiley, Pp.481-492.

Monkhouse, F., (1995). *Principles Of Physical Geography*. London: Hodder & Stoughton.

Morris, C., Simmonds, I. And Plummer, N., 2001. Quantification Of The Influences Of Wind And Cloud On The Nocturnal Urban Heat Island Of A Large City. *Journal Of Applied Meteorology*, 40(2), Pp.169-182.

Nazari-Sharabian, M. And Karakouzian, M., 2020. Relationship Between Sunspot Numbers And Mean Annual Precipitation: Application Of Cross-Wavelet Transform— A Case Study. *J — Multidisciplinary Scientific Journal*, 3(1), Pp.67-78.

Nica, A., Popescu, A. & Ibanescu, D. (2019) Human Influence On The Climate System, *Curr Trends Nat Sci* 8 (15): 209-215

Ningrum, W. (2018). Urban Heat Island Towards Urban Climate. *Iop Conference Series: Earth And Environmental Science*, 118, P.012048.

NOAA, 2021. Solar Cycle Progression | Noaa / Nws Space Weather Prediction Center. [Online] [Swpc.Noaa.Gov](https://www.swpc.noaa.gov). Available At: <<https://www.swpc.noaa.gov/products/solar-cycle-progression>> [Accessed 27 December 2021].

Norusis, M. (1988). *The Spss Guide To Data Analysis For Spss With Additional Instructions For Spss/Pc*. Chicago, Il: Spss.

Nunez, M. And Oke, T., 1977. The Energy Balance Of An Urban Canyon. *Journal Of Applied Meteorology*, 16(1), Pp.11-19.

Nuruzzaman, M. (2015) Urban Heat Island: Causes, Effects And Mitigation Measures - A Review, *International Journal Of Environmental Monitoring And Analysis* 3 (2): 67

Oke, T. (1973). City Size And The Urban Heat Island. *Atmospheric Environment* (1967), 7(8), Pp.769-779.

Oke, T. (1982) The Energetic Basis Of The Urban Heat Island, *Quarterly Journal Of The Royal Meteorological Society* 108 (455): 1-24.

Oke, T. (1987) *Boundary Layer Climates*, London: Routledge, Taylor & Francis Group

Oke, T. (1988) The Urban Energy Balance Process In Physical Geography, *Progress In Physical Geography* 12 (4): 471-508



Oke, T. (1995). Classics In Physical Geography Revisited. Progress In Physical Geography, 19(1), Pp.107-113

Oke, T. (1997) Urban Environments, In: Bailey, W., Oke, T. & Rouse, W. The Surface Climates Of Canada, Montreal: McGill-Queens University Press, Pp.303 - 327

Oke, T. (2008) Guide To Meteorological Instruments And Methods Of Observation, Geneva: Wmo

Oke, T., (1997). Urban Climates And Global Environmental Change. In: A. Perry And R. Thompson, Ed., Applied Climatology: Principles And Practice, 1st Ed. London: Routledge, Pp.273 - 287.

Oke, T., Mills, G., Christen, A. And Voogt, J., 2017. Urban Climates. Cambridge, United Kingdom: Cambridge University Press.

Oke, T.R., 1976. The Distinction Between Canopy And Boundary-Layer Urban Heat Islands. Atmosphere, 14(4), Pp.268-277.

Oke. T. (2004) Urban Observations, Instruments And Methods Of Observation Programme,, Geneva: World Meteorological Organization [Accessed: 3 April 2018].

ONS (1997) Uk Data Service Discover, Available From:

<[Http://Dx.Doi.Org/10.5257/Census/Aggregate-1991-1](http://dx.doi.org/10.5257/Census/Aggregate-1991-1)> [Accessed: 7 May 2018]

ONS (2005) Uk Data Service Discover, Available From:

<[Http://Dx.Doi.Org/10.5257/Census/Aggregate-2001-1](http://dx.doi.org/10.5257/Census/Aggregate-2001-1)> [Accessed: 7 May 2018]

ONS 2016. Standard Area Measurements (2016) For Administrative Areas In The United Kingdom. [Online] Ons.Maps.Arcgis.Com. Available At:

<[Https://Ons.Maps.Arcgis.Com/Home/Item.Html?Id=A79de233ad254a6d9f76298e666abb2b](https://ons.maps.arcgis.com/home/item.html?id=A79de233ad254a6d9f76298e666abb2b)> [Accessed 14 August 2021].

Ordnance Survey, 2020. Terrain 50 | Visualise And Analyse Landscapes In 3d | Tools & Support. [Online] Ordnancesurvey.Co.Uk. Available At: <<https://www.ordnancesurvey.co.uk/business-government/tools-support/terrain-50-support>> [Accessed 8 January 2022].

Pallant, J. (2010). *Spss Survival Manual: A Step By Step Guide To Data Analysis Using Spss*. Open University Press.

Peng, S., Feng, Z., Liao, H., Huang, B., Peng, S. And Zhou, T., 2019. Spatial-Temporal Pattern Of, And Driving Forces For, Urban Heat Island In China. *Ecological Indicators*, 96, Pp.127-132.

Perez-Sindin, X., 2017. Secondary Data: Sources, Advantages And Disadvantages. In: M. Allen, Ed., *Sage Encyclopedia Of Communication Research Methods*. New York: Sage, Pp.1577-1579.

Perkins, S., 2015. A Review On The Scientific Understanding Of Heatwaves—Their Measurement, Driving Mechanisms, And Changes At The Global Scale. *Atmospheric Research*, 164-165, Pp.242-267.

Perkins, S., 2019. Core Concept: Albedo Is A Simple Concept That Plays Complicated Roles In Climate And Astronomy. *Proceedings Of The National Academy Of Sciences*, 116(51), Pp.25369-25371.

Perkins-Kirkpatrick, S. And Lewis, S., 2020. Increasing Trends In Regional Heatwaves. *Nature Communications*, 11(1).

Pinho, O. & Orgaz, M. (2000) The Urban Heat Island In A Small City In Coastal Portugal, *International Journal of Biometeorology* 44 (4): 198-203

- Priyadarsini, R., Hien, W. & Wai David, C. (2008) Microclimatic Modeling Of The Urban Thermal Environment Of Singapore To Mitigate Urban Heat Island, *Solar Energy* 82 (8): 727-745
- Rao, P.K., 1972. Remote Sensing Of Urban " Heat Islands" From An Environmental Satellite. *Bulletin Of The American Meteorological Society*, 53(7), Pp.647-648.
- Rauf, S., Pasra, M. & Yuliani (2020) Analysis Of Correlation Between Urban Heat Islands (Uhi) With Land-Use Using Sentinel 2 Time-Series Image In Makassar City, *Iop Conference Series: Earth And Environmental Science* 419 (1): 012088
- Reichel, R., Thejll, P. And Lassen, K., 2001. The Cause-And-Effect Relationship Of Solar Cycle Length And The Northern Hemisphere Air Surface Temperature. *Journal Of Geophysical Research: Space Physics*, 106(A8), Pp.15635-15641.
- Reichle, D. (2020) Anthropogenic Alterations To The Global Carbon Cycle And Climate Change, *The Global Carbon Cycle and Climate Change*: 209-251
- Rembold, F., Carnicelli, S., Nori, M. And Ferrari, G., 2000. Use Of Aerial Photographs, Landsat Tm Imagery And Multidisciplinary Field Survey For Land-Cover Change Analysis In The Lakes Region (Ethiopia). *International Journal Of Applied Earth Observation And Geoinformation*, 2(3-4), Pp.181-189.
- Richards, M., Rogers, M. & Richards, D. (2009) Long-Term Variability In The Length Of The Solar Cycle, *Publications of the Astronomical Society of the Pacific* 121 (881): 797-809
- Robinson, P. And Henderson-Sellers, A., 1999. *Contemporary Climatology*. 2nd Ed. Essex: Pearson Education Limited.

Sakakibara, Y. & Matsui, E. (2005) Relation Between Heat Island Intensity And City Size Indices/Urban Canopy Characteristics In Settlements Of Nagano Basin, Japan, *Geographical Review Of Japan* 78 (12): 812-824

Schmittner, A., 2018. *Introduction To Climate Science*. 1st Ed. Oregon State University.

Silso, 2020. Sunspot Number And Long-Term Solar Observations. [Online] Wdc-Silso. Available At: <[Http://Www.Sidc.Be/Silso/](http://www.sidc.be/Silso/)> [Accessed 12 July 2020].

Siu, L. & Hart, M. (2012) Quantifying Urban Heat Island Intensity In Hong Kong Sar, China, *Environmental Monitoring And Assessment* 185 (5): 4383-4398.

Smith, C., Webb, A., Levermore, G., Lindley, S. And Beswick, K. (2011). Fine-Scale Spatial Temperature Patterns Across A Uk Conurbation. *Climatic Change*, 109(3-4), Pp.269-286.

Smoliak, B., Snyder, P., Twine, T., Mykleby, P. And Hertel, W., 2015. Dense Network Observations Of The Twin Cities Canopy-Layer Urban Heat Island. *Journal Of Applied Meteorology And Climatology*, 54(9), Pp.1899-1917.

Sobrino, J., Oltra-Carrió, R., Sòria, G., Jiménez-Muñoz, J., Franch, B., Hidalgo, V., Mattar, C., Julien, Y., Cuenca, J., Romaguera, M., Gómez, J., De Miguel, E., Bianchi, R. And Paganini, M. (2013). Evaluation Of The Surface Urban Heat Island Effect In The City Of Madrid By Thermal Remote Sensing.

Solheim, J., Stordahl, K. And Humlum, O., 2012. The Long Sunspot Cycle 23 Predicts A Significant Temperature Decrease In Cycle 24. *Journal Of Atmospheric And Solar-Terrestrial Physics*, 80, Pp.267-284.

Steenneveld, G., Koopmans, S., Heusinkveld, B., Van Hove, L. & Holtslag, A. (2011) Quantifying Urban Heat Island Effects And Human Comfort For Cities Of Variable Size And Urban Morphology In The Netherlands, *Journal Of Geophysical Research* 116 (D20).

Stephens, G. And L'ecuyer, T., 2015. The Earth's Energy Balance. *Atmospheric Research*, 166, Pp.195-203.

Stewart, I. & Oke, T. (2012) Local Climate Zones For Urban Temperature Studies, *Bulletin of the American Meteorological Society* 93 (12): 1879-1900

Stewart, I. (2011). A Systematic Review And Scientific Critique Of Methodology In Modern Urban Heat Island Literature. *International Journal Of Climatology*, 31(2), Pp.200-217.

Svensson, M., Eliasson, I. & Holmer, B. (2002) A GIS Based Empirical Model To Simulate Air Temperature Variations In The Göteborg Urban Area During The Night, *Climate Research* 22: 215-226

Taeslar, R., 1986. *Urban Climatological Methods And Data..* Mexico City: World Meteorological Organization, Pp.199-238.

Taha, H., Konopacki, S. & Gaberseck, S. (1999) Impacts Of Large-Scale Surface Modifications On Meteorological Conditions And Energy Use: A 10-Region Modeling Study, *Theoretical And Applied Climatology* 62 (3-4): 175-185

Theeuwes, N., Barlow, J., Teuling, A., Grimmond, C. And Kotthaus, S., 2019. Persistent Cloud Cover Over Mega-Cities Linked To Surface Heat Release. *Npj Climate And Atmospheric Science*, 2(1).

Tian, L., Li, Y., Lu, J. & Wang, J. (2021) Review On Urban Heat Island In China: Methods, Its Impact On Buildings Energy Demand And Mitigation Strategies, Sustainability 13 (2): 762

Trenberth, K., Miller, K., Mearns, L. And Rhodes, S., 2000. Effects Of Changing Climate On Weather And Human Activities. Sausalito: University Science Books.

Tursilowati, L., Pemanfaatan, P., Atmosfer, S. And Lapan, I. (2018). Urban Heat Island Dan Kontribusinya Pada Perubahan Iklim Dan Hubungannya Dengan Perubahan Lahan. [Ebook] Prosiding Seminar Nasional Pemanasan Global Dan Perubahan Global – Fakta, Mitigasi, Dan Adaptasi, Pp.89-94. Available At: [https://www.researchgate.net/publication/265112122\\_Urban\\_Heat\\_Island\\_Dan\\_Kontribusiny\\_Pada\\_Perubahan\\_Iklim\\_Dan\\_Hubungannya\\_Dengan\\_Perubahan\\_Lahan?Enrichid=RgregFfe5b4ced7882a8a1a33b250962a8aa4Xxx&Enrichsource=Y292zxjqywdlozi2ntexmjeymitbuzoymtynjy4ntaxndiyndlamQyodu0otywmtmwma%3d%3d&EI=1\\_X\\_3&Esc=Publicationcoverpdf](https://www.researchgate.net/publication/265112122_Urban_Heat_Island_Dan_Kontribusiny_Pada_Perubahan_Iklim_Dan_Hubungannya_Dengan_Perubahan_Lahan?Enrichid=RgregFfe5b4ced7882a8a1a33b250962a8aa4Xxx&Enrichsource=Y292zxjqywdlozi2ntexmjeymitbuzoymtynjy4ntaxndiyndlamQyodu0otywmtmwma%3d%3d&EI=1_X_3&Esc=Publicationcoverpdf) [Accessed 8 Apr. 2018].

UKCEH, 2020. Land Cover Map 1990 Dataset Documentation. [Ebook] Uk Centre For Ecology An Hydrology, Pp.1-21. Available At: [https://www.ceh.ac.uk/sites/default/files/202111/lcm1990\\_dataset\\_document\\_0ct2020.pdf](https://www.ceh.ac.uk/sites/default/files/202111/lcm1990_dataset_document_0ct2020.pdf) [Accessed 29 December 2021].

Voogt, J. And Oke, T. (2003). Thermal Remote Sensing Of Urban Climates. Remote Sensing Of Environment, 86(3), Pp.370-384.

Wake, B., 2015. Global Versus Local. Nature Climate Change, 5(11), Pp.974-974.

Wallace, J. And Hobbs, P., 2006. The Earth System. Atmospheric Science, Pp.25-61.

Wang, B., Ding, S., Qiao, G., Guo, Y. And Xu, Y., 2015. Study On The Urban Heat Islands And The Meteorological Elements Over The Pearl River Delta. [Ebook] Guangzhou: International Conference On Urban Climate, Pp.1 - 5. Available At: <[Http://Www.Meteo.Fr/Icuc9/Longabstracts/Poster\\_1-5-2401253\\_A.Pdf](http://www.meteo.fr/icuc9/longabstracts/poster_1-5-2401253_A.pdf)> [Accessed 30 January 2022].

WDC-SILSO, 2021. Daily Total Sunspot Number | Silso. [Online] [Wwwbis.Sidc.Be](http://wwwbis.sidc.be). Available At: <[Https://Wwwbis.Sidc.Be/Silso/Infosndtot](https://wwwbis.sidc.be/silso/infosndtot)> [Accessed 9 December 2021].

Webb, J. And Meaden, G., 2000. Daily Temperature Extremes For Britain. *Weather*, 55(9), Pp.298-315.

Webb, J. And Meaden, G., 2012. Daily Temperature Extremes For Britain. *Weather*, 55(9), Pp.298-315.

White, I., Mottershead, D. And Harrison, S., 1998. *Environmental Systems*. Cheltenham, England: Stanley Thornes.

White, M., Nemani, R., Thornton, P. And Running, S., 2002. Satellite Evidence Of Phenological Differences Between Urbanized And Rural Areas Of The Eastern United States Deciduous Broadleaf Forest. *Ecosystems*, 5(3), Pp.260-273.

Wienert, U. & Kuttler, W. (2005) The Dependence Of The Urban Heat Island Intensity On Latitude A Statistical Approach, *Meteorologische Zeitschrift* 14 (5): 677-686

Wittich, K.-P., 1997: Some Simple Relationships Between Land-Surface Emissivity, Greenness And Plant Cover Fraction For Use In Satellite Remote Sensing. *International Journal Of Biometeorology*

WMO (2010) Guide To Climatological Practices, World Meteorological Organization

Available From:

<[http://www.wmo.int/pages/prog/gcos/documents/gruanmanuals/cimo/cimo\\_guide-7th\\_edition-2008.pdf](http://www.wmo.int/pages/prog/gcos/documents/gruanmanuals/cimo/cimo_guide-7th_edition-2008.pdf)> [Accessed: 9 May 2018].

WMO, 2018. Guidelines On The Definition And Monitoring Of Extreme Weather And Climate Events. [Ebook] World Meteorological Organization Commission For

Climatology. Available At:

<[http://www.wmo.int/pages/prog/wcp/ccl/documents/guidelinesonthedefinitionandmonitoringofextremeweatherandclimateevents\\_09032018.pdf](http://www.wmo.int/pages/prog/wcp/ccl/documents/guidelinesonthedefinitionandmonitoringofextremeweatherandclimateevents_09032018.pdf)> [Accessed 27 December 2021].

Word Bank (2021) World Development Indicators | Databank, Available From:

<<https://databank.worldbank.org/source/world-development-indicators>>

[Accessed: 27 December 2021]

Wuebbles, D., Fahey, D., Hibbard, K., Stewart, B. And Maycock, T., 2017. Climate Science Special Report: Fourth National Climate Assessment, Volume 1. [Ebook]

Washington: Usgcrp, Pp.1-477. Available At:

<[https://science2017.globalchange.gov/downloads/cssr2017\\_fullreport.pdf](https://science2017.globalchange.gov/downloads/cssr2017_fullreport.pdf)>

[Accessed 28 January 2022].

Xu, Y., Zhou, D. & Li, Z. (2016) Research On Characteristic Analysis Of Urban Heat Island In Multi-Scales And Urban Planning Strategies, *Procedia Engineering* 169:

175-182

Yow, D. & Carbone, G. (2006) The Urban Heat Island And Local Temperature

Variations In Orlando, Florida, *Southeastern Geographer* 46 (2): 297-321



Yow, D. (2007) Urban Heat Islands: Observations, Impacts, And Adaptation, Geography Compass 1 (6): 1227-1251

Zhao, L., Lee, X., Smith, R. & Oleson, K. (2014) Strong Contributions Of Local Background Climate To Urban Heat Islands, Nature 511 (7508): 216-219

Zhou, B., Rybski, D. And Kropp, J., 2017. The Role Of City Size And Urban Form In The Surface Urban Heat Island. Scientific Reports, 7(1).

Zipper, S., Schatz, J., Kucharik, C. & Loheide, S. (2017) Urban Heat Island-Induced Increases In Evapotranspirative Demand, Geophysical Research Letters 44 (2): 873-881

Živković, J., 2018. Urban Form And Function. Encyclopedia Of The Un Sustainable Development Goals, Pp.1-10.